



ESA – Bare PHOTOVOLTAIC TETHER

WP1 - Mechanical Testing

UniPD Team: E. Lorenzini, D. Mattinelli, A. Valmorbidia

Presented by Enrico Lorenzini

University of Padova 19-01-2023



UNIVERSITÀ
DEGLI STUDI
DI PADOVA



PRESENTATION OUTLINE

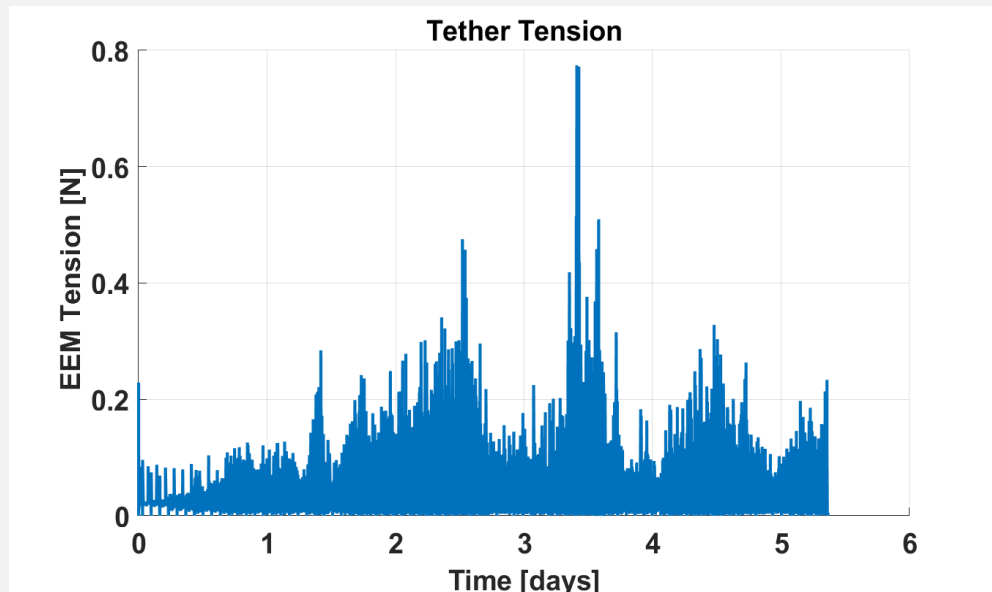
- Tape mechanical loads
 - Derived from numerical simulations and tape handling requirements
- Mechanical testing of tapes
 - Servo-hydraulic machine *MTS 858 Mini Bionix II* used to measure:
 - Mechanical strength
 - Axial stiffness
 - Two independent methods with *Bose ElectroForce®* machine and *Laser Vibrometer* utilized to measure:
 - Damping coefficients
- Deployment test of photovoltaic tape
 - Used tape deployer drive-pulleys assembly to evaluate effects on cells power performance

REQUIREMENT ON TAPE AXIAL LOAD

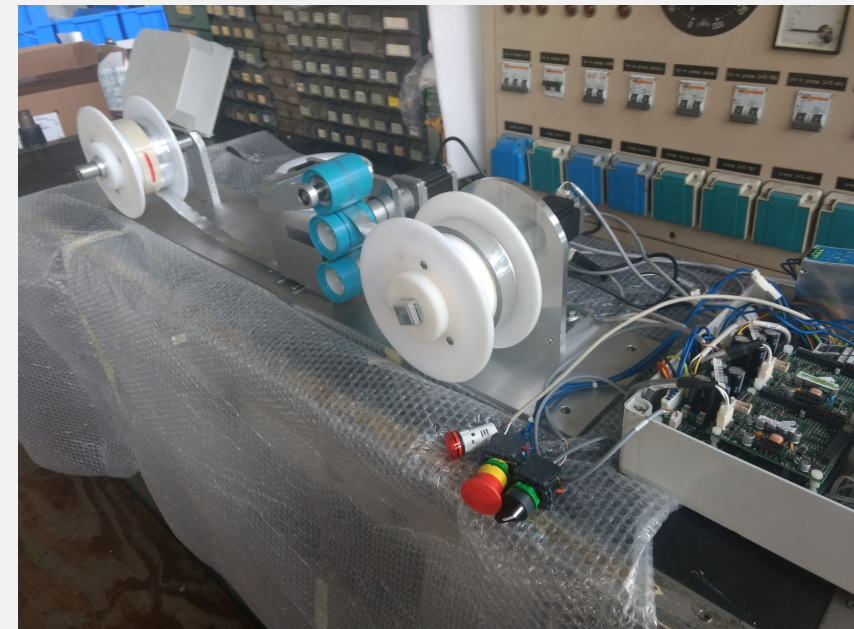
- Requirement on tether axial force

- The requirement of 10 N maximum axial load (BPT-P-0020) stems from the process of spooling the tape onto a stable spool that is launch-load-resistant (as tested on shaker for the project E.T.PACK)
- The maximum tension value during deorbiting from numerical simulations due to dynamics is < 1 N

Tether tension during deorbit from sim



Tape spooling machine at UniPD



TEST PLAN

Test items and test conditions

Test items	Test conditions
3x Aluminum tape-substrate samples of different lengths	Ambient
3x Steel tape-substrate samples of different lengths (same as aluminum)	Ambient

Test plan for measuring mechanical characteristics

Test type	Methodology	Finality	Conditions
Hysteresis cycles	30 cycle at 0.5 Hz in a load range from TBD to TBD with force control	Measure the damping coefficient	Ambient
Pull test	slow ramp with displacement control up to a moderate load	Measure stiffness	Ambient
Pull test	increase displacement up to breakage	Measure yield & break strengths	Ambient

PULL TESTS TO MEASURE STIFFNESS AND STRENGTH

- Pull tests done on Aluminum and Stainless substrates with servo-hydraulic machine controlled in displacement or pulling force (MTS 858 Mini Bionix II): max machine load 1.5 kN
- Samples instrumented with 4 strain gauges to improve strain measurement resolution

Effective sample length	10 cm	25 cm	40 cm	Data from Materials Selector
Mechanical properties				
Stainless Steel – annealed (50μm)				
K [N/m]	1318 \cdot 10 ³	627 \cdot 10 ³	553 \cdot 10 ³	
E [GPa]	105	176	177	190-200 GPa
σ^y [MPa]	~	800 – 880	800 – 856	520-960 MPa
σ^U [MPa]	~	947	946	760-1270 MPa
Aluminum – 1200 H18 (40μm)				
K [N/m]	330 \cdot 10 ³	213 \cdot 10 ³	126 \cdot 10 ³	
E [GPa]	33	53	50	69 GPa
σ^y [MPa]	120 – 140	115 – 135	118 – 130	150 Mpa
σ^U [MPa]	161	161	159	165 MPa

MTS 858 Mini Bionix II at UNIPD



Strain gauges

MEASURED AXIAL STRENGTH

- Tape strength vs. axial force requirement

Material	Cross section	Axial Yield (N)	Axial Ultimate (N)	Linear mass (kg/km)
Stainless Steel	50 μ m x 25mm	1000-1100 N	1180 N	9.7
Aluminum	40 μ m x 25 mm	115-140 N	200 N	2.7
BPT-P-0020	BPT Axial Force BPT shall withstand an axial force of, at least, 10 N. Rationale: this is conservative value attained in non-stationary conditions <i>Added Note: the tape is spooled on a coil at ~8 N of tension</i>			

- **Conclusions:**
 - both substrates satisfy the axial force requirement with *very ample margins of safety*
 - Aluminum substrate is considerably lighter than Stainless Steel

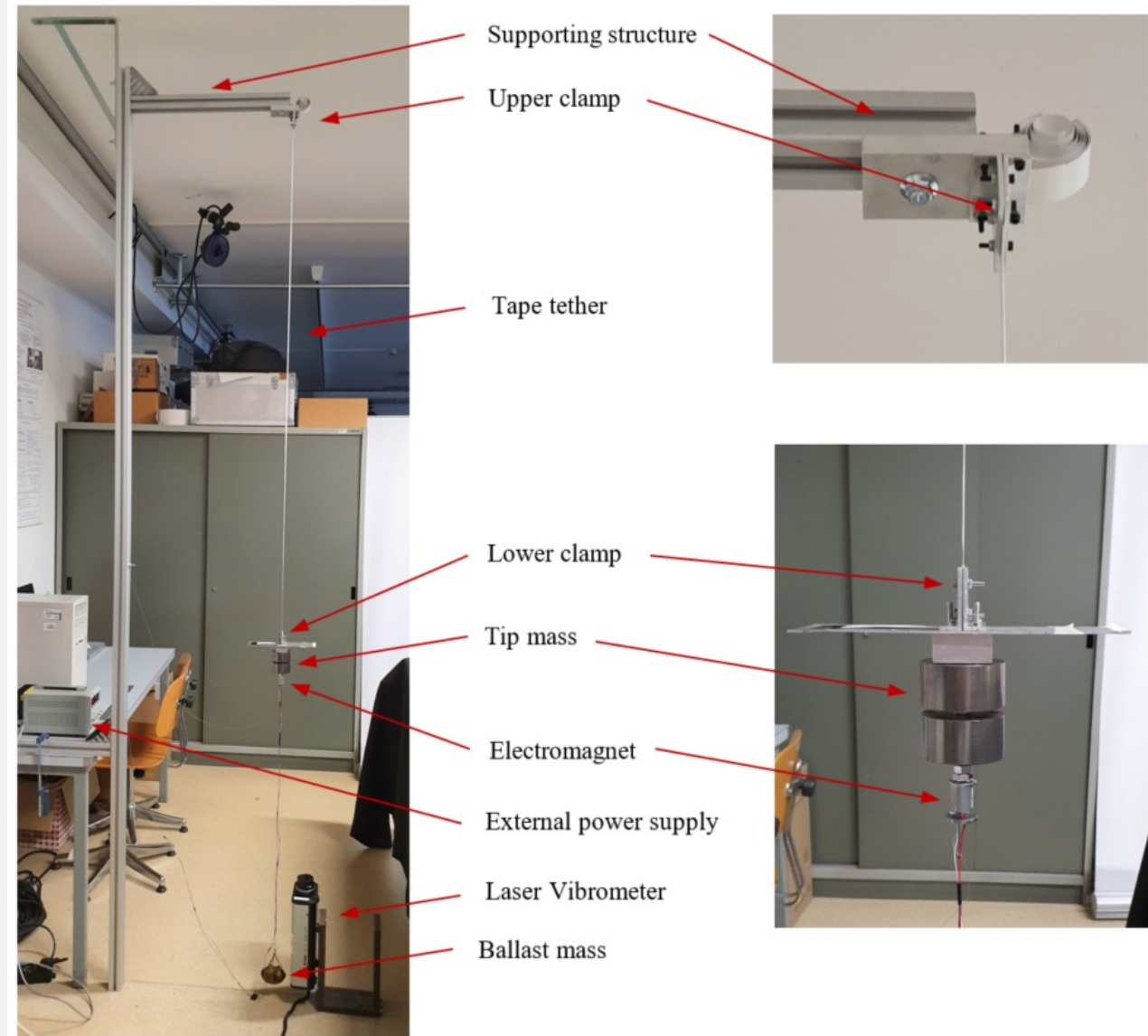
MEASUREMENT OF DAMPING COEFFICIENT

- The Mini Bionix II machine proved *not to have enough* displacement and force resolutions to estimate reliably the damping coefficients of short samples
- We adopted two alternative and independent measurements with different equipment:
 - *Laser vibrometer*: the tether sample is hanged vertically and put under tension with a weight. Other weights are then attached at the bottom and held by an electromagnet. When the electromagnet is deactivated the mass falls forcing the tape to oscillate. The oscillation amplitude is measured by a laser vibrometer. The damping coefficient is estimated from the analysis of the oscillation amplitude decay
 - *Bose ElectroForce[®] machine*: this machine differs from the Mini-Bionix II because it uses electromagnetic forces as opposed to hydraulics. The Bose has a smaller dynamic range of 400 N max, a position accuracy of 1 micron, and a force resolution better than 0.1 N

LASER VIBROMETER SETUP

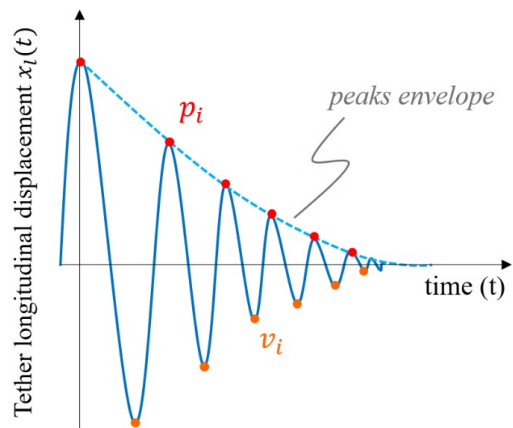
- The tape is hanged from a support at one end and kept in tension by a set of weights at the other end.
- Through an electromagnet other weights are attached at the bottom. The weights can be suddenly released with a switch putting the system into oscillation.
- A laser vibrometer is used to measure the oscillation of the plate after release
- The damping of the oscillation follows an exponential decay described by $x(t) = X e^{-\zeta \omega_n t}$ from which the damping coefficient can be derived as

$$c = 2\zeta \sqrt{EAm/L}$$



ALUMINUM WITH PV CELLS – LASER VIBROMETER

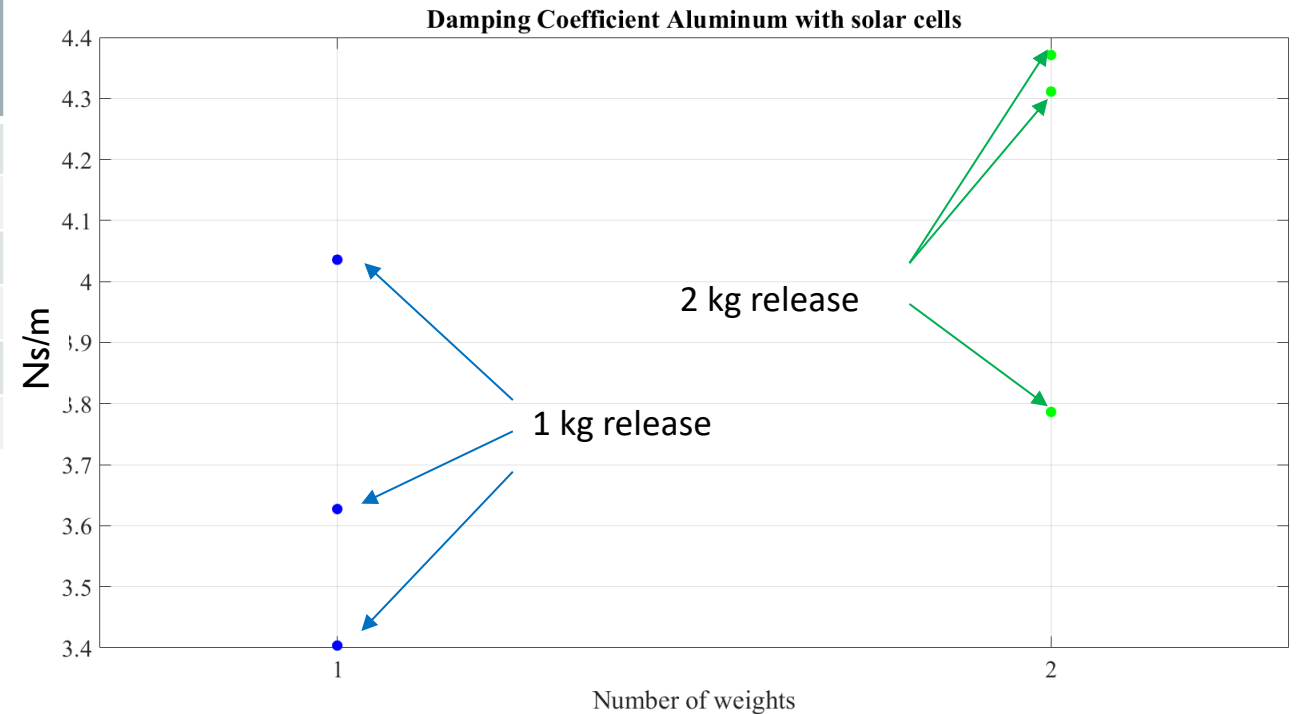
# Test	Length [cm]	# Weights	Damping coefficient [Ns/m]	ζ ratio
1	143	1	4.04	0.00691
2	143	1	3.40	0.00586
3	143	1	3.63	0.00624
4	143	2	4.37	0.00754
5	143	2	4.31	0.00743
6	143	2	3.79	0.00653



$$p(t) = a e^{-\zeta \omega_n t}$$

$$\omega_n = \sqrt{\frac{E A}{m L}}$$

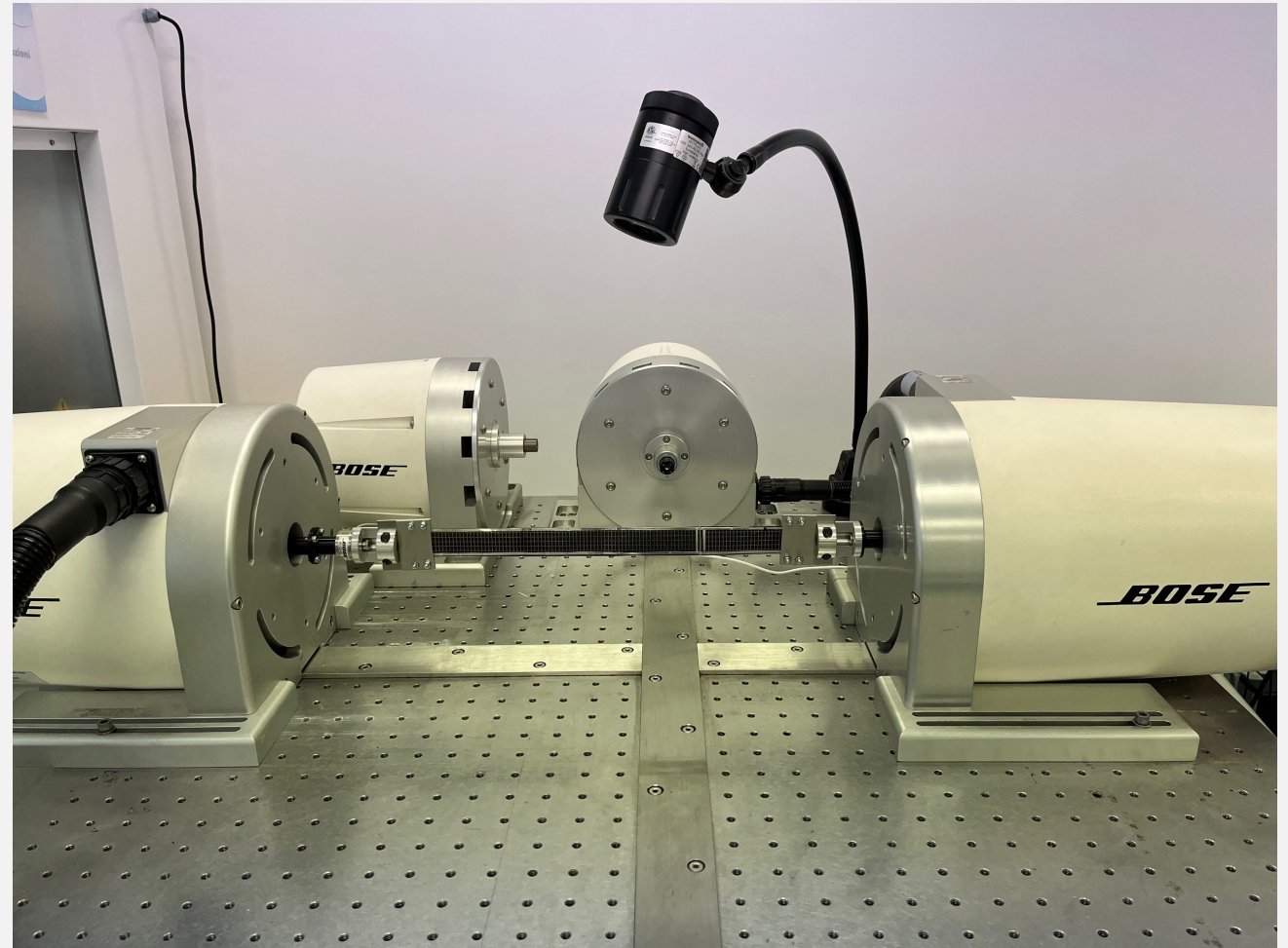
Damping coefficient estimated from oscillation decay



With this method the *mean value* of damping coefficient is in the range 3.7 – 4.2 Ns/m

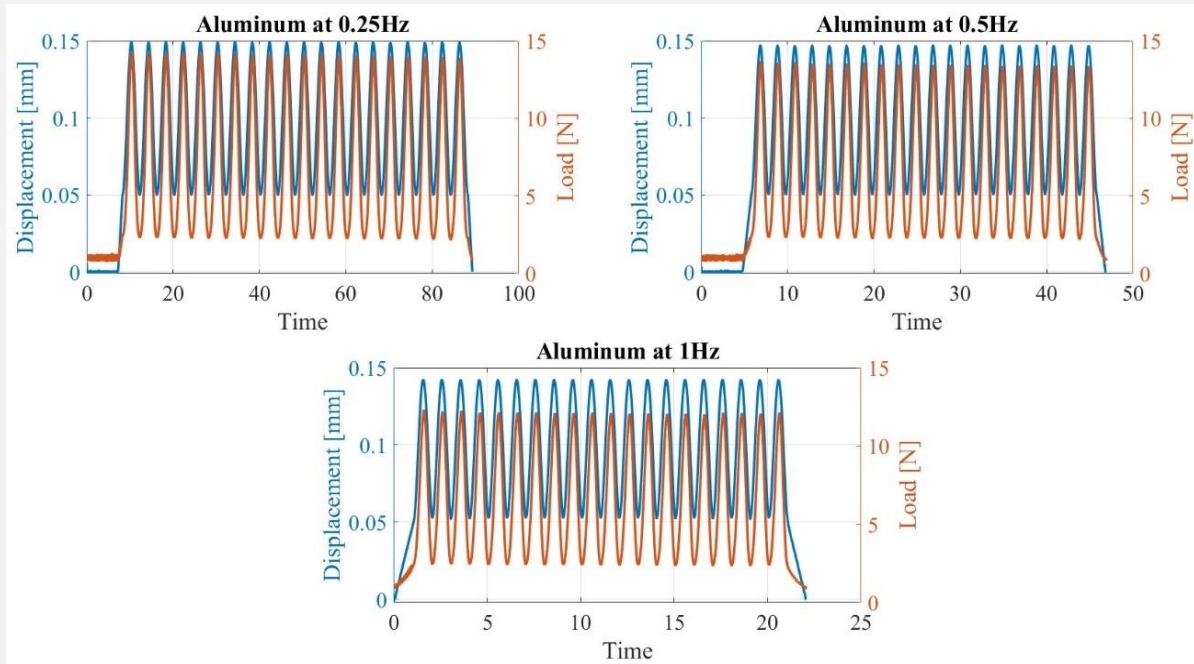
TESTS WITH BOSE ELECTROFORCE® MACHINE

- *Bose ElectroForce*® machine utilizes electromagnetic forces to generate very accurate displacement profiles. The force dynamic range is 400 N with a position accuracy of 1 micron and a force resolution better than 0.1 N
- This equipment was used to generate many hysteresis cycles at the desired frequencies and compute the damping from the energy dissipated in those cycles
- Samples tested
 - 1 bare Aluminum tape, 30-cm long with loading at frequencies of 0.25Hz, 0.5Hz and 1Hz
 - 5 Aluminum tape with solar cells, 30-cm long with loading at frequencies of 0.25Hz, 0.5Hz, 1Hz

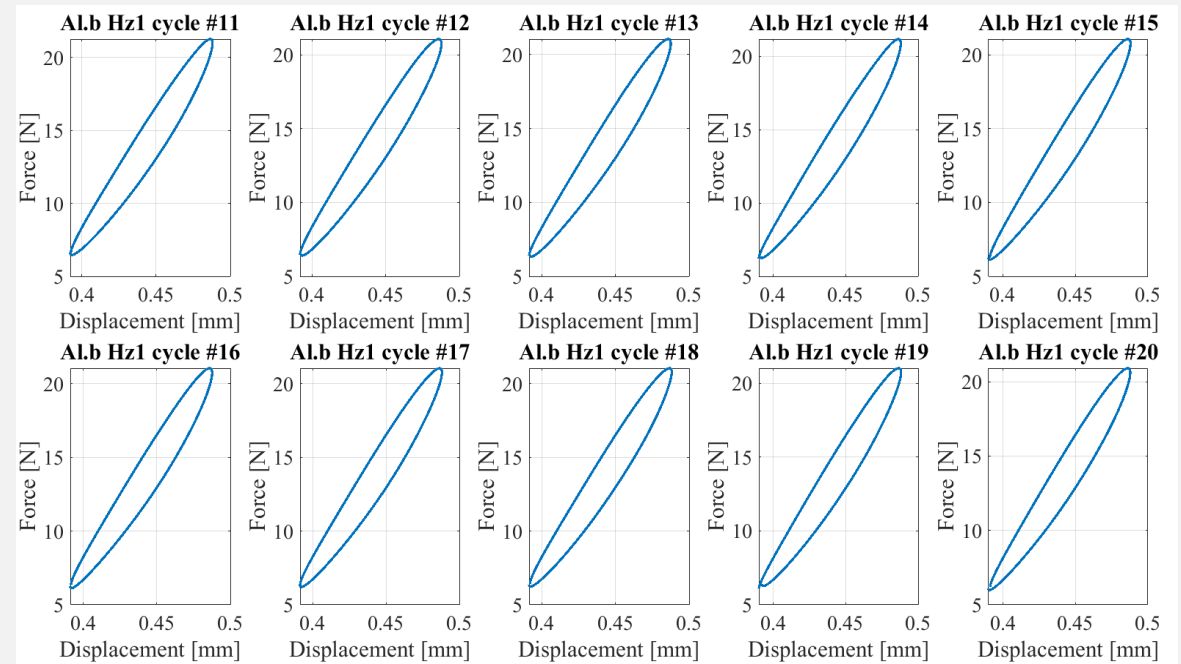


A SAMPLE OF HYSTERESIS CYCLES

Raw data from Bose ElectroForce©



Set of cycles of Aluminum tape with solar cells at 1Hz after filtering

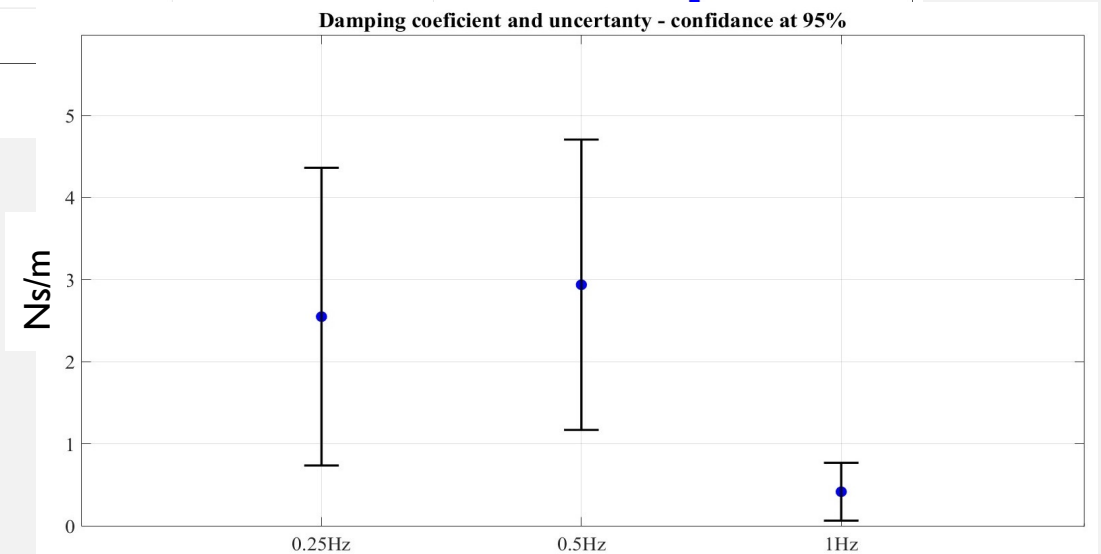
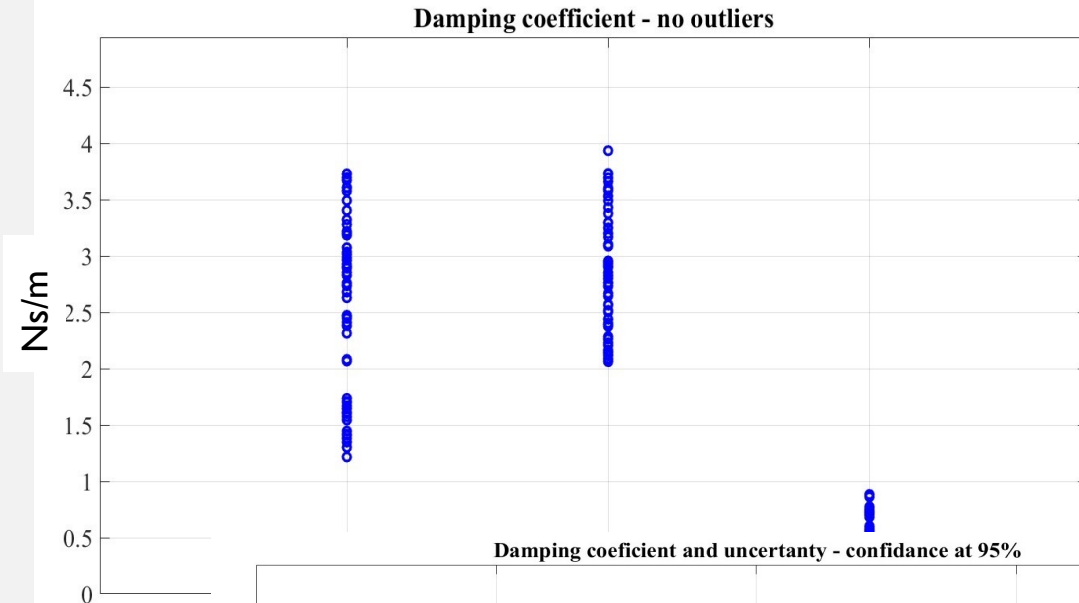


ESTIMATION OF DAMPING COEFFICIENT FROM HYSTERESIS

- Dissipated energy per cycle (with c the damping coefficient)

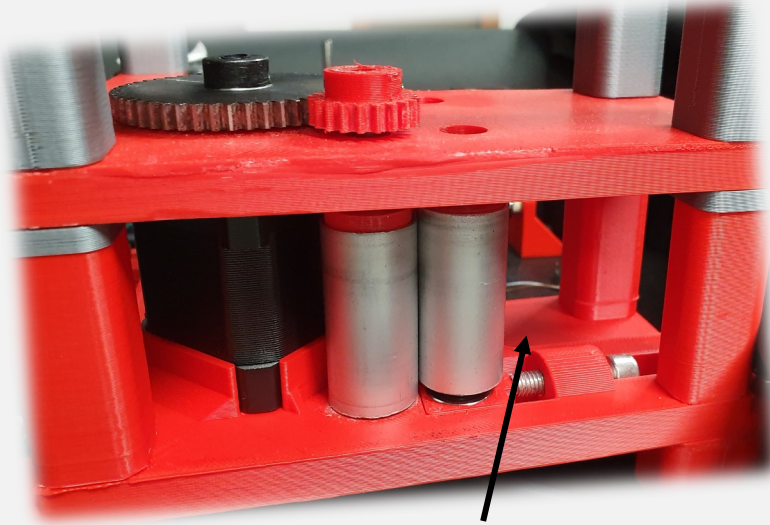
$$E_d = \pi \cdot c \cdot \omega \cdot y_{max}^2$$

- Results are well in line with those obtained from the technique with *Laser Vibrometer*
- *Mean value* of damping coefficients is in the approx. range 2 – 3 Ns/m, excluding the data at 1 Hz that does not match the test with Vibrometer



Average values of damping coeff. with 95% uncertainty bands

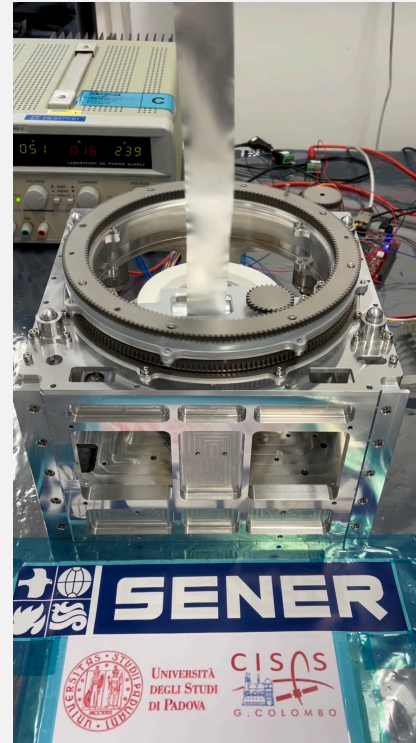
DEPLOYMENT TEST AND ESTIMATION OF CELLS PERFORMANCE



Spring-loaded drive-pulleys of breadboard



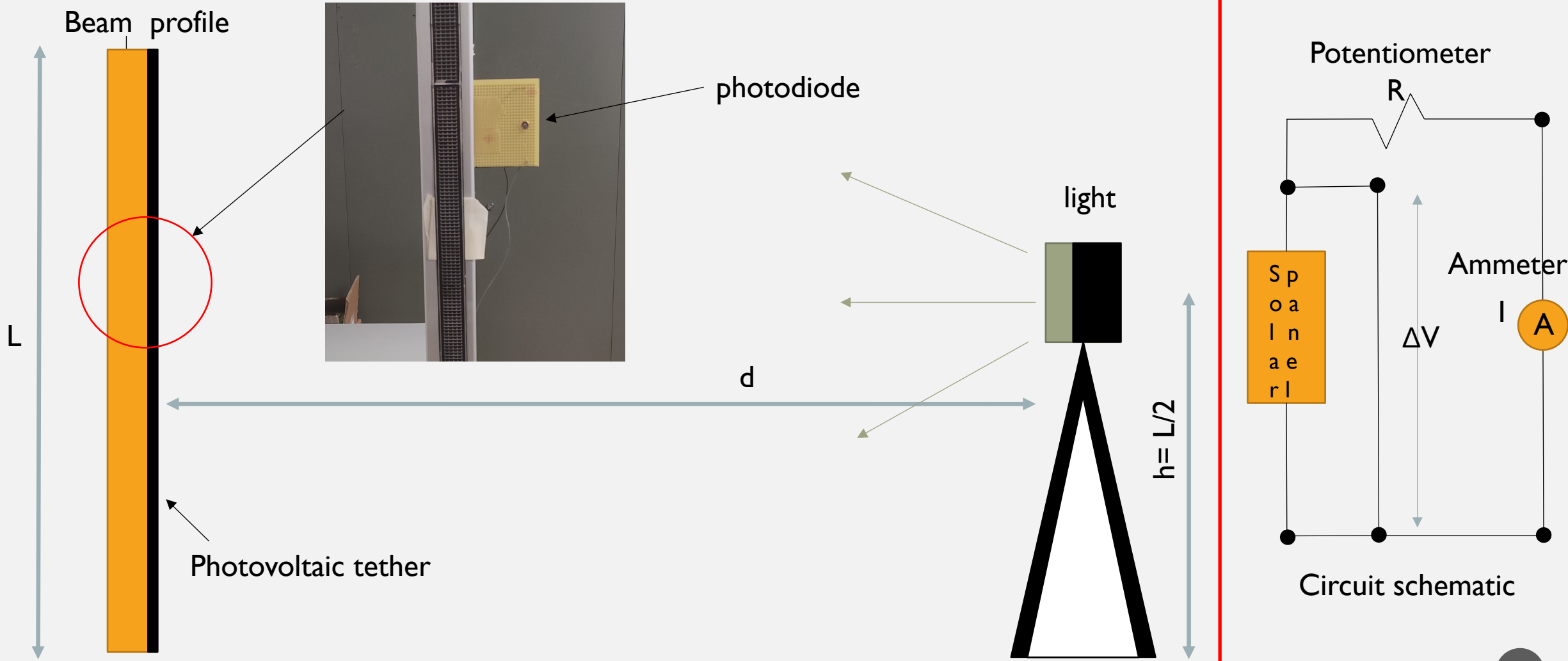
3-m-long pv tape sample



E.T.PACK deployer

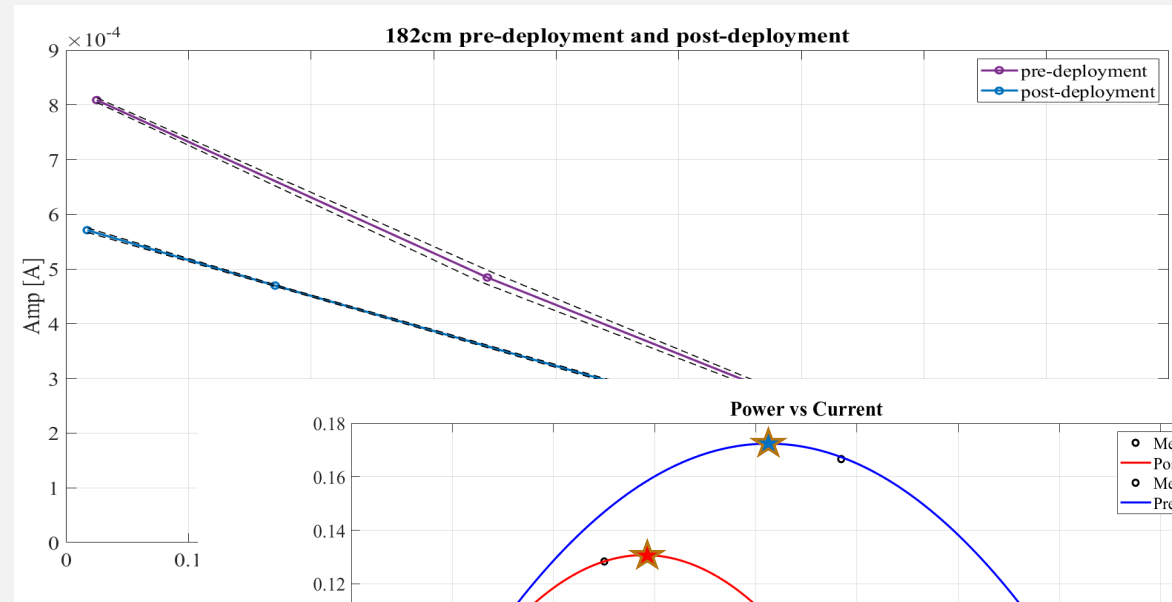
- A 3-m-long tape with pv cells was deployed through the drive pulleys of the deployer breadboard
- Tape was inspected for damages (none detected)
- Power produced by the sample under controlled illumination was measured

PHOTOVOLTAIC PERFORMANCE - SETUP

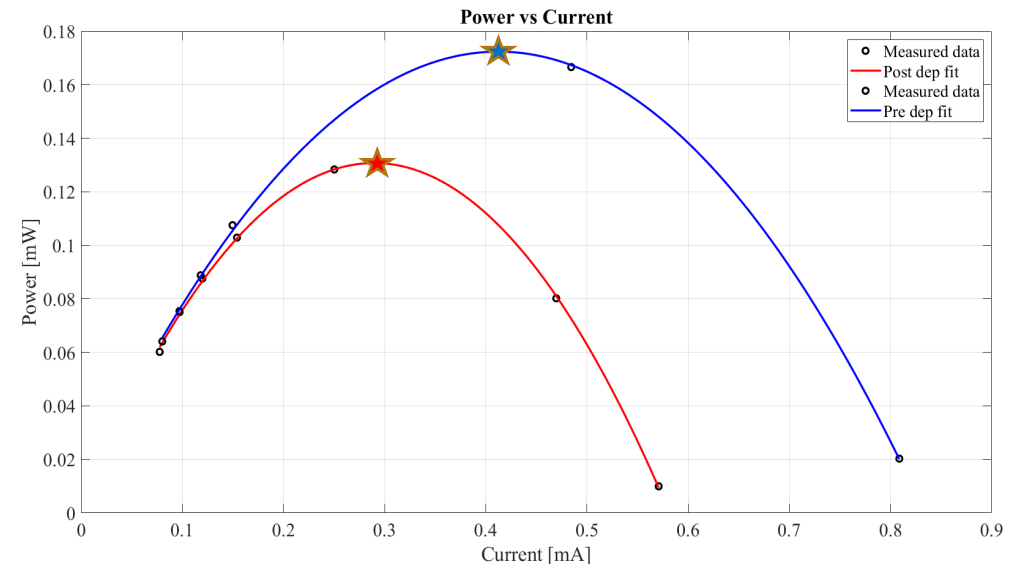


RESULTS – POWER PRODUCED PRE & POST DEPLOYMENT

- **Results summary**
- Deployment through the drive pulleys moderately affects the PTS performance
- In the case analyzed we detected a maximum loss of peak power post-deployment of 24% when compared to the pre-deployment performance
- Note that drive pulleys have a hard metallic surface and were not designed for handling the pv cells
- Drive pulleys could be modified to handle “more softly” the pv cells



I-V curve v
with light s



Power vs. current pre & post deployment

CONCLUSIONS

- Performance of the photovoltaic tape is moderately influenced by deployment
 - ✓ A peak power reduction of 24% was measured between before and after the BPT deployment through the drive pulleys
- Tape with pv cells was not visually damaged after deployment
- Note that drive pulleys could be redesigned to handle the tape “*more softly*”
- The axial strength of either substrates – Aluminum and Stainless Steel – is well above the required value of 10 N (with ample safety margin)
- Aluminum substrate is preferable to Stainless Steel because of its lighter mass
- Damping coefficient of the pv tape is low and of order 2-4 Ns/m
- The system will require additional damping like for example a passive damper in series to the tape as it is currently being developed for the E.T.PACK system



THANK YOU FOR THE ATTENTION

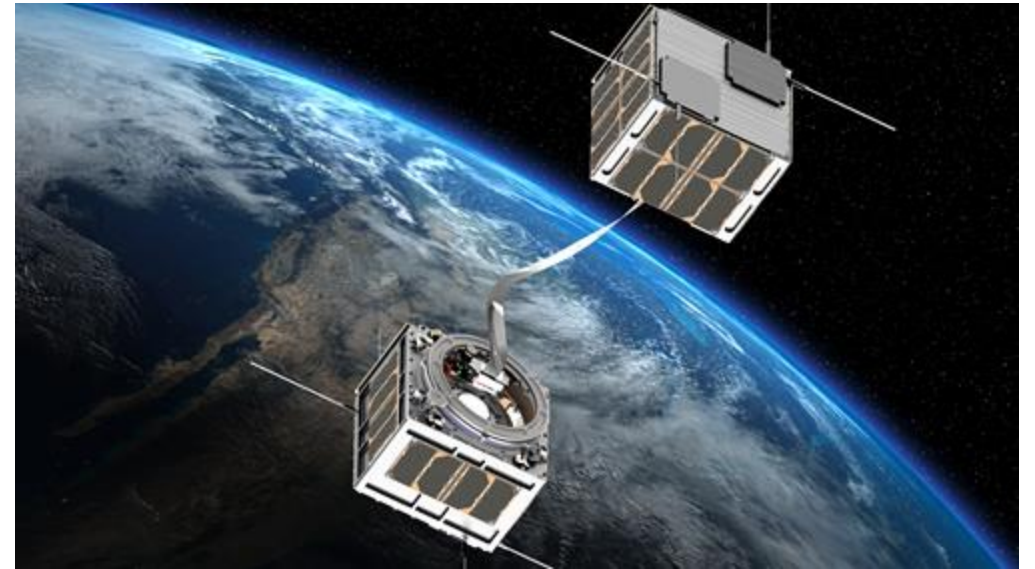
We would like to acknowledge the contributions at the University of Padova of Prof. Nicola Petrone and Giuseppe Zullo for their work with the pull tests on the Bionix II machine and Prof. Piero Pavan for the tests with the Bose ElectroForce© machine. We sincerely thank them for their essential help and advice.

Questions ?

A Consumable-less Propulsion System Based on a Bare-Photovoltaic Tether

Universidad Carlos III de Madrid, TU Dresden,
University of Padova and SENER Aeroespacial

ESA Contract No. 4000135893/ 21/ NL/ GLC/ ov



INDEX

- **Coordination (UC3M)**
- Bare-Photovoltaic Tether (BPT) Design (UC3M)
- BPT Manufacturing and Electrical Testing (TUD)
- BPT Mechanical Testing (UNIPD)
- BPT Modelling and Simulation (UC3M)
- BPT Modelling Roadmap (SENER)
- Open Discussion

The Bare-Photovoltaic Tether (BPT)

Goal of the Project

“demonstrate the feasibility of the BPT and assess its potential impact on EDT technology”

Objective of the Project

- Identify the most promising pv technology and make an electrical and mechanical design of the bare-pv tether.
- Perform a detailed electrical and mechanical characterization.
- Incorporate a bare-pv model into a mission analysis software and study its performances.



Coordination

WP		Task	Partner	M1	M2	M3	M4	M5	M6	M7	M8	M9	M10	M11	M12
				PHASE A				PHASE B							
1000	1100	User Requirements	UC3M/TUD/UniPD/SENER												
	1200	Electrical Design	UC3M/TUD												
	1300	Mechanical Design	SENER/UniPD												
2000	2100	Solar cell trade-off	TUD												
	2200	PV segment Procurement	UC3M/TUD												
	2300	PV-bare tether assembly	SENER												
3000	3100	Test Plan	TUD/UniPD												
	3200	Electrical and Thermal Testing	TUD												
	3300	Mechanical Testing	UniPD												
4000	4100	Software Development	UC3M												
	4200	ETPACK IOD application	UC3M/UniPd												
	4300	Results summary and design update	TUD/UC3M/UniPD/SENER												
	4400	PV development Roadmap	UC3M/SENER												
Milestone								MS1	MS2	MS3					
Event				KoM				PM1	PM2	PM3				FM	
Deliverable								D1.1	D2.1	D3.1				D4.1	

- The work plan was implemented following the Gantt chart with no major issue.

Coordination

Code	Name	WP	Type
D1.1	Requirements and preliminary design of a bare-pv tether	1000	Document
D2.1	Samples of PV tethers and PV-Bare Tethers	2000	Hardware
D3.1	Electrical and mechanical characteristics of a bare-pv tether	3000	Document
D4.1	Performances, and Development Plan of a Bare-PV Tether.	4000	Document



Table 6. Technical Deliverables

Other information sent to ESA

- Final Report
- Executive Summary
- Final Presentation slides
- Illustration of the activity in one self standing image
- 5 min video summarizing the main results of the activity.

Coordination

Event	Type	Description	Date	Deliverable/ Output
KOM	Kick Off Meeting	Videoconference	KO	None
PM1	Progress Meeting	Videoconference	KO+3	D1.1
MS1	Milestone	End of PHASE A	KO+4	None
MS2	Milestone	Bare-PV Tether assembled	KO+6	D2.1
PM2	Progress Meeting	Videoconference	KO+6	None
MS3	Milestone	Bare-PV tether model implemented in BETsMA v2.0	KO+8	None
PM3	Progress Meeting	Videoconference	KO+10	None
MS4	Milestone	PV-Tether is Characterized electrically and mechanically	KO+11	D3.1
FM	Final Meeting	Presential (ESA Premises)	KO+12	D4.1



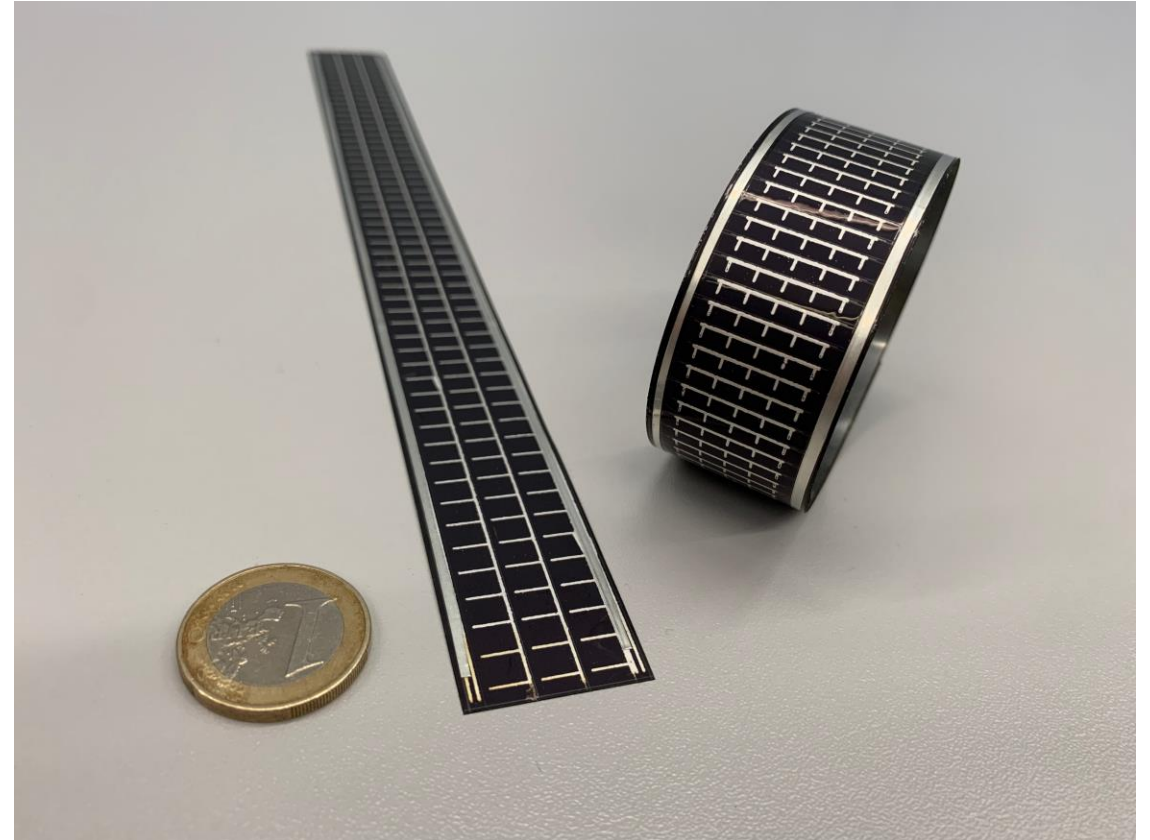
Table 9. Event and Milestone Planning

Coordination

Problem Areas and Risks identified in the proposal	Solution implemented in the project
Procurement of the pv-cells	Sunplugged was able to manufacture all the samples order by the team
Personnel availability	Young team members were hired and worked fully focussed on the Project.
Resilience to Micrometeoroid impact of the pv-segment	The new design allows to decouple the pv cells from the EDT.
Joint between the pv tether and the bare tether	SENER proposed a solution in case it is needed. However, the BPT design does not require any joint (pv cells are printed in the bare Al)
Endurance in space and storage on the ground of the pv segments	Testing activities showed that the BPT is feasible. High vacuum has a regenerative effect.

Conclusions of the project

- Design, manufacturing and testing activities showed that the BPT concept is feasible.
- Simulation work revealed that the pv segment enhances EDT performances.
- The combination of thin-film solar cells and EDT technology can be used to prepare compact systems to provide in-space propellant-less propulsion and power.
- The BPT is compatible with the E.T.PACK-F IOD, which is the perfect opportunity to increase the TRL.



Sample of Bare Photovoltaic Tether.

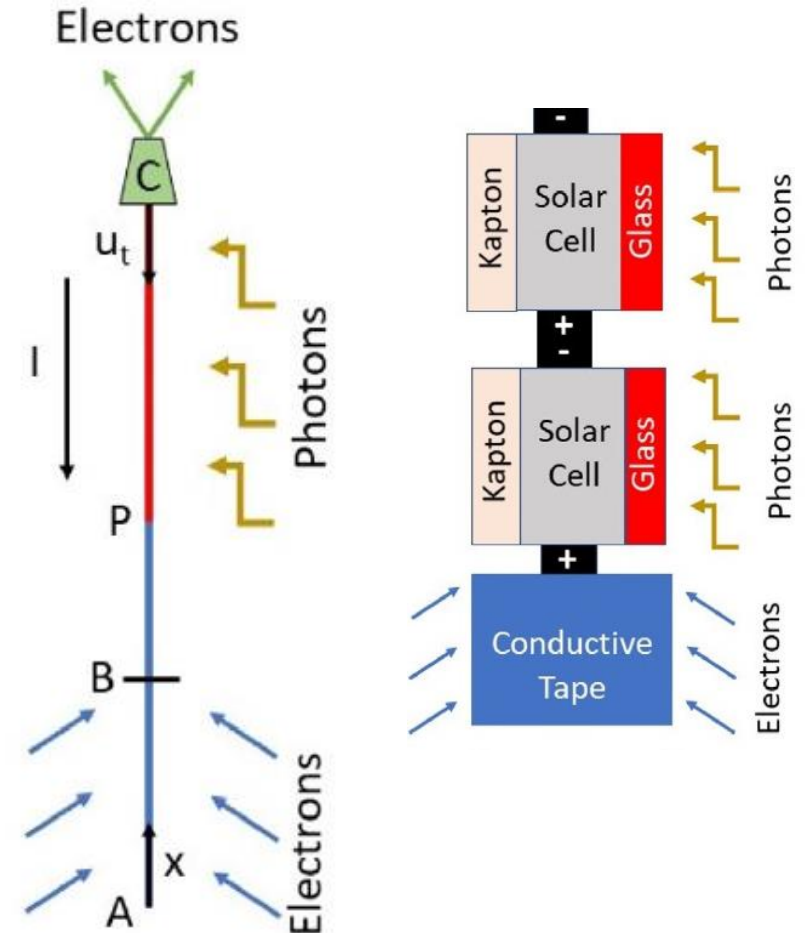
INDEX

- Coordination (UC3M)
- **Bare-Photovoltaic Tether (BPT) Design (UC3M)**
- BPT Manufacturing and Electrical Testing (TUD)
- BPT Mechanical Testing (UNIPD)
- BPT Modelling and Simulation (UC3M)
- BPT Modelling Roadmap (SENER)
- Open Discussion

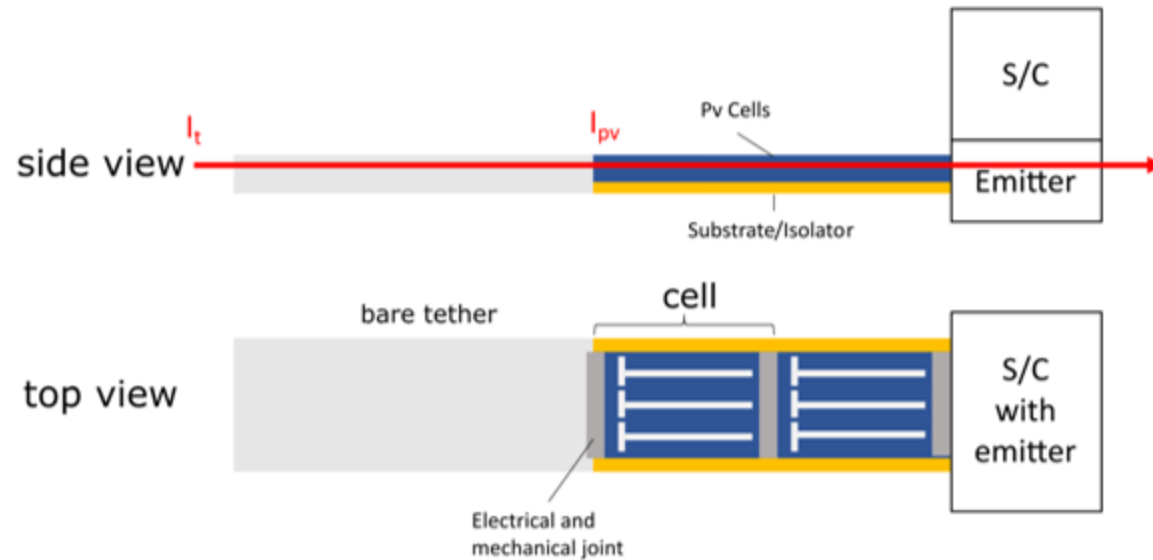
The Bare-Photovoltaic Tether (BPT)

- The original design of the BPT proposed in [1] has some drawbacks/issues:
 - A failure of the photovoltaic tether segment (PTS) make the tether fail.
 - Bypass diodes are needed to allow the current flow in shadowed cells.
- 2 alternative configurations were proposed.

[1] M. Tajmar and G. Sanchez-Arriaga, *A bare-photovoltaic tether for consumable-less and autonomous space propulsion and power generation*, Acta Astronautica 180, 2021.



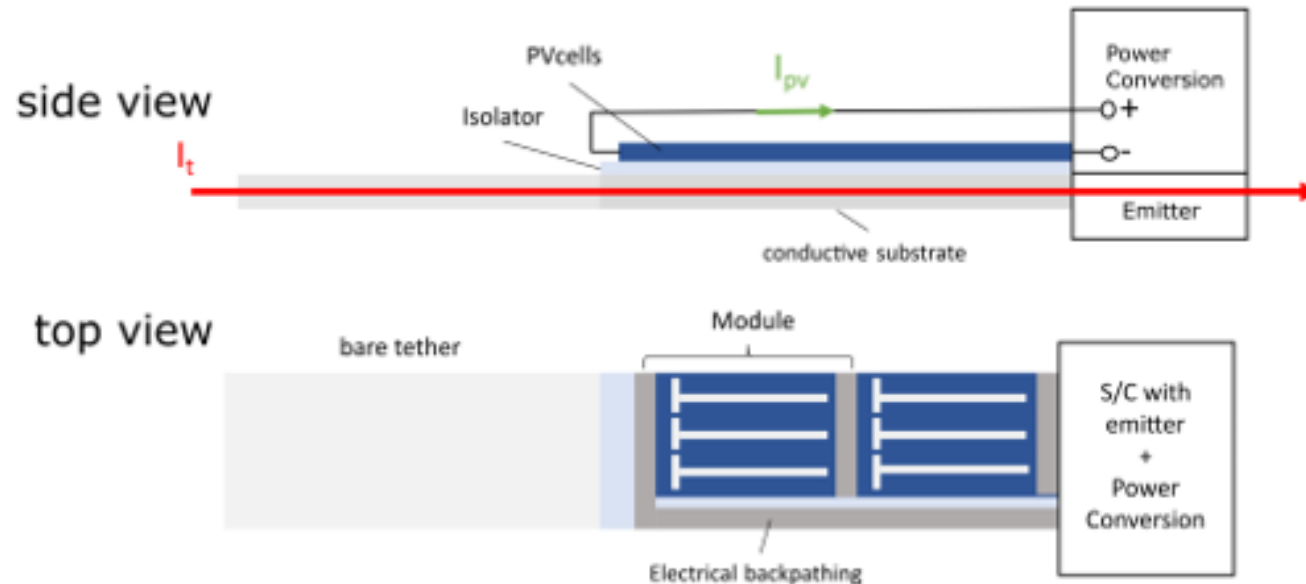
BPT Design: Configuration 1



Characteristics

- The current collected by the bare tether passes through the pv cells.
- Fully electrical coupling between the pv-cells and the bare tether.
- High voltage gain and constant current.
- Bypass diodes are needed.
- The area used to harvest power is maximized.

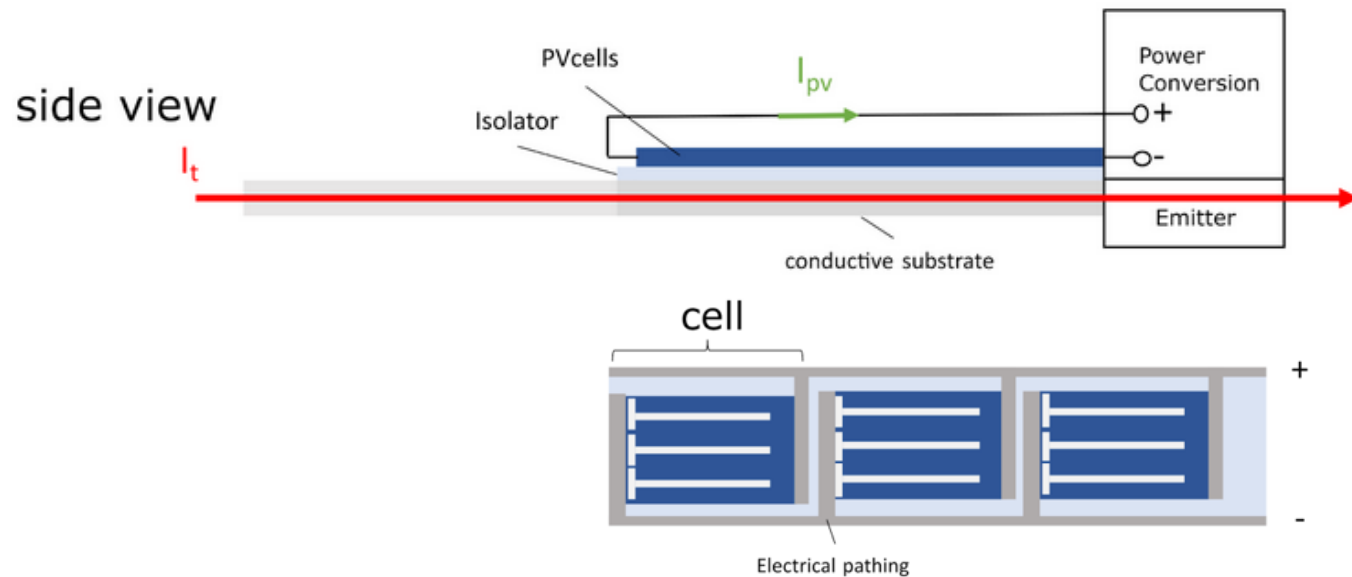
BPT Design: Configuration 2



Characteristics

- The pv cells and the bare tether are separated by a layer of insulation.
- The pv cells are organized into cell/submodules that are connected in series.
- The submodules are connected to one electrical path.
- The two poles are at the S/C

BPT Design: Configuration 3



Characteristics

- The pv cells and the bare tether are separated by a layer of insulation.
- The pv cells are organized into cell/submodules that are connected in parallel.
- The submodules are connected to two electrical paths.
- The two poles are at the S/C

BPT Design: Trade-off

	Configuration 1	Configuration 2	Configuration 3
Characteristics	Series connection	Series connection	Parallel connection
	Current collected passes through the cells Fully coupled bare/pv	Current collected passes through the substrate Switchable bare/pv coupling Ordered samples with and without diodes	Current collected passes through substrate Switchable bare/pv coupling Ordered samples with and without diodes
Advantages	High voltage gain and constant current	High voltage gain and constant current Can harvest power with pv segment	Can harvest power with pv segment No diodes needed
Drawbacks	Use of diodes. System failure for a single shaded module	Use of diodes.	Two extra backpathing strings Current limited (thermal issues)
	Cannot harvest power	One extra backpathing string	

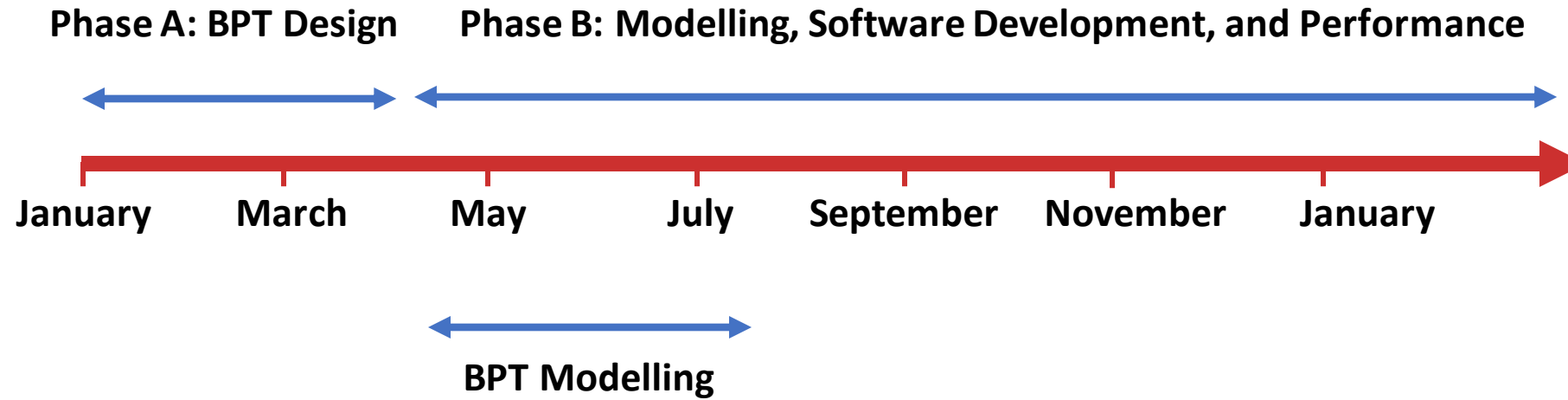
Conclusions

- Samples of Configuration 2 and 3 were manufactured and tested.
- Configuration 3 was selected.
- Configurations 2 and 3 are similar to a conventional solar panels, but with a lower efficiency (thin film solar cells).
- However, the lower efficiency is largely compensated by
 - a) The price of the thin film solar cells
 - b) Having two key subsystems (propulsion and power) integrated in the same device.
 - c) No additional support structure -> good specific power (W/kg)

INDEX

- Coordination (UC3M)
- Bare-Photovoltaic Tether (BPT) Design (UC3M)
- BPT Manufacturing and Electrical Testing (TUD)
- BPT Mechanical Testing (UNIPD)
- **BPT Modelling and Simulation (UC3M)**
- BPT Modelling Roadmap (SENER)
- Open Discussion

Schedule of the Activities at UC3M



1. BPT Modelling: Passive and Active Mode

Assumptions:

- Straight tether with High-bias Orbital-Motion-Limited (OML) current collection in bare segment
- No electron collection in the tether face that has the pv-cells.
- The power harvested by the pv cells inserted in the model as a power supply between the tether and the EE
- Ideal Cathode: emit any current for a given $V_c < 0$

Methodology:

- Compute semi-analytical solutions of the profiles.
- Verify the code
- Integrate the code in BETsMAv2.0

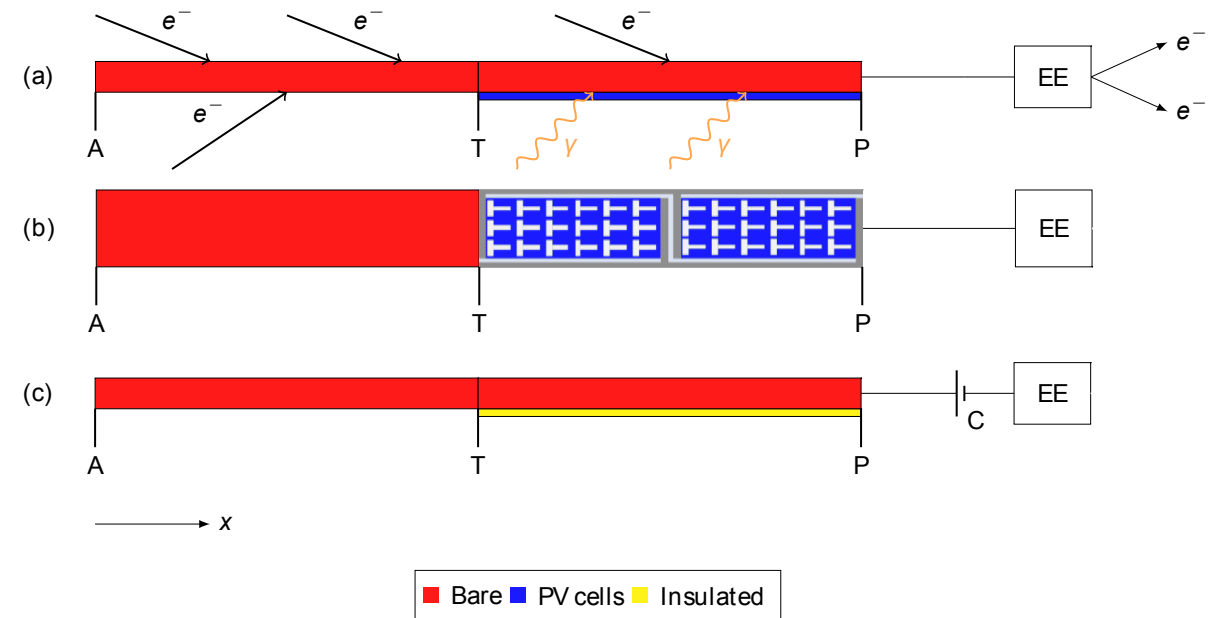


Figure 1. Sketch of a BPT in the Passive Mode

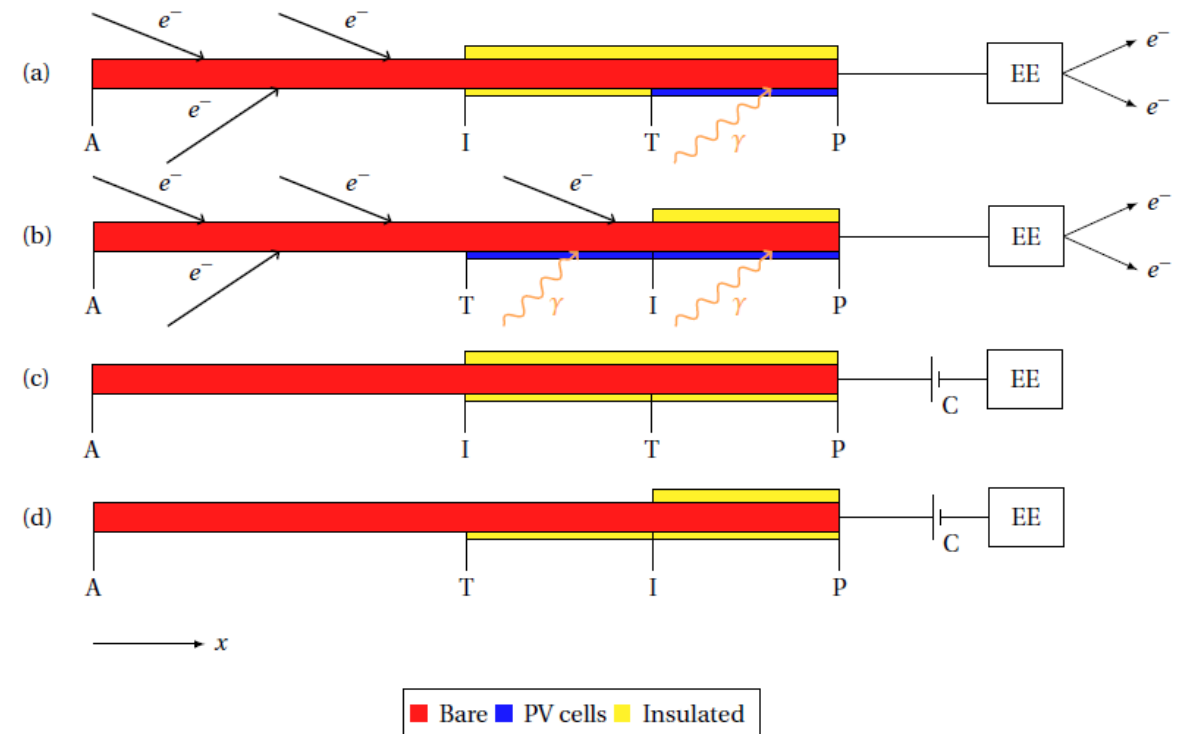
1. BPT Modelling: Passive and Active Mode

Assumptions:

- Straight tether with High-bias Orbital-Motion-Limited (OML) current collection in bare segment
- No electron collection in the tether face that has the pv-cells.
- The power harvested by the pv cells inserted in the model as a power supply between the tether and the EE
- Ideal Cathode: emit any current for a given $V_c < 0$

Methodology:

- Compute semi-analytical solutions of the profiles.
- Verify the code
- Integrate the code in BETsMAv2.0



1. BPT Model in the Passive Mode

Following standard methods in bare tether analysis we introduced the following dimensionless variables:

$$i \equiv I/I_*; \quad \phi \equiv V/V_*; \quad \xi \equiv x/L_*;$$

$$I_* \equiv E_m \sigma_b A_b; \quad V_* \equiv E_m L_* \quad L_* \equiv \left(\frac{2 A_b}{p_b} \right)^{2/3} \left(\frac{9\pi^2 m_e \sigma_b E_m}{128 e^3 N_\infty^2} \right)^{1/3}$$

The profiles depend on the following dimensions-less parameters

$$\xi_t \equiv \frac{L_b}{L_*} + \frac{L_{pv}}{L_*} \equiv \xi_b + \xi_{pv} \quad f_{pv} \equiv \frac{L_{pv}}{L_b + L_{pv}} \quad \phi_c \equiv \frac{V_c}{E_m L_*}$$

$$\alpha \equiv \frac{p_{pv}}{p_b} \quad \beta \equiv \frac{\sigma_b A_b}{\sigma_{pv} A_{pv}} \quad w_e \equiv \frac{W_e}{\sigma_b E_m^2 A_b L_*}$$

For a given tether segment, and after a proper rescaling, the normalized current (y) and voltage (u) are governed by

Parameter-Free ODE

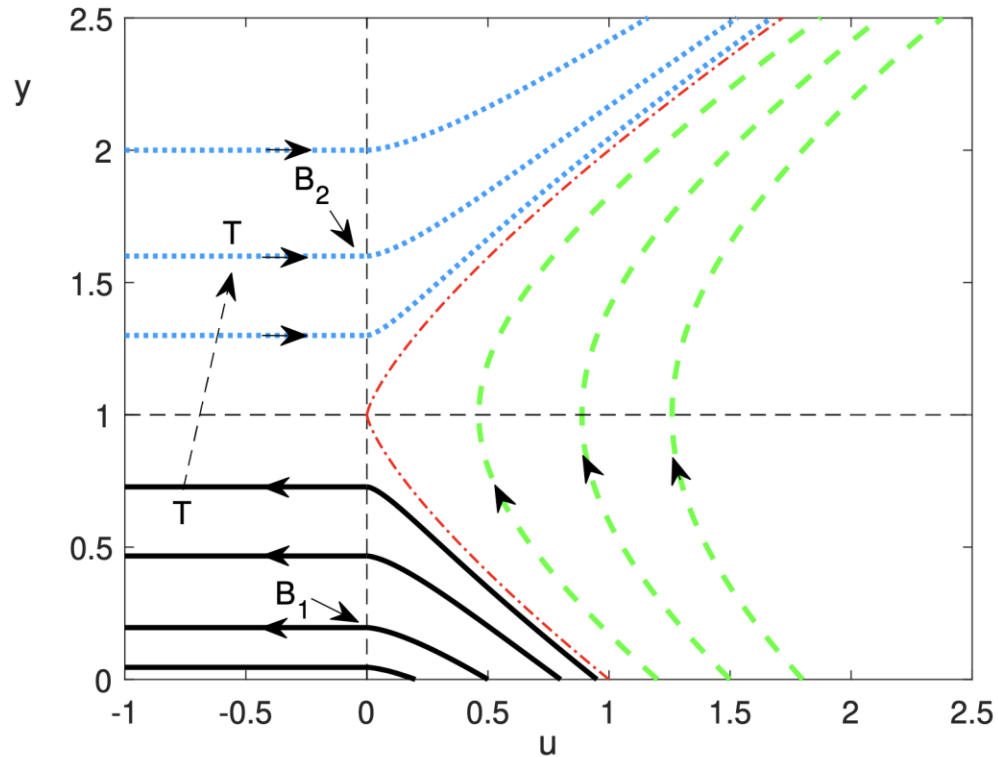
Valid for $\forall \xi < \xi_b + \xi_{pv}$

$$\frac{dy}{ds} = \begin{cases} 0 & \text{if } u < 0 \\ \frac{3}{4} \sqrt{u} & \text{if } u > 0 \end{cases}$$

$$\frac{du}{ds} = y - 1$$

$$u(s_0) = u_0; \quad y(s_0) = y_0$$

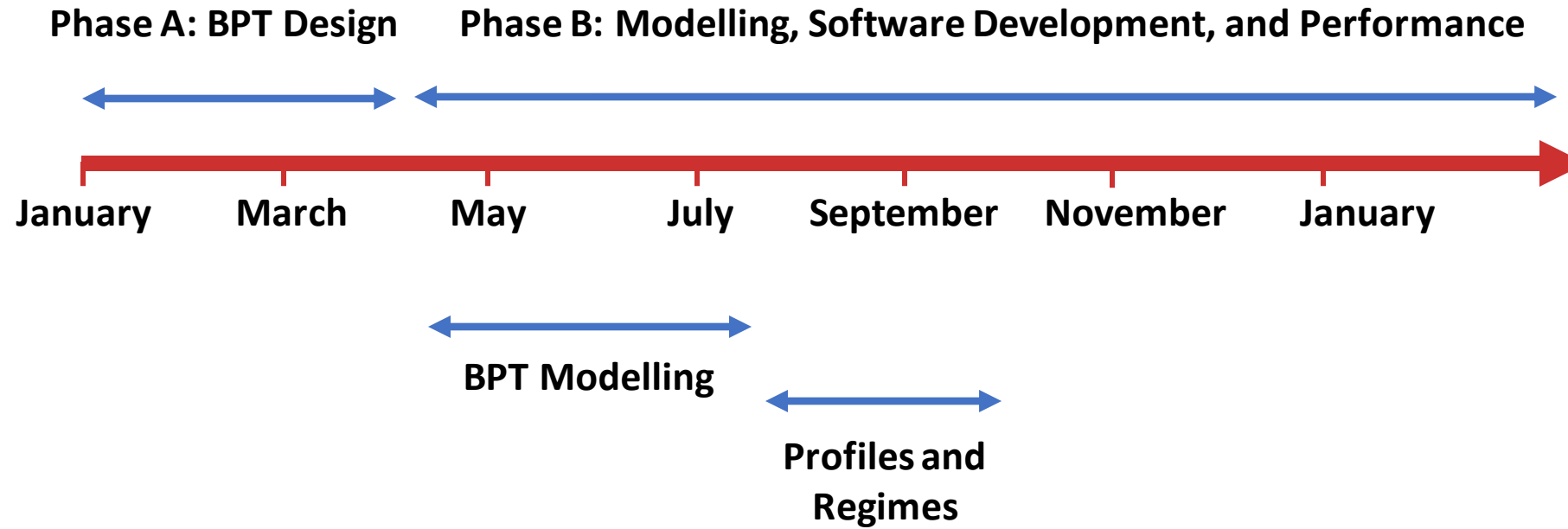
1. BPT Model in the Passive Mode



- BPTs profiles can explore any region in the current-voltage plane.
- Two zero bias points (B_1 and B_2) are possible.
- There are 4 solutions in phase space (one of them is new).

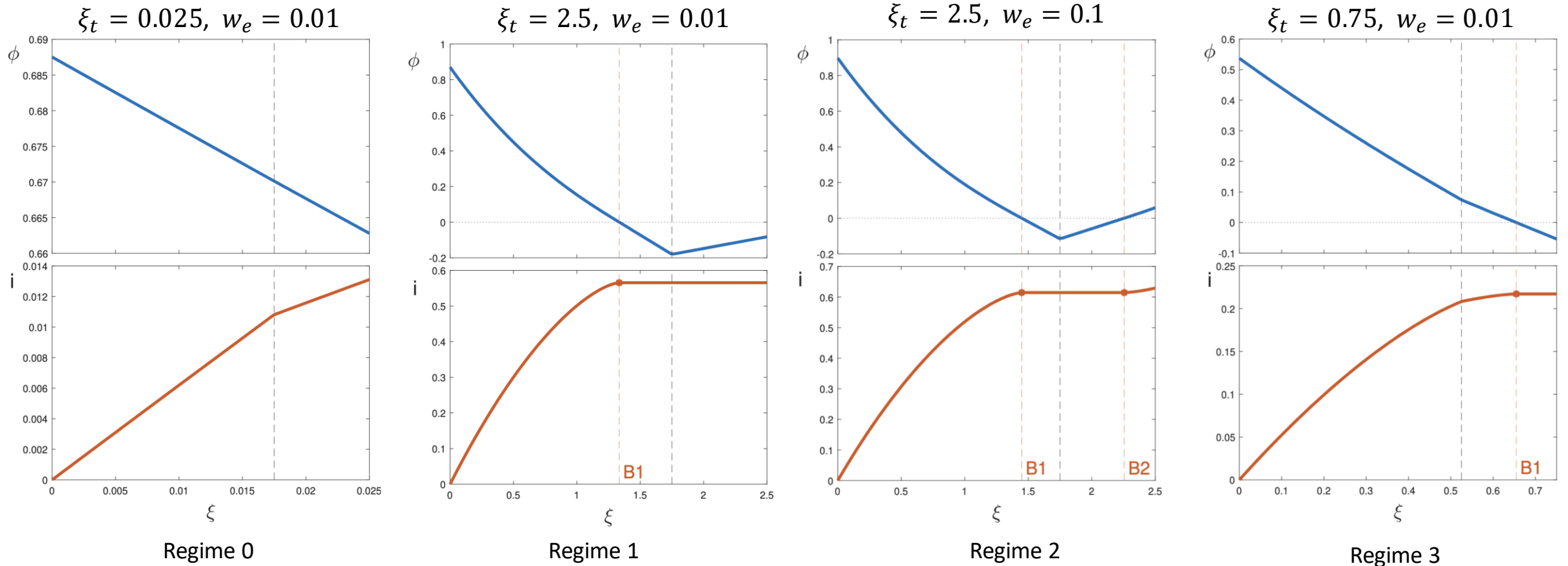
	Conventional bare tether
	Bare tethers + power supply
	Separatrix
	Tethers with different segments (like BPTs)

Schedule of the Activities at UC3M



2. BPT Profiles and Regimes

- Depending on the number and location of the zero-bias points, we identify four regimes.
- Example for $\alpha = 0.5$, $\beta = 2$, $f_{pv} = 0.3$, $\phi_C = -0.1$



Operational Regimes as a function of

$$f_{pv} \equiv \frac{L_{pv}}{L_b + L_{pv}}$$

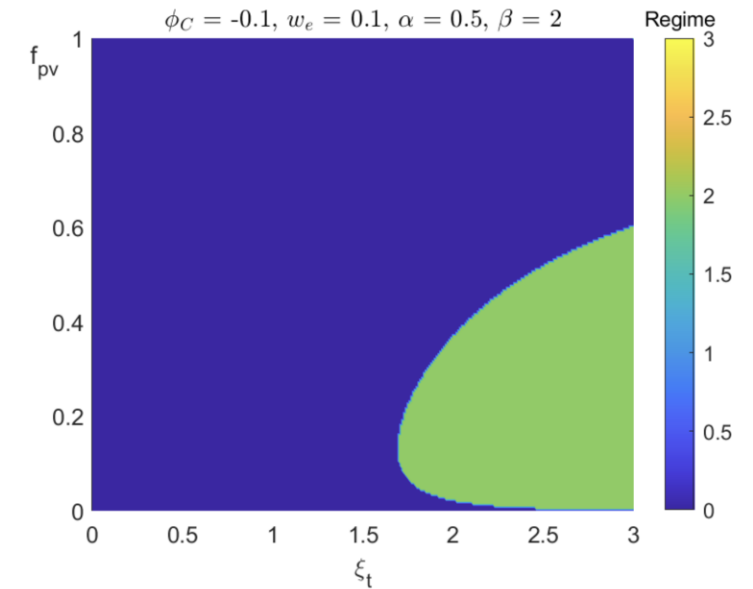
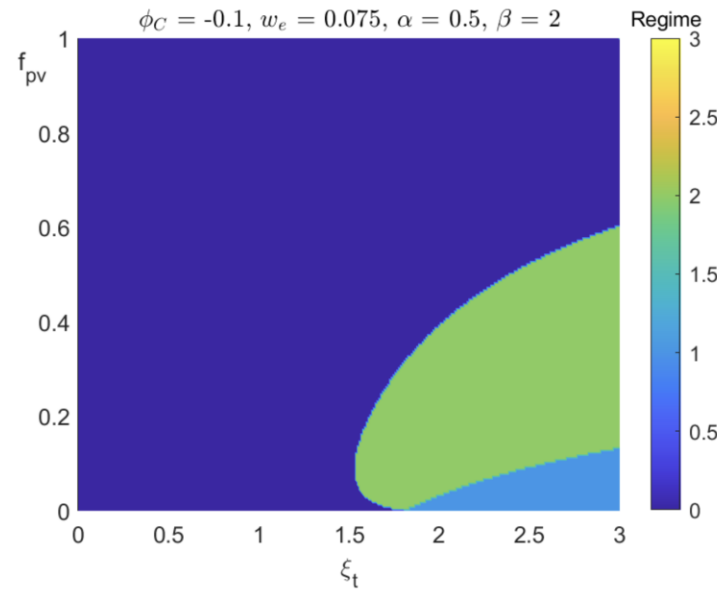
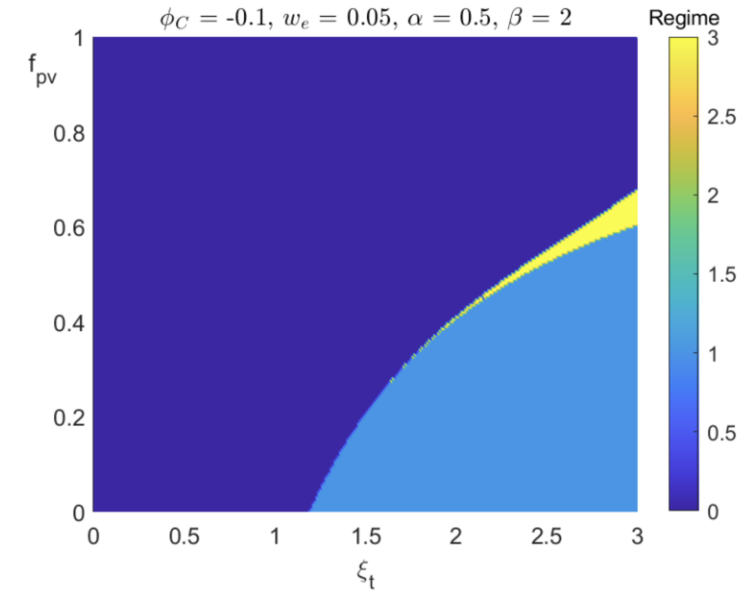
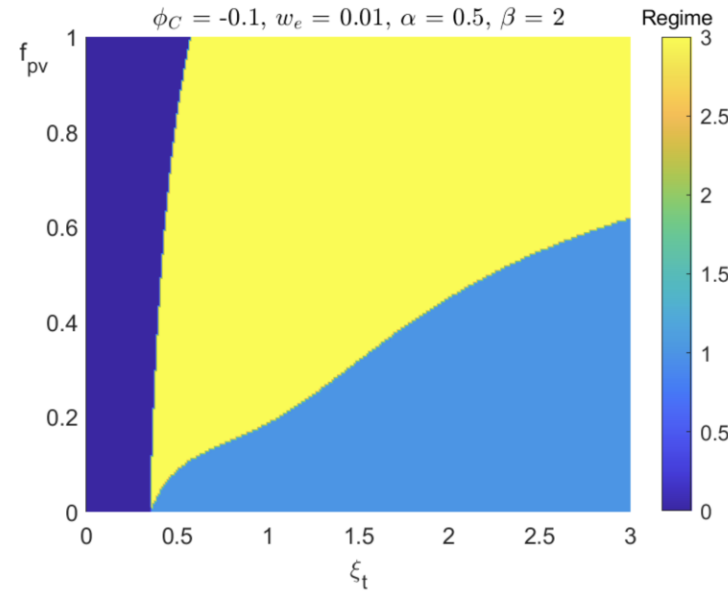
$$\xi_t \equiv \frac{L_b}{L_*} + \frac{L_{pv}}{L_*} \equiv \xi_b + \xi_{pv}$$

for

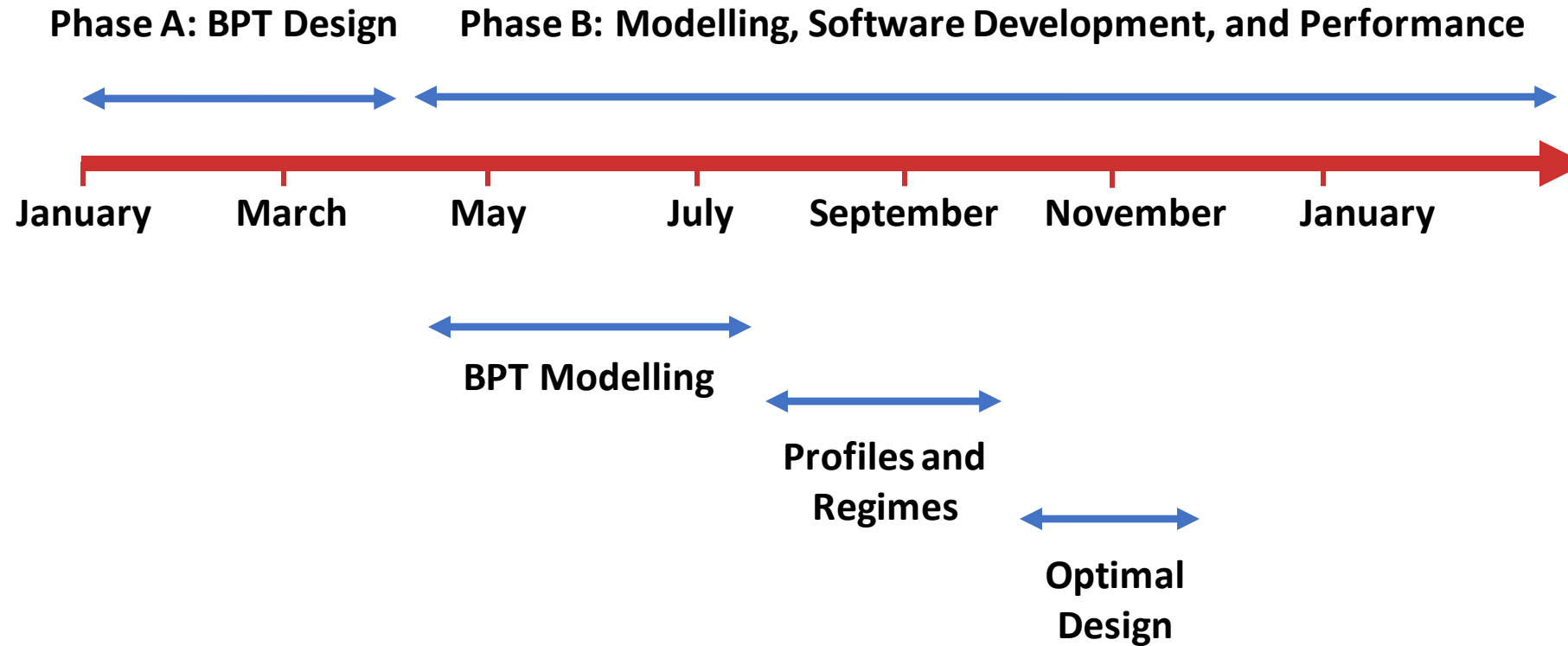
$$\alpha = 0.5, \quad \beta = 2, \quad \phi_C = -0.1$$

Conclusions:

- Since L_* depends on ambient variables, different regimes can be present for the same tether design.
- Our software is robust and it works for any regime.



Schedule of the Activities at UC3M



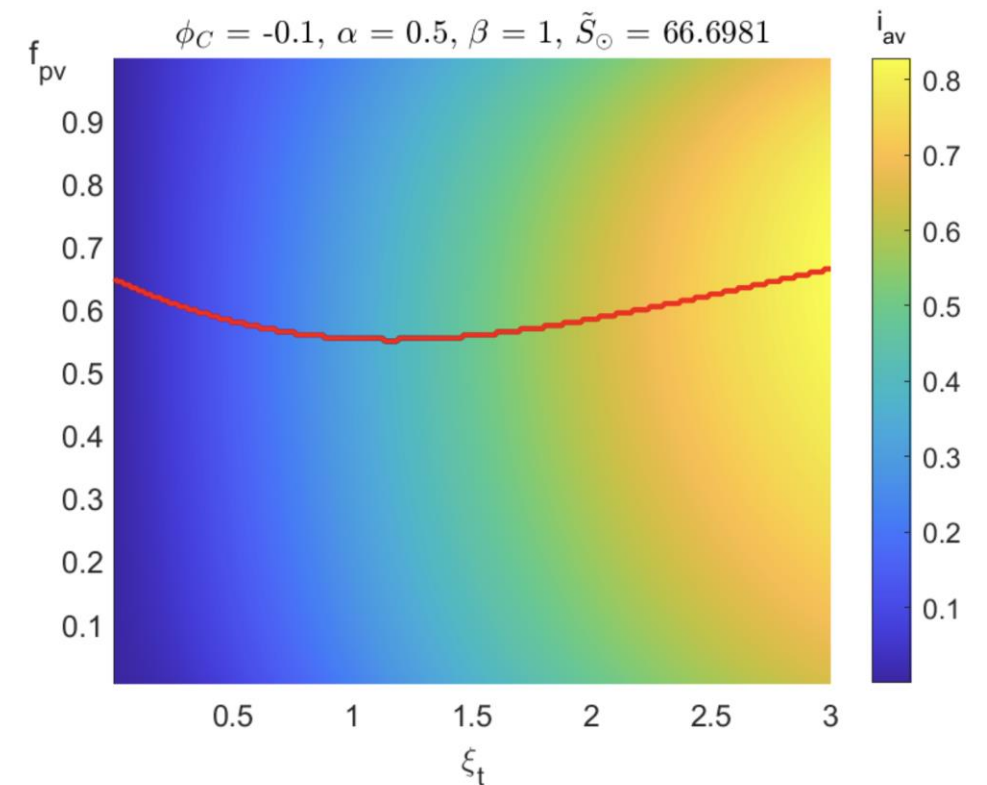
3. Optimal Design

- Take a fully autonomous system and fix tether thickness h_{pv}

$$w_e(f_{pv}, \xi_t) = \frac{\eta_{pv}}{\pi\beta} \frac{S_{\odot}}{\sigma_{pv} E_m^2 h_{pv}} \times f_{pv} \times \xi_t$$

- BPT design involves 3 parameters: L_t , f_{pv} , and w_t .
- To select these parameters optimally, we followed two approaches:
 - Optimize the tether efficiency (i_{av}) for a given set of ambient variables.

BPT with a Hollow Cathode



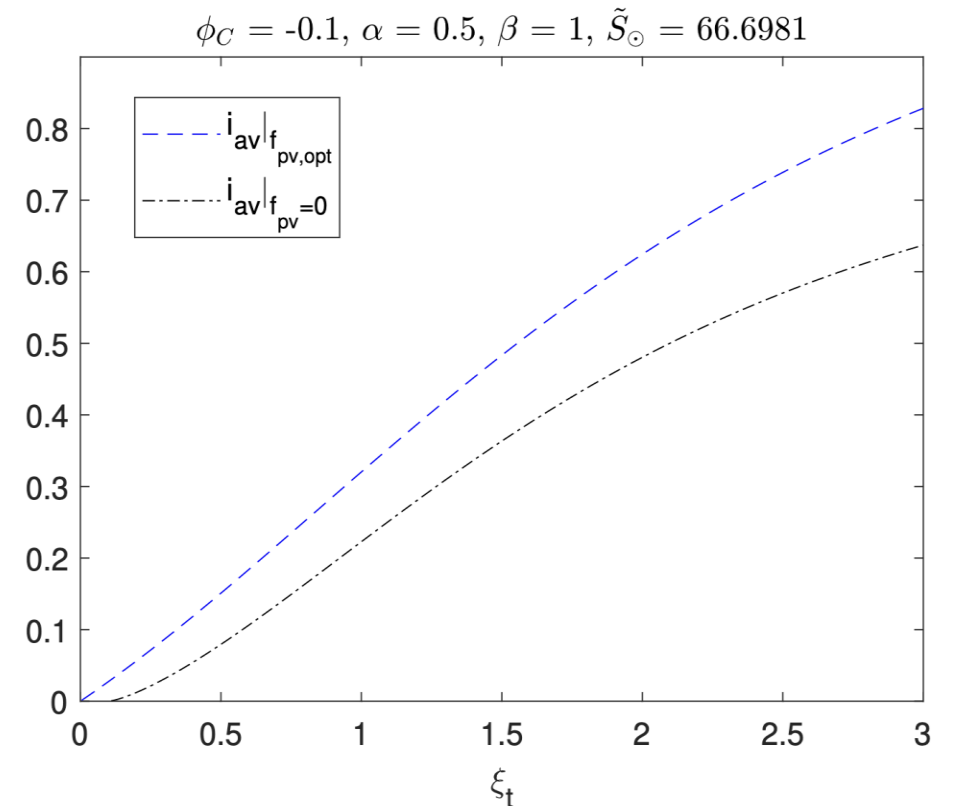
3. Optimal Design

- Take a fully autonomous system and fix tether thickness h_{pv}

$$w_e(f_{pv}, \xi_t) = \frac{\eta_{pv}}{\pi\beta} \frac{S_{\odot}}{\sigma_{pv} E_m^2 h_{pv}} \times f_{pv} \times \xi_t$$

- BPT design involves 3 parameters: L_t , f_{pv} , and w_t .
- To select these parameters optimally, we followed two approaches:
 - Optimize the tether efficiency (i_{av}) for a given set of ambient variables.

BPT with a Hollow Cathode and optimum $f_{pv} \sim 0.6$



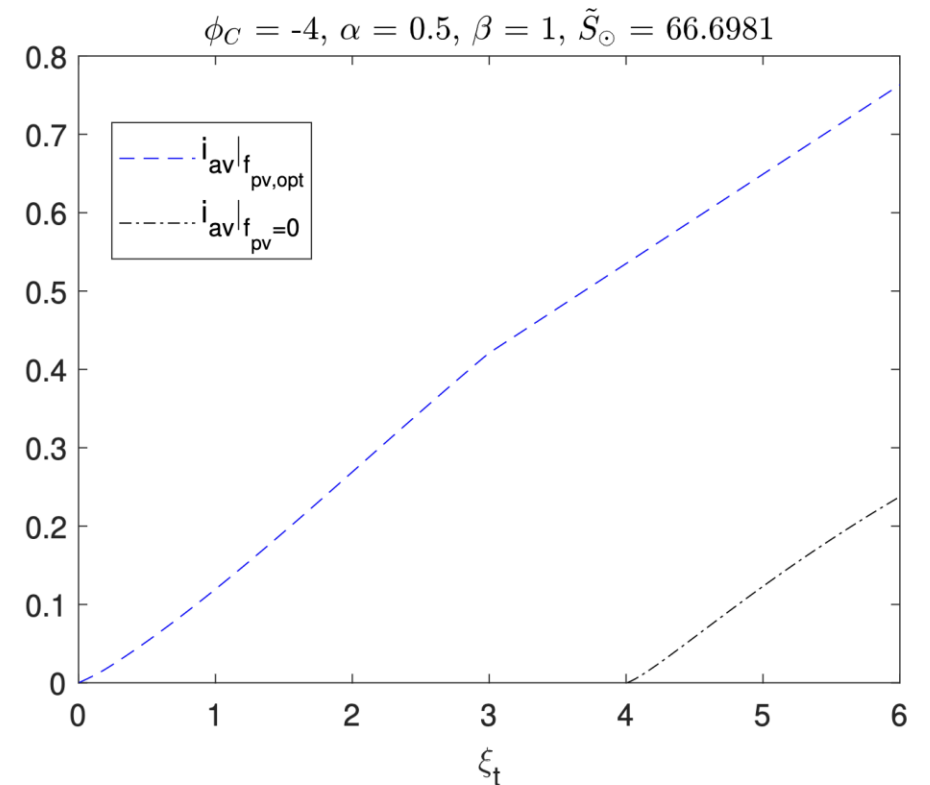
3. Optimal Design

- Take a fully autonomous system and fix tether thickness h_{pv}

$$w_e(f_{pv}, \xi_t) = \frac{\eta_{pv}}{\pi\beta} \frac{S_{\odot}}{\sigma_{pv} E_m^2 h_{pv}} \times f_{pv} \times \xi_t$$

- BPT design involves 3 parameters: L_t , f_{pv} , and w_t .
- To select these parameters optimally, we followed two approaches:
 - Optimize the tether efficiency (i_{av}) for a given set of ambient variables.

BPT with a Electron Field Emitter and optimum $f_{pv} \sim 0.9$



3. Optimal Design

- Take a fully autonomous system and fix tether thickness h_{pv}

$$w_e(f_{pv}, \xi_t) = \frac{\eta_{pv}}{\pi\beta} \frac{S_{\odot}}{\sigma_{pv} E_m^2 h_{pv}} \times f_{pv} \times \xi_t$$

- BPT design involves 3 parameters: L_t , f_{pv} , and w_t .
- To select these parameters optimally, we followed two approaches:
 - Optimize the tether efficiency (i_{av}) for a given set of ambient variables.
 - Optimize a global figure of merit (deorbit time) for a given mission

$$T_D(w_t, L_{pv}, f_{pv}) \simeq \int_{H_F}^{H_0} \frac{m_{DD}}{R_1 m_t + R_0 m_{DD}} dH$$

Parameters of E.T.PACK-F IOD

Parameter	Value	Parameter	Value
H_0	600 km	L_t	$L_b + L_{pv} = 500 m$
β_M	80 kg/m ²	C_D	2
H_F	350 km	h_t	40 μm
i	51°	α	0.5
ρ_b, ρ_{pv}	2700 kg/m ³	β	1
σ_b, σ_{pv}	$3.54 \cdot 10^7$ 1/Ωm	f_i	1/π
V_C	-30V		
m_t	2 kg	m_M	22 kg

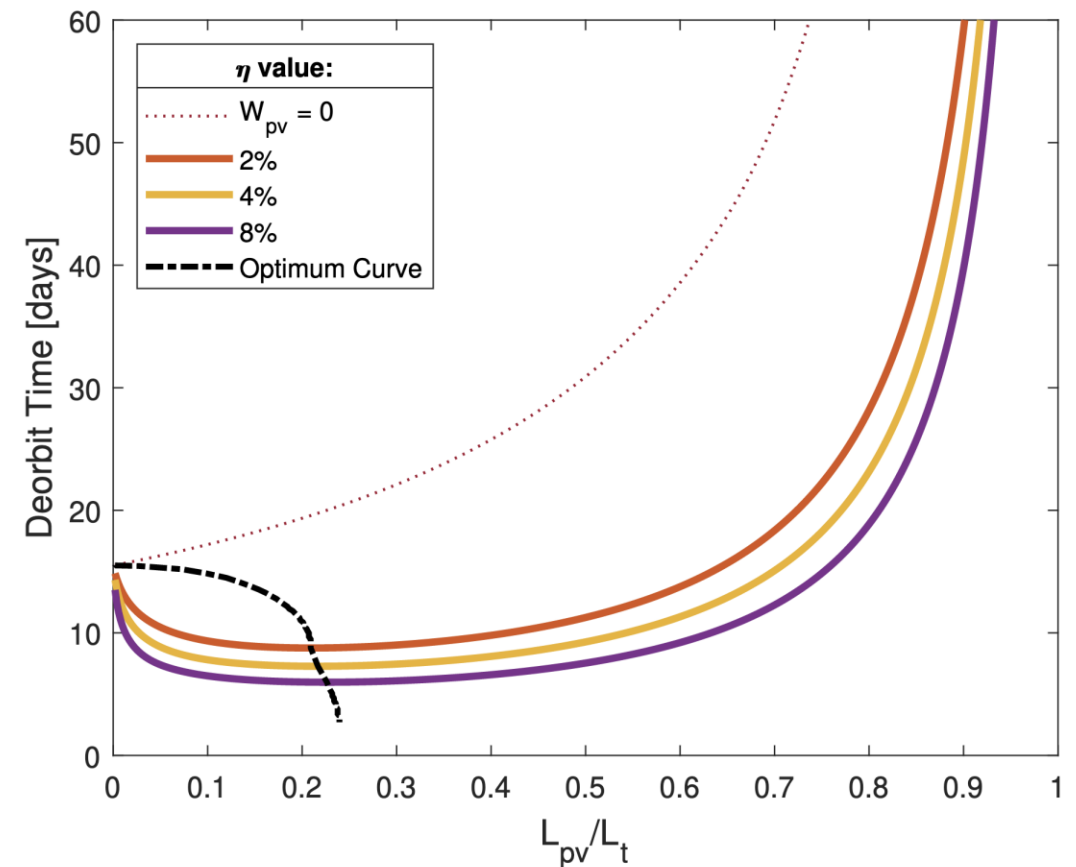
3. Optimal Design

- Take a fully autonomous system and fix tether thickness h_{pv}

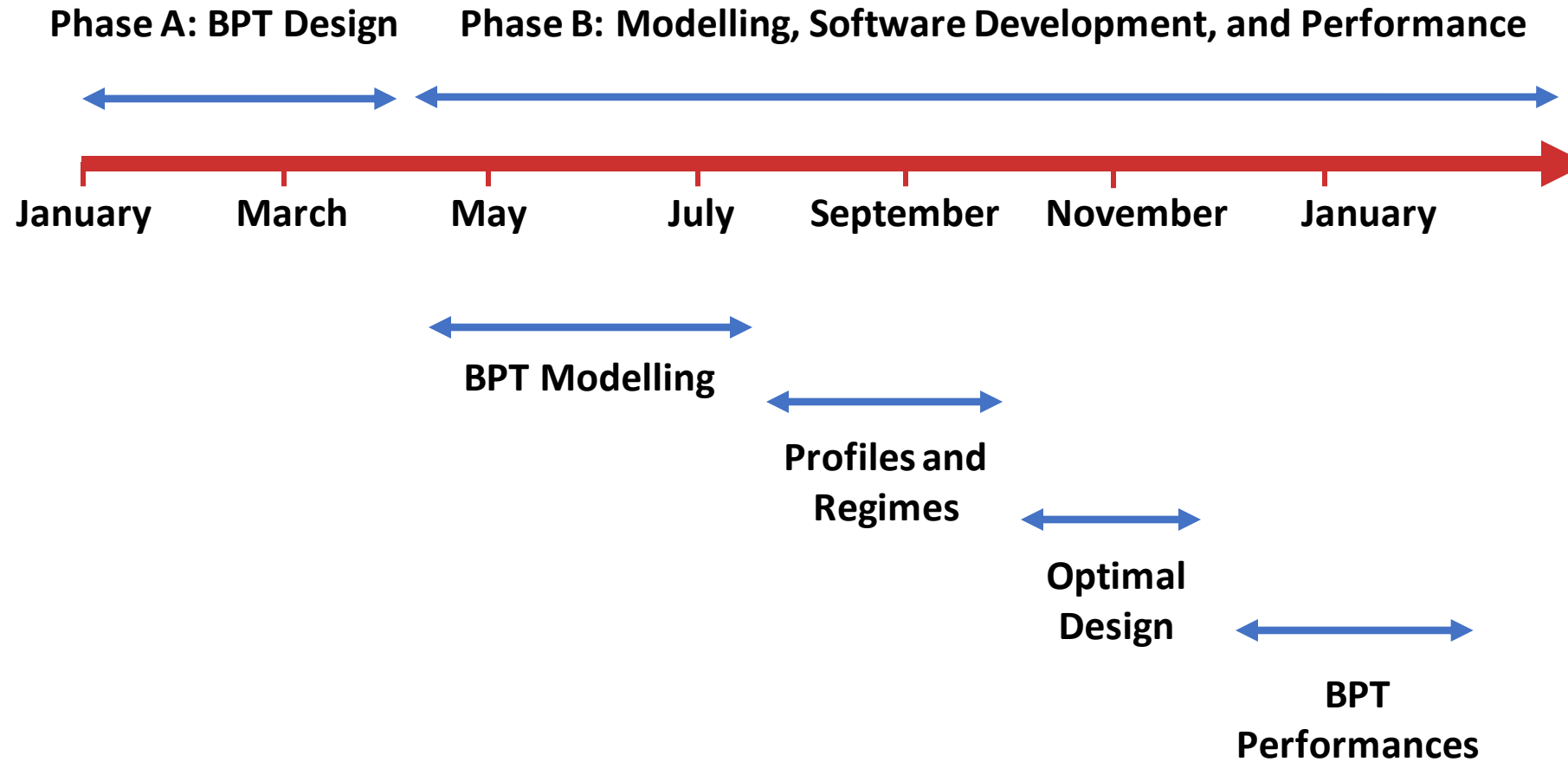
$$w_e(f_{pv}, \xi_t) = \frac{\eta_{pv}}{\pi\beta} \frac{S_{\odot}}{\sigma_{pv} E_m^2 h_{pv}} \times f_{pv} \times \xi_t$$

- BPT design involves 3 parameters: L_t , f_{pv} , and w_t .
- To select these parameters optimally, we followed two approaches:
 - Optimize the tether efficiency (i_{av}) for a given set of ambient variables.
 - Optimize a global figure of merit (deorbit time) for a given mission

$$T_D(w_t, L_{pv}, f_{pv}) \simeq \int_{H_F}^{H_0} \frac{m_{DD}}{R_1 m_t + R_0 m_{DD}} dH$$



Schedule of the Activities at UC3M

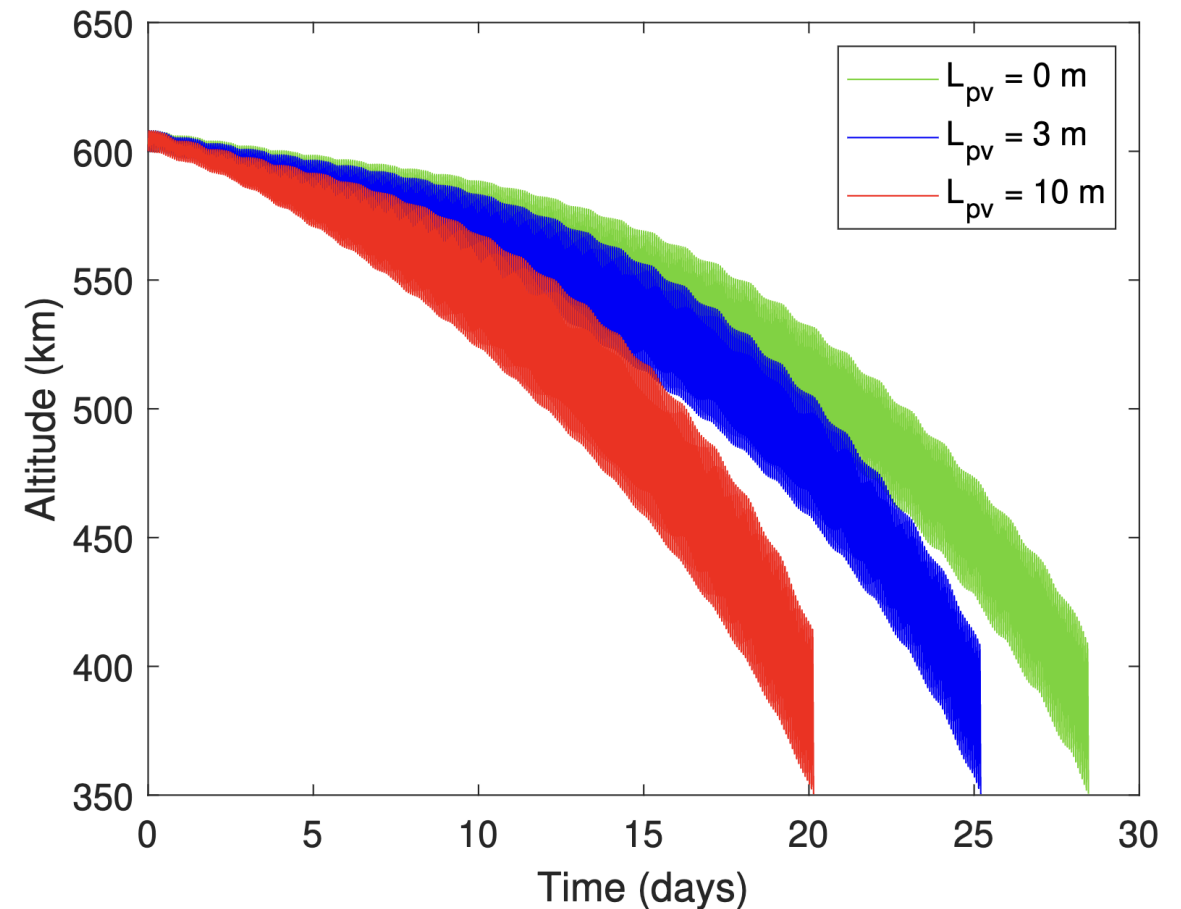


4. BPT Performance: E.T.PACK-F IOD

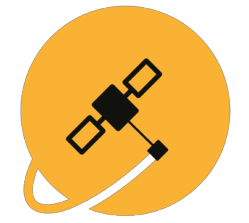


BETsMA v2.0

Parameter	Value	Parameter	Value
m	24 kg	BC	80kg/m^2
w_t	2.5cm	h_t	$40\mu\text{m}$
α_t	0.12	ϵ_t	0.12
H_0	600km	inc	51°
H_F	350km	V_C	-30 V
L_{inert}	25 m	L_t	525 m
I_{min}	0.2 A	I_{max}	0.5 A
f_i	$1/\pi$	η_{pv}	0.02



4. BPT Performance: Commercial scenarios



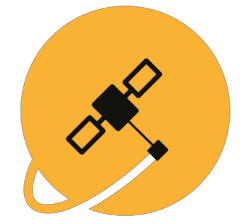
BETsMA v2.0

Parametric analysis for

- Three masses: 250, 500 and 1000kg.
- Two altitudes: 600 and 800kg.
- Two inclinations
- 6 different deorbit devices.

	Deorbit Device	L_t (m)	L_{inert} (m)	L_b (m)	L_{pv} (m)	Mass (kg)	V_C (V)
ANACONDA	Anaconda+EFE	500	50	0	450	11	-500
	Anaconda+HC	500	50	225	225	16	-30
BOA	Boa+EFE	1500	150	0	1350	15	-500
	Boa+HC	1500	150	675	675	25	-30
COBRA	Cobra+EFE	3000	300	0	2700	18	-500
	Cobra+HC	3000	300	1350	1350	35	-30

4. BPT Performance: Commercial scenarios



BETsMA v2.0

M_s (kg)	H_0 (km)	inclination (deg)	DD Type	N_c (%)	T_D (Days)
250	600	53	Anaconda+EFE	0.14	288
			Anaconda+HC	0.05	96
250	600	98	Anaconda+HC	0.24	374
			Boa+EFE	0.17	92
			Boa+HC	0.08	45
250	800	53	Boa+EFE	0.19	79
			Boa+HC	0.08	32
250	800	98	Boa+HC	0.56	175
			Cobra+EFE	0.49	78

M_s (kg)	H_0 (km)	inclination (deg)	DD Type	N_c (%)	T_D (Days)
1000	600	53	Boa+EFE	0.18	125
			Boa+HC	0.06	42
1000	600	98	Boa+HC	0.38	219
			Cobra+EFE	0.39	110
1000	800	53	Boa+HC	0.31	127
			Cobra+EFE	0.36	76
1000	800	98	Cobra+EFE	2.41	398
			Cobra+HC	1.19	172

M_s (kg)	H_0 (km)	inclination (deg)	DD Type	N_c (%)	T_D (Days)
500	600	53	Boa+EFE	0.08	58
500	600	98	Boa+EFE	0.37	207
			Boa+HC	0.17	92
			Cobra+EFE	0.19	53
500	800	53	Boa+EFE	0.38	166
			Boa+HC	0.16	63
			Cobra+EFE	0.19	37
500	800	98	Boa+HC	1.26	389
			Cobra+EFE	1.06	179
			Cobra+HC	0.5	63

Conclusions:

- Fully autonomous deorbit within a few months is perfectly possible thanks to the BPT

5. Conclusions

- Theoretical models for BPTs in the passive and the active modes have been prepared.
- Robust and efficient algorithms to compute the profiles have been developed.
- The code has been verified and integrated in BETsMA v2.0.
- A total of four regimes for BPTs in the passive mode have been found (3 in the active mode).
- Two algorithms to make optimal sizing of BPTs have been constructed.
- The analysis highlighted the benefits of using BPTs:
 - Performance improvement (~30%).
 - Possibility of preparing autonomous DDs with expellant-less emitters
- Simulation campaign with BETsMA v2.0
 - E.T.PACK-F: 10 m of pv-segment reduces the deorbit time a 30% and increases the capacity factor.
 - Commercial scenarios: fully autonomous and light DD based on BPTs can deorbit within a few months.

Peiffer, Leo
Tajmar, Martin

BPT Manufacturing and Electrical Testing

Final Meeting

Final Meeting// Thursday 19.01.2023

Peiffer, Leo
Tajmar, Martin

BPT Manufacturing and Electrical Testing

Final Meeting



Table of Contents

- I. Trade-off: solar cell technology**
- II. Manufacturing of the photovoltaic tether segment (PTS)**
- III. Electrical characteristics of the PTS**
- IV. Atomic oxygen robustness**
- V. Conclusion**

I. Trade-off: solar cell technology

Thin-film solar cell technologies

technology	η^* [%]	flexible substrates	manufacturers on flexible substrates	scalability for a PTS	costs
<u>a-Si:H</u>	13.6	yes	no	yes	low to moderate
<u>CdTe</u>	22.1	only academic	no	yes	low to moderate
<u>CIGS</u>	22.3	yes	yes	yes	low to moderate
<u>GaAs multijunction</u>	37.75	in development	very limited	no	high
<u>PSC</u>	25.2	yes	no	no	low to moderate

← promising for the future

ELO: Epitaxial Lift-OFF

- GaAs solar cells as thin-film technology
- tf2 devices (Netherlands) + Fraunhofer ISE (also Airbus and Azurspace)
→ ALFAMA-Project "Advanced Lightweight and Flexible Array with Mechanical Architecture"

I. Trade-off: solar cell technology

Thin-film solar cell technologies

technology	η^* [%]	flexible substrates	manufacturers on flexible substrates	scalability for a PTS	costs
<u>a-Si:H</u>	13.6	yes	no	yes	low to moderate
<u>CdTe</u>	22.1	only academic	no	yes	low to moderate
<u>CIGS</u>	22.3	yes	yes	yes	low to moderate
<u>GaAs multijunction</u>	37.75	in development	very limited	no	high
<u>PSC</u>	25.2	yes	no	no	low to moderate

← technology for the BPT

CIGS: Copper-Indium-Gallium-Selenide

- Moderate efficiencies
- Competitive market
- Low costs
- Good radiation hardness

I. Trade-off: solar cell technology

CIGS Manufacturers

Manufacturer	state	substrate	η_{module} [%]	thickness [μm]	bend radius [cm]
<u>Global Solar</u>	USA	stainless steel	14.5	3000	50
<u>Midsummer</u>	SWE	stainless steel	11	2000	50
<u>Miasolé</u>	USA	stainless steel	14	330	5
<u>Flisom</u>	CHE	Polyimide	13	60	1
<u>Ascent Solar</u>	USA	stainless steel	9	80	3
<u>Sunplugged</u>	AUT	stainless steel, Polyimide	9	60	4

← manufacturer for PTS

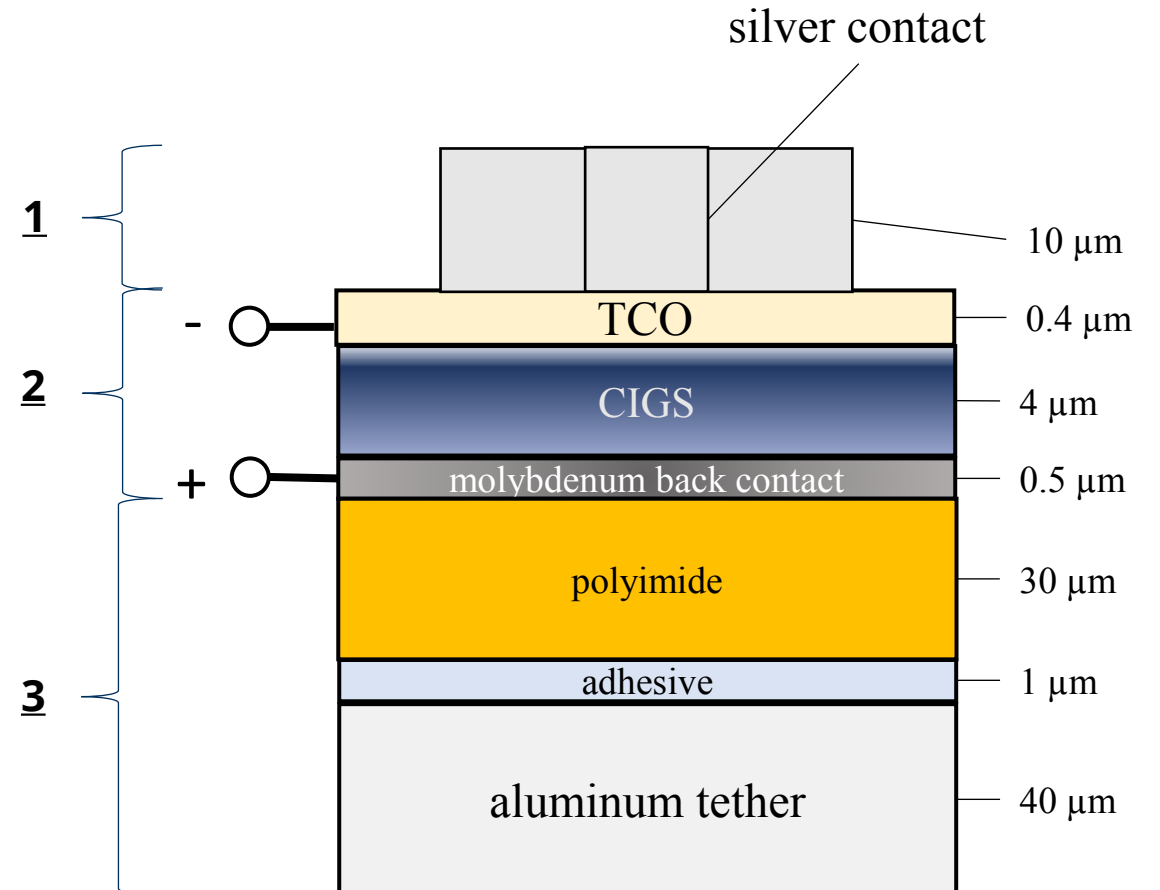
Sunplugged

- specialized on custom solutions
- main focus on Building Integrated Photovoltaics (BIPV)
- experience in solar integrated products for vehicles and other electronic devices (also non-CIGS)
- **they were interested in a collaboration**

II. Manufacturing of the photovoltaic tether segment (PTS)

PTS layering

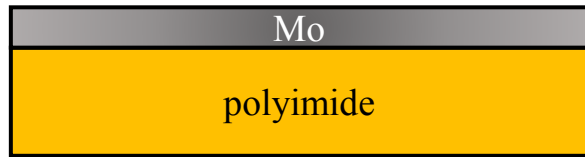
- 1 Electron collecting grid
- 2 Solar cell
 - Transparent Conductive Oxide (TCO) as front contact
 - CIGS absorber crystal (graded absorber)
 - Molybdenum back contact
- 3 Substrate
 - Kapton (solar cell is directly deposited on top)
 - bare aluminum tether



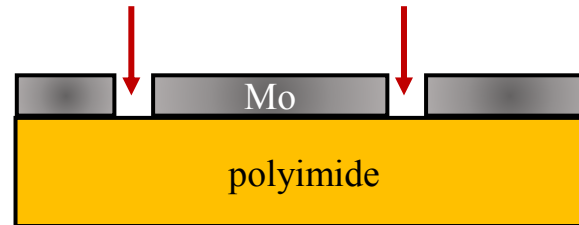
II. Manufacturing of the photovoltaic tether segment (PTS)

Rough description of the manufacturing process

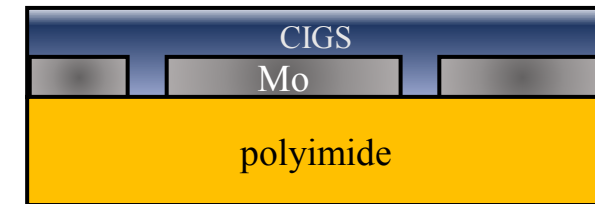
1) Application of back contact



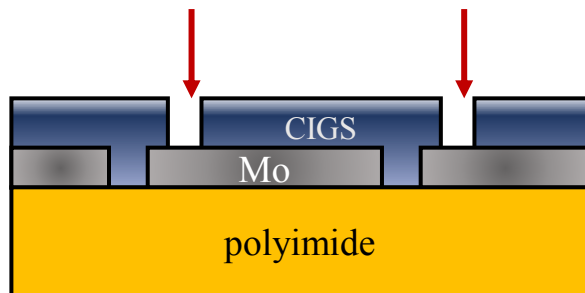
2) Laser structuring



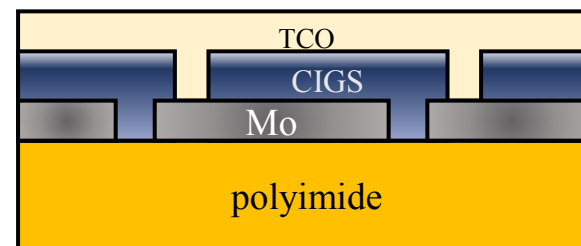
3) Deposition of absorber material



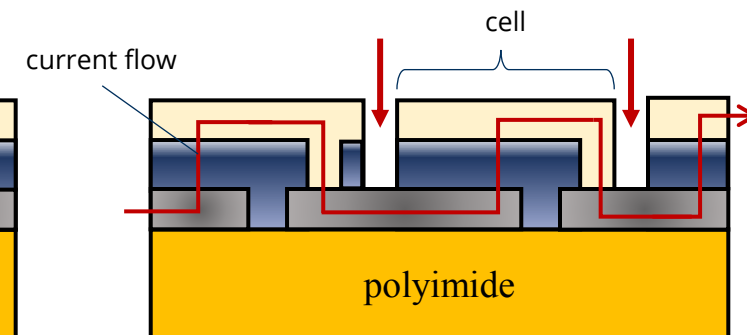
4) Laser structuring of absorber



5) Application of TCO front contact



6) Laser structuring of TCO

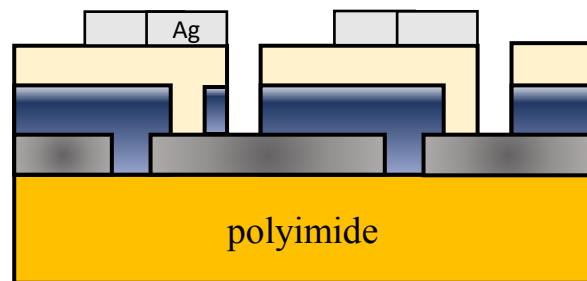


Dimensions are not to scale!

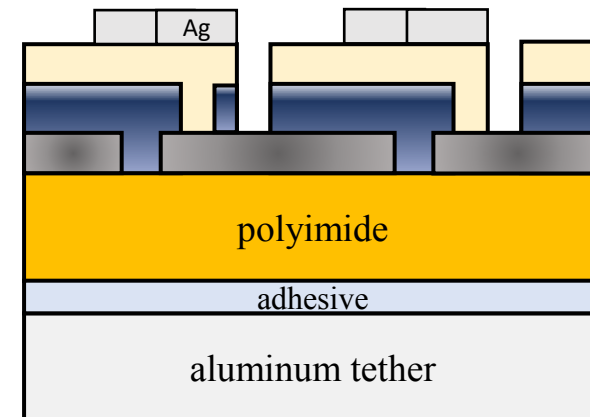
II. Manufacturing of the photovoltaic tether segment (PTS)

Rough description of the manufacturing process

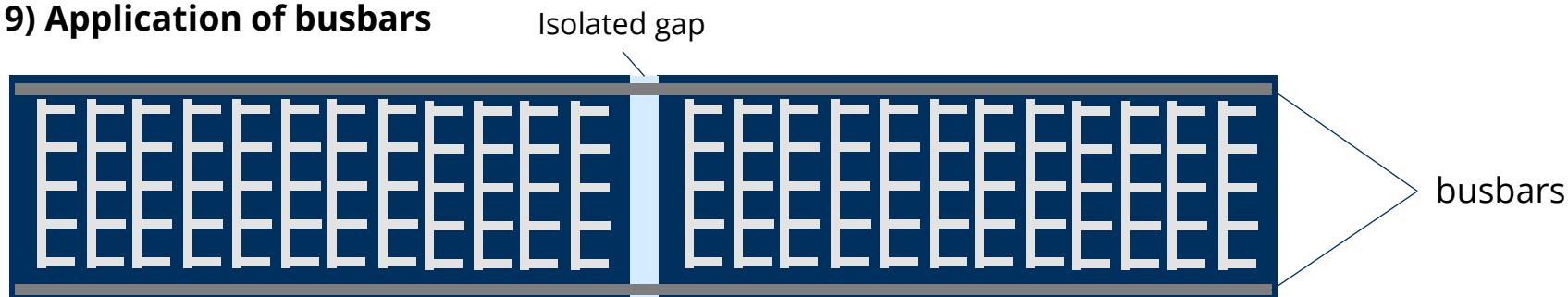
7) Printing of silver grid



8) Application on the aluminum tether



9) Application of busbars

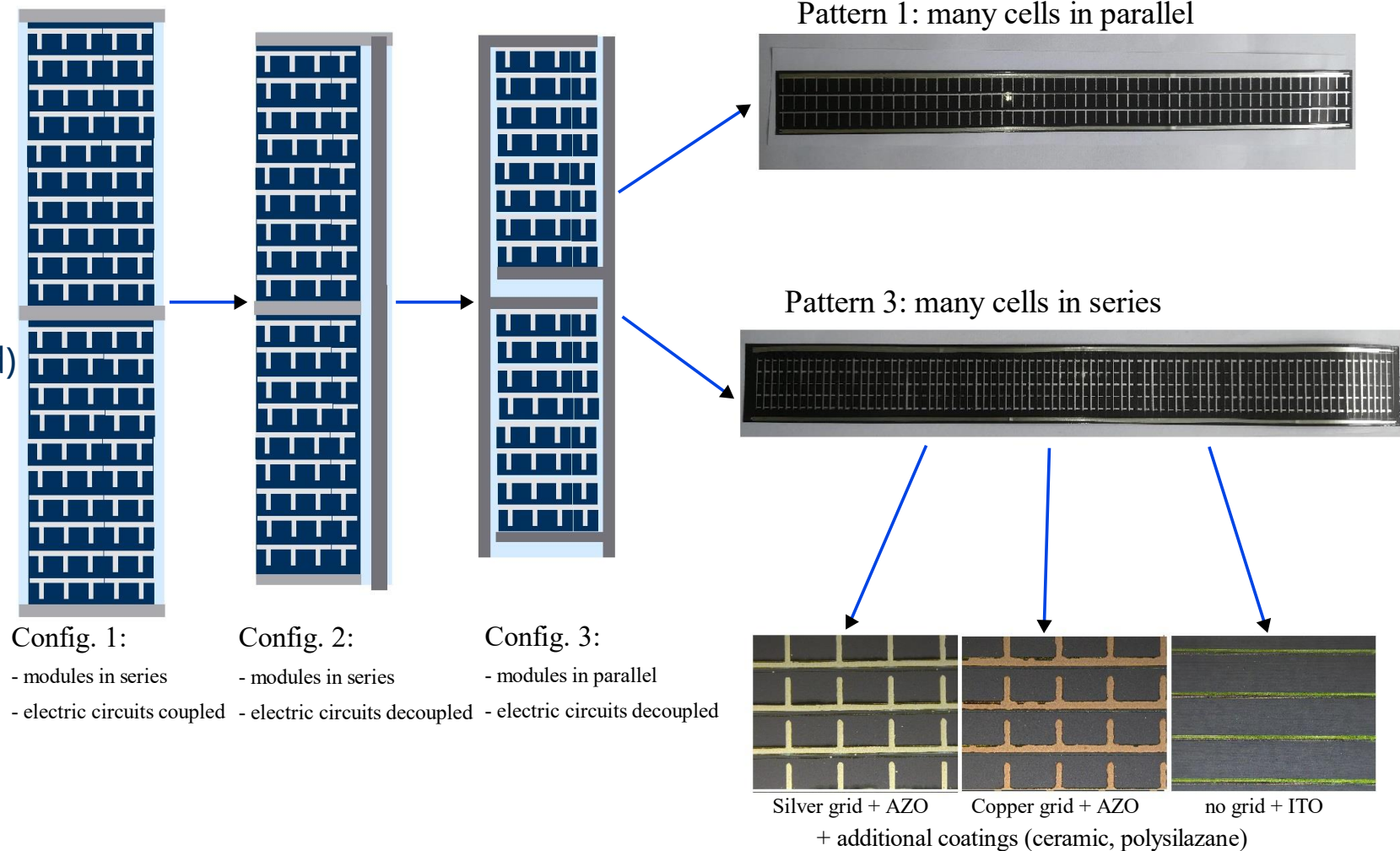


Dimensions are not to scale!

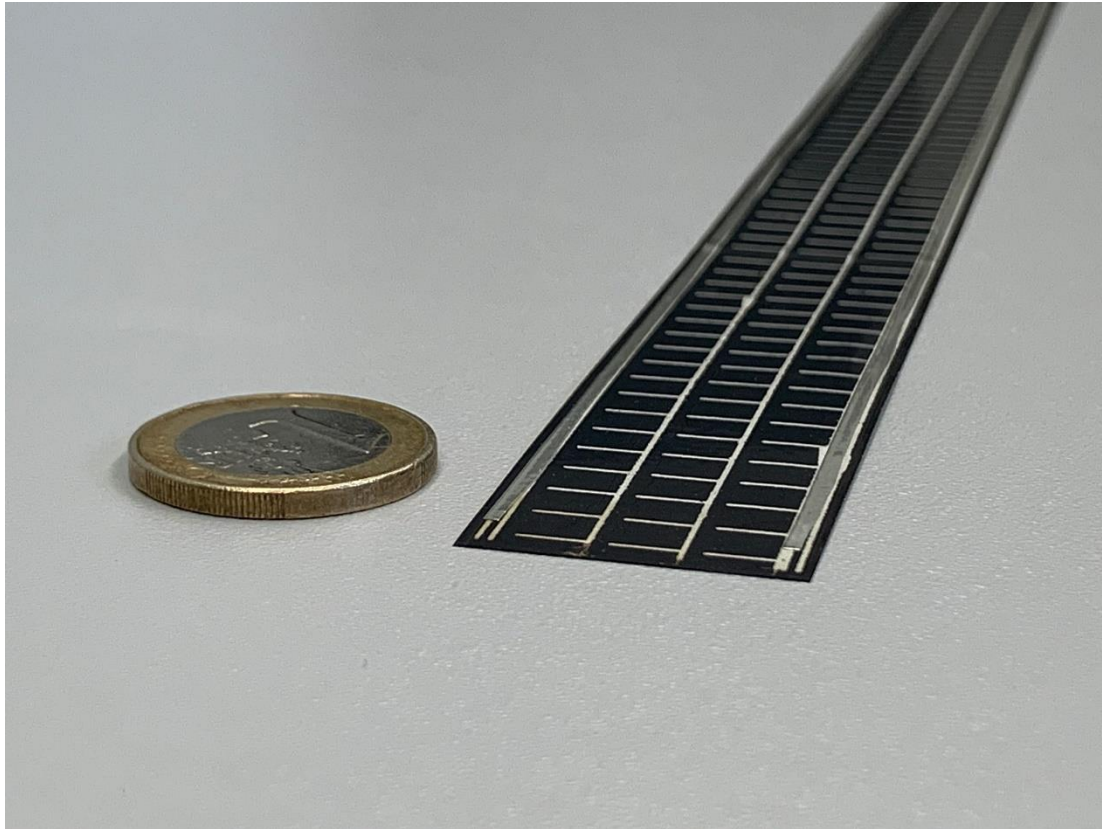
II. Manufacturing of the photovoltaic tether segment (PTS)

Samples:

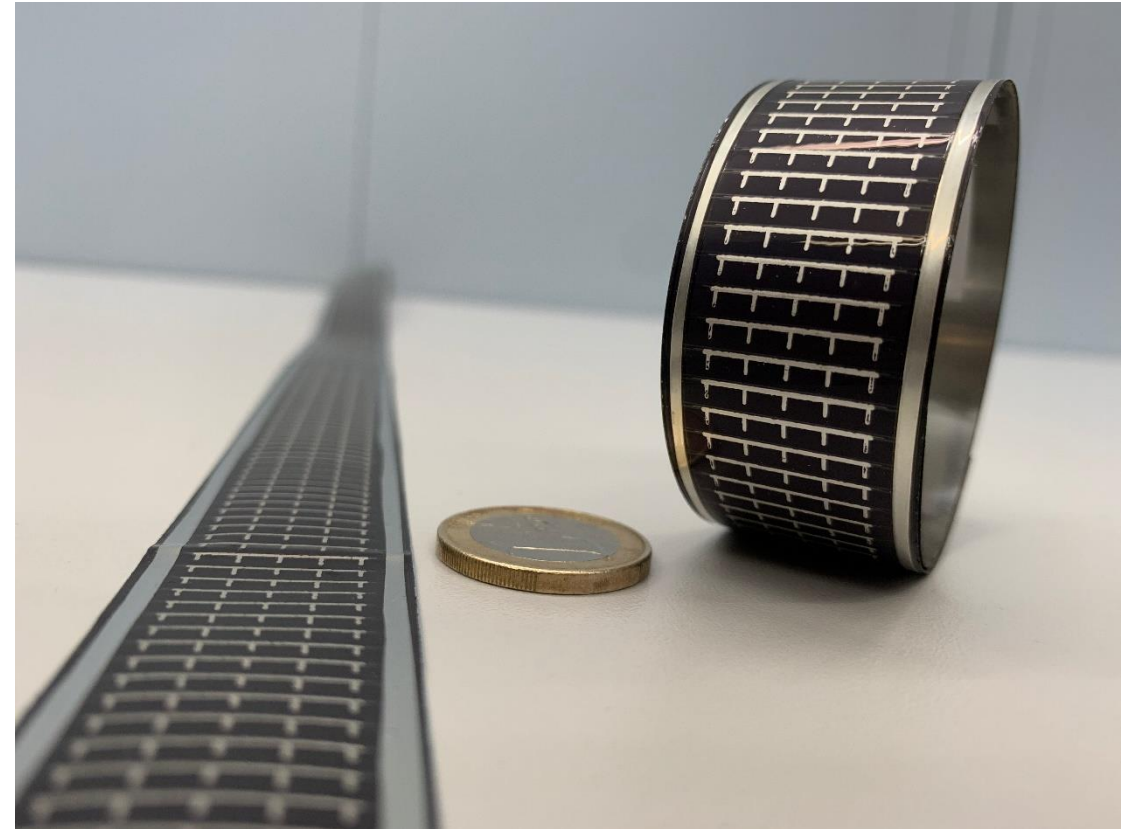
- **Submodules** (25x250 mm²)
 - Pattern 1 on stainless-steel
 - Pattern 3 on stainless-steel
 - Pattern 3 on aluminum
- **Assembled PTS** (non-optimized)
 - 1x 3 m PTS
 - 6x 1.5 m PTS
- **Material Demonstrators**
 - (40x40mm²)
 - 7 material combinations
 - Atomic oxygen robustness tests



II. Manufacturing of the photovoltaic tether segment (PTS)



Submodule of pattern 1



Right: coiled-up submodule of pattern 3
Left: 1.5 m PTS sample made of 6 submodules of pattern 3

III. Electrical characteristics of the PTS

General considerations and restrictions

- **Appropriate testing** of 1.5 m and 3 m PTS samples **was not possible**
 - Establishing the solar constant in a test plane of 3 m x 25 mm was out of the scope of the project
 - Assembled PTS samples were manufactured for mechanical testing and electrically unoptimized

- **Only submodules** of different patterns with length 25 cm **were tested in detail**

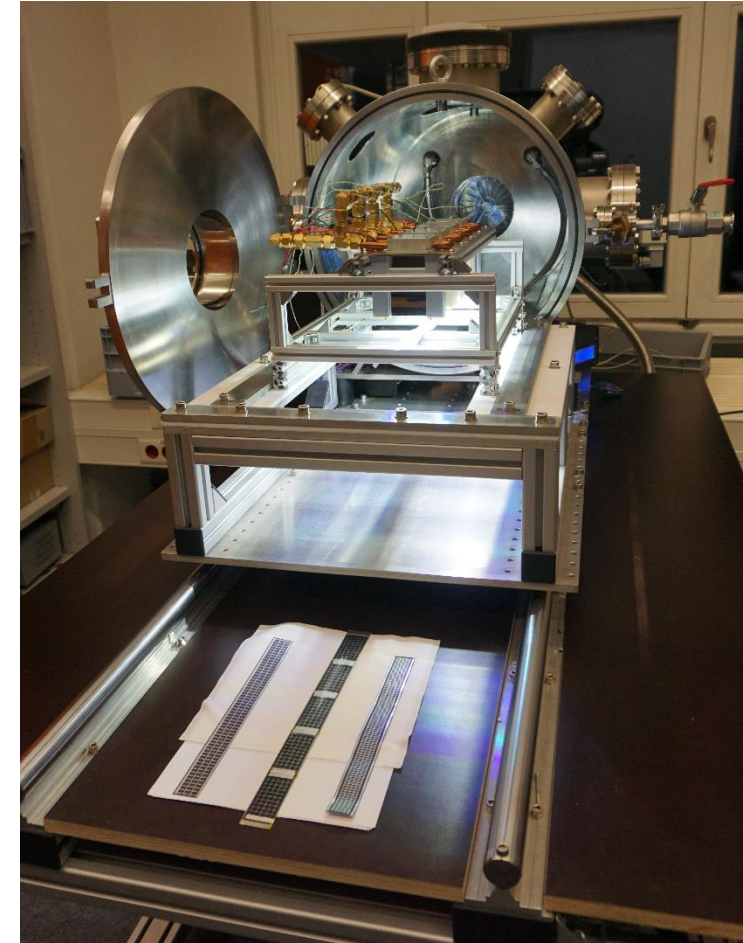
- **Reference Measurement** with commercial LED Sunbrick Solar Simulator (g2voptics) **for each submodule**

- **Measurements under self-built LED Solar Simulator** inside vacuum chamber
 - Investigation of the **influence of vacuum**
 - Investigation of the **influence of temperature**

III. Electrical characteristics of the PTS

Test-Setup

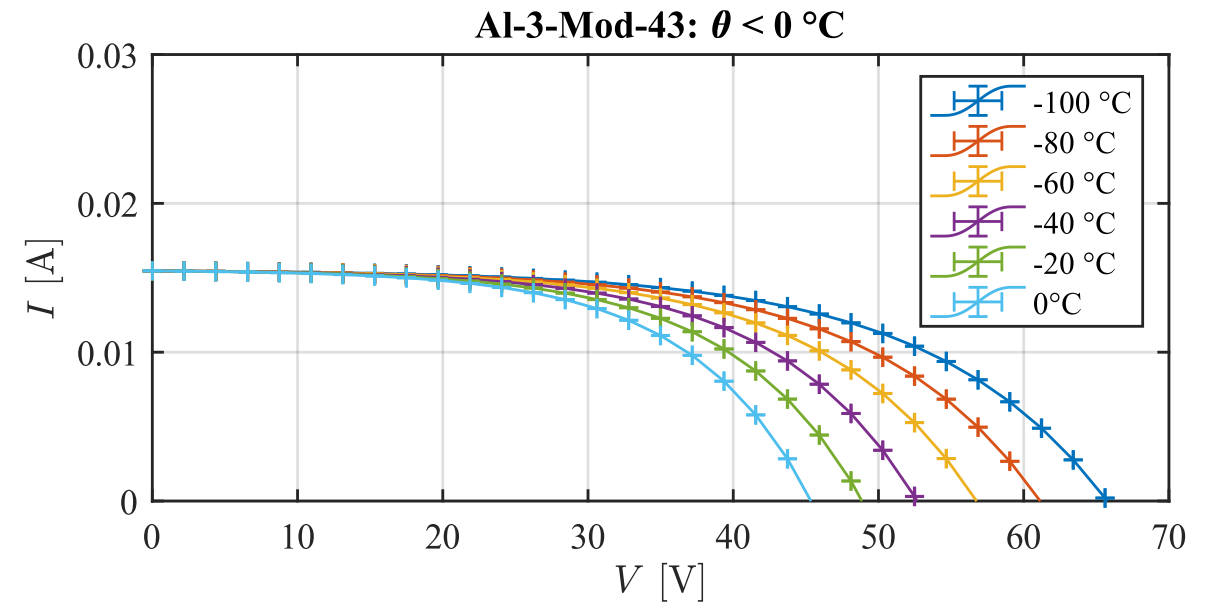
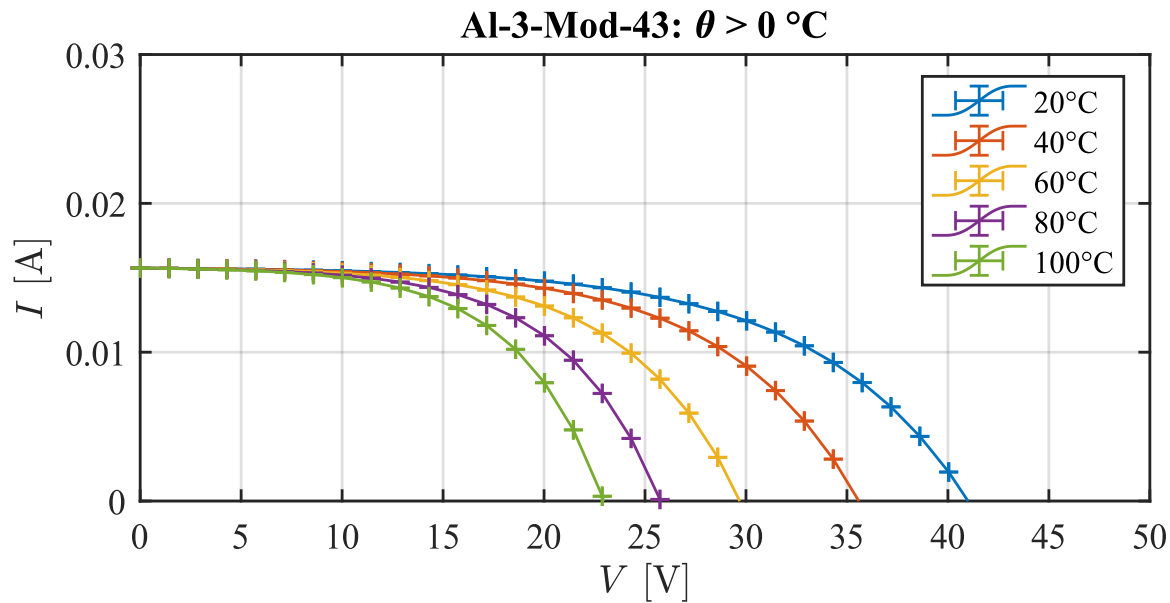
- LED-Based **SoSi of class BCA** in the wavelength range 400 nm to 1000 nm
 - Class B spectral match
 - Class C spatial uniformity
 - Class A temporal stability
- Vacuum chamber
 - $p = 1 \times 10^{-5}$ mbar with full SoSi inside
- Thermal plate
 - Flushing with water or liquid nitrogen for cooling
 - 20 W heating foil for heating



III. Electrical characteristics of the PTS

Influence of Temperature: I-V characteristic

Exemplary submodule of pattern 3 on aluminum:

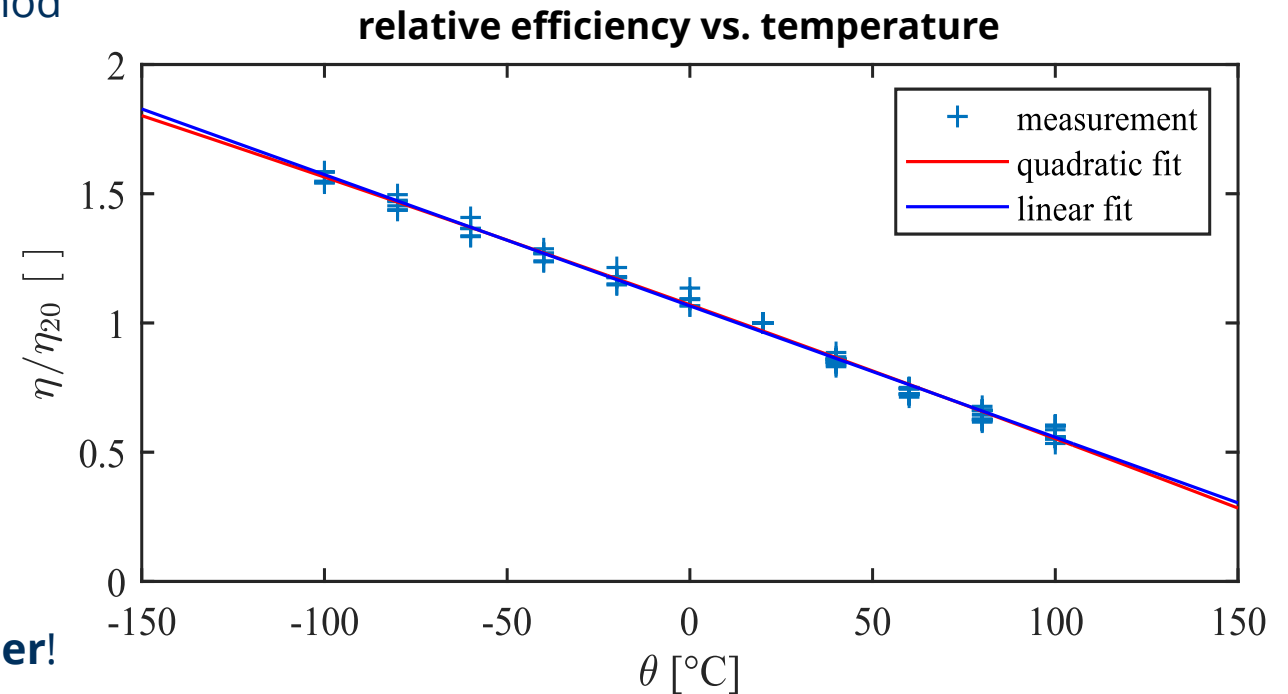


→ Voltage peaks, if spacecraft comes from eclipse

III. Electrical characteristics of the PTS

Influence of Temperature: power conversion efficiency

- Nearly linear function $\eta(\theta)$ with least square method
 - Temperature coefficient: **-0.508 %/K**
 - **But:** gets unprecise above 150 °C
 - For example Mod 43 (see slide before):
 - $\eta = 5.35\%$ at 20 °C
 - $\eta = 2.99\%$ at 100 °C
 - Estimated Operation temperature: 120 °C
 - low heat capacity
 - suboptimal thermo optical properties
- **Temperature is the most influential parameter!**



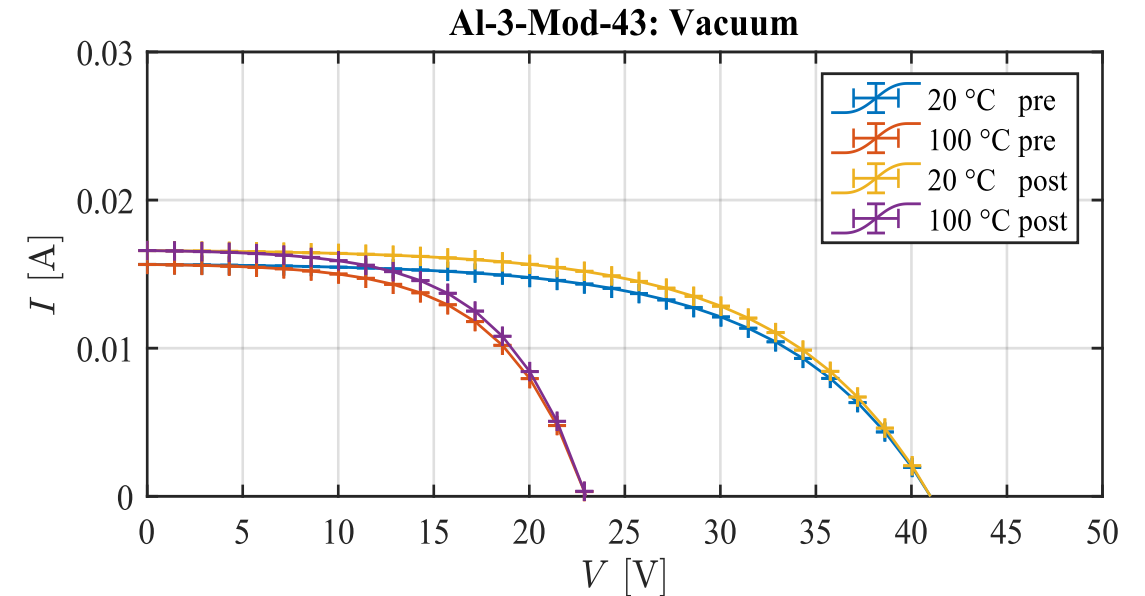
III. Electrical characteristics of the PTS

Influence of Vacuum: I-V characteristic

- **1x10⁻⁵ mbar for 72 hours at 100 °C**
- An increase in current was observed for all samples
 - Average **increase of current by 5 %**
- An increase in efficiency was observed for all samples
 - Average **increase of efficiency by 5.2 %** before vs. after
 - E.g. mod 43 at 20 °C: 5.35 % → 5.67 %

→ **Vacuum has no detrimental effect**

→ **Storage under inert atmosphere would be recommended pre-flight**



IV. Atomic oxygen robustness

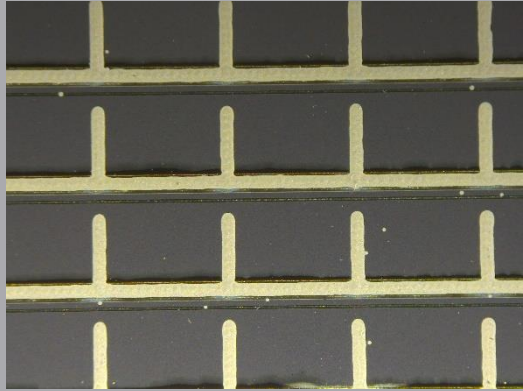
Considerations

- Scenario: E.T.PACK-F would be in a residual **atmosphere, dominated by atomic oxygen**
- BETSMA simulation: atomic oxygen fluence of **0.96×10^{19} Atoms/cm² to 1.45×10^{19} Atoms/cm²** for IOD mission
- Two susceptible PTS materials:
 - **Silver** of the electron grid → **unprotected**
 - **Polyimide** of the solar cell substrate → **protected** by cell structure and aluminum tether
- Task: **protect silver grid** or find different materials
 - change metal ink for the grid
 - avoid using a metal grid
 - use coatings as encapsulation

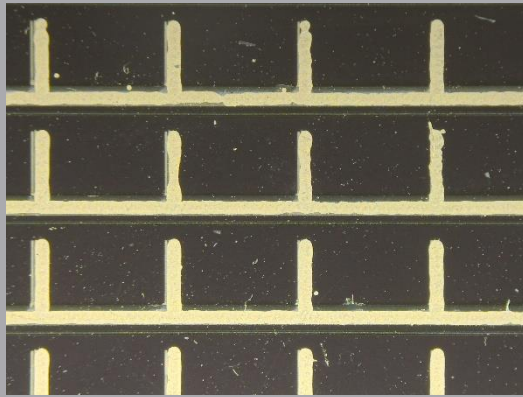
IV. Atomic oxygen robustness

Silver Ink + TCO (Al:ZnO)

no coating

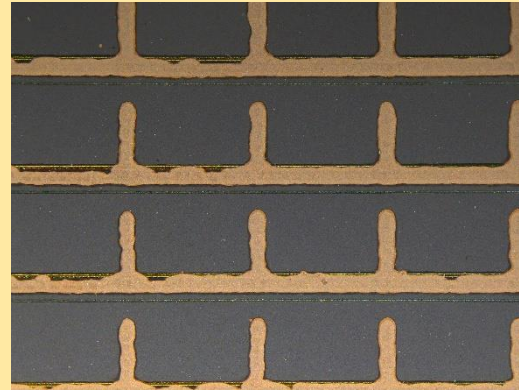


Standard Coating (Sol-gel)

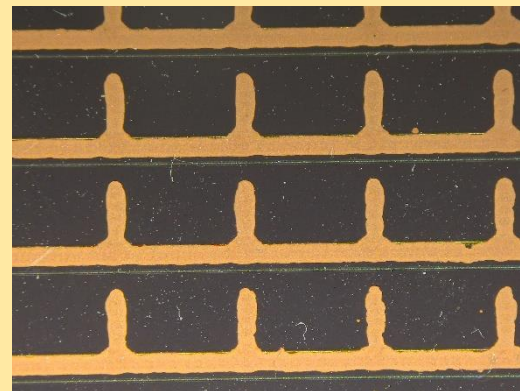


Copper Ink + TCO (Al:ZnO)

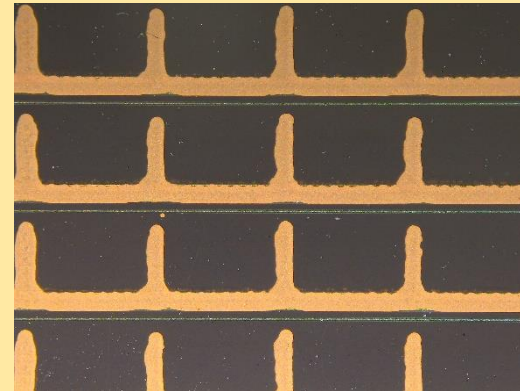
no coating



Standard Coating (Sol-gel)



CAG37

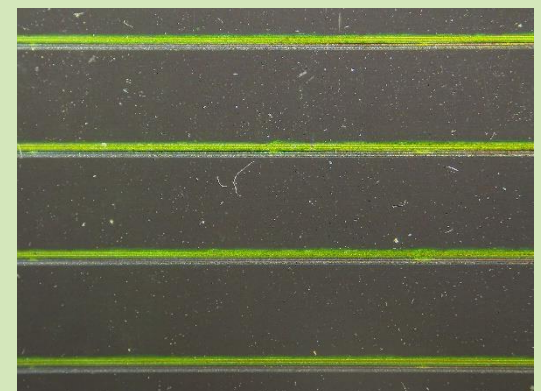


No Ink, only TCO (ITO)

no coating



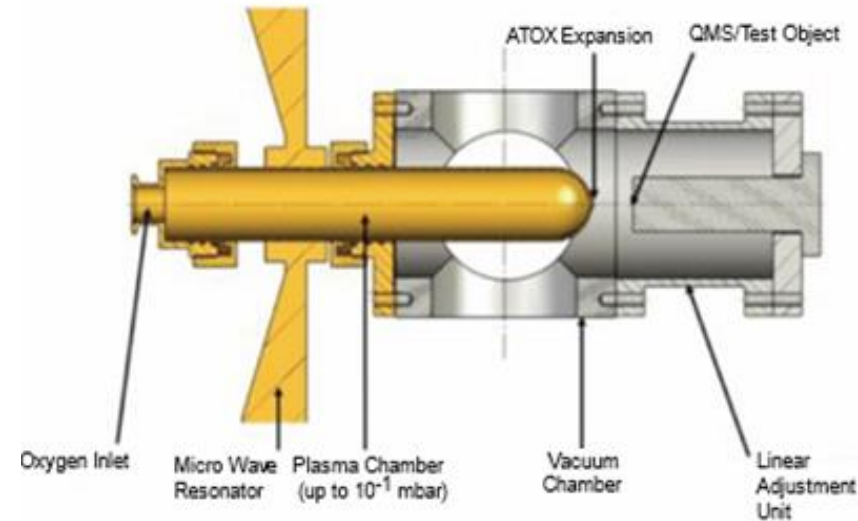
Standard Coating (Sol-gel)



IV. Atomic oxygen robustness

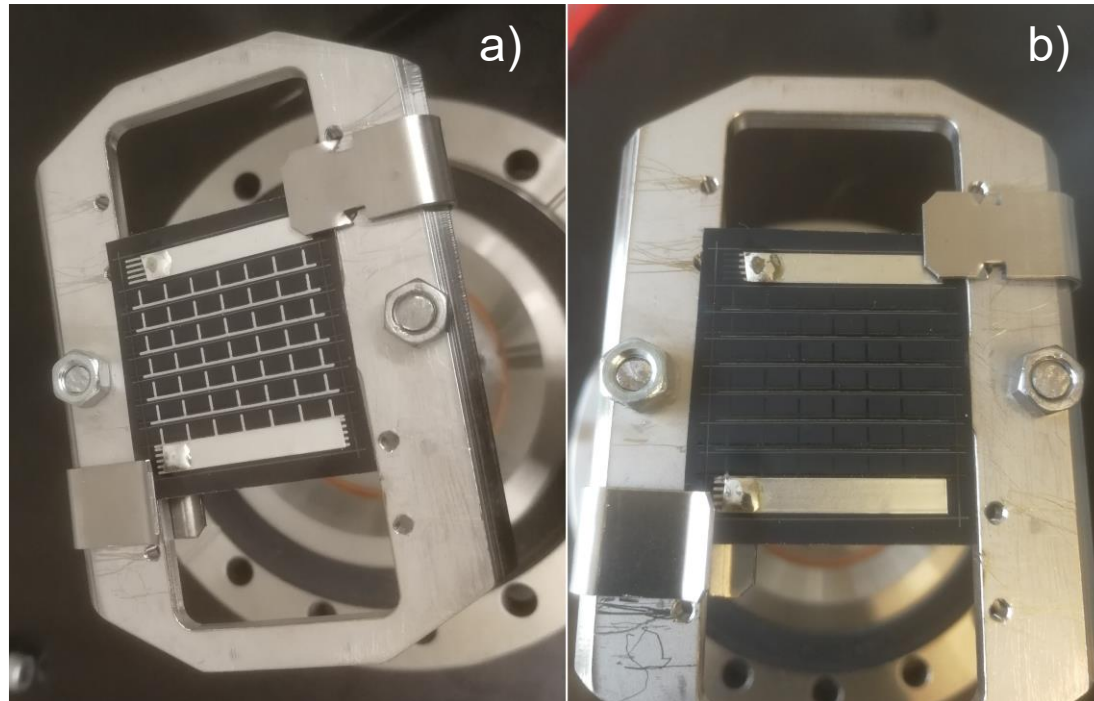
Test Setup: micro wave plasma-based atomic oxygen source

- Flux: $(2.43 \pm 0.92) \times 10^{14}$ Atoms/cm²s
→ testing duration of 20 h for 1×10^{19} Atoms/cm²
- Vacuum quality: $p = 1.1 \times 10^{-5}$ mbar
→ LEO: $p < 10^{-7}$ mbar
- Sample temperature: $\theta = (30 \pm 10)$ °C
→ LEO: -100 °C $< \theta < 150$ °C
- Particle kinetic energy: $E_{kin} < 0.05$ eV
→ LEO: $E_{kin} = 4.5$ eV

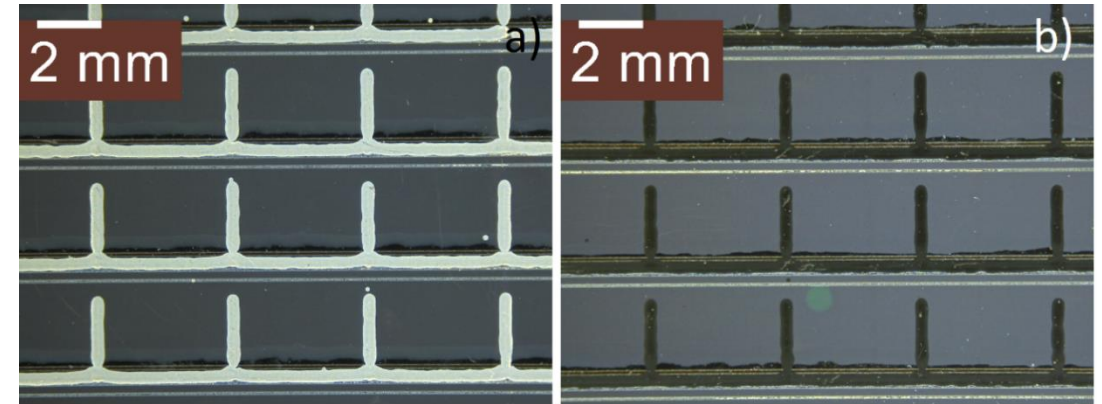


IV. Atomic oxygen robustness

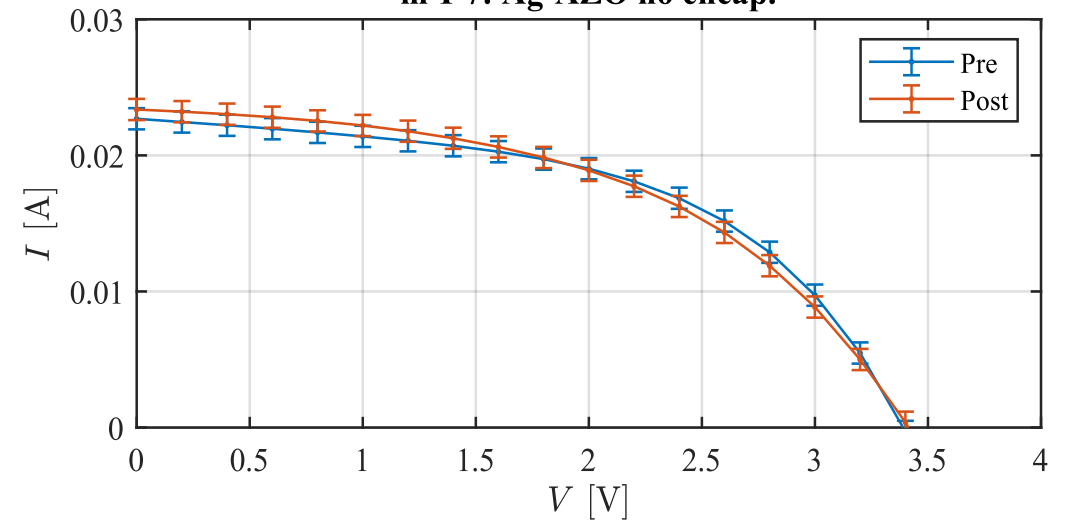
Results: Silver electron collecting grid



→ Ag electron collecting grid was visually degraded
→ But: Degradation had no effect on I-V characteristic



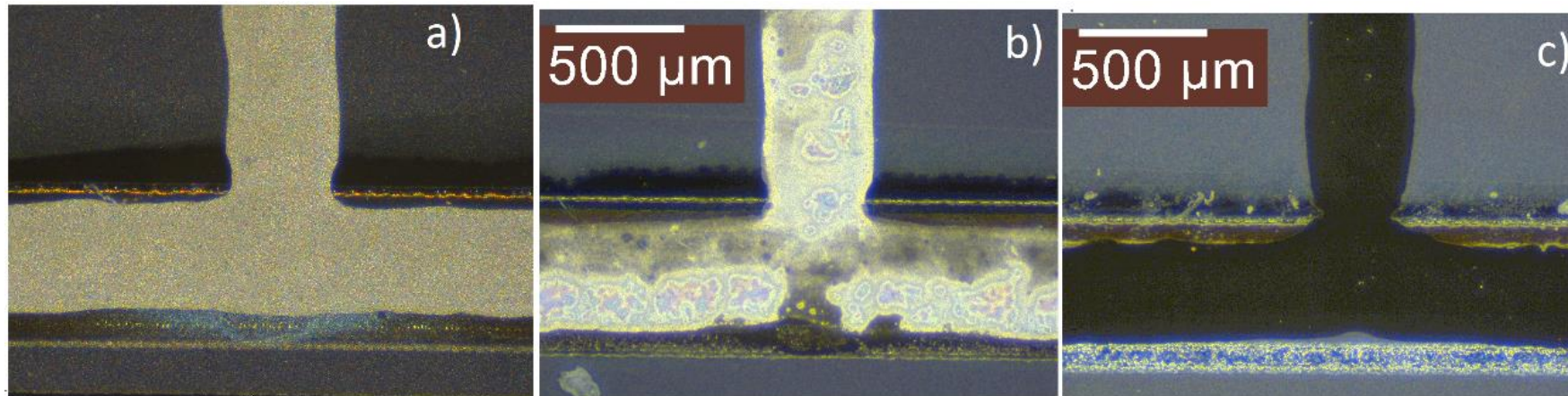
m-I-7: Ag-AZO no encap.



IV. Atomic oxygen robustness

Results: Silver electron collecting grid

- Optical microscopy revealed severe material change at the silver contacts
 - a) non-degraded
 - b) partially degraded
 - c) Completely degraded



Images show different spots on onesample

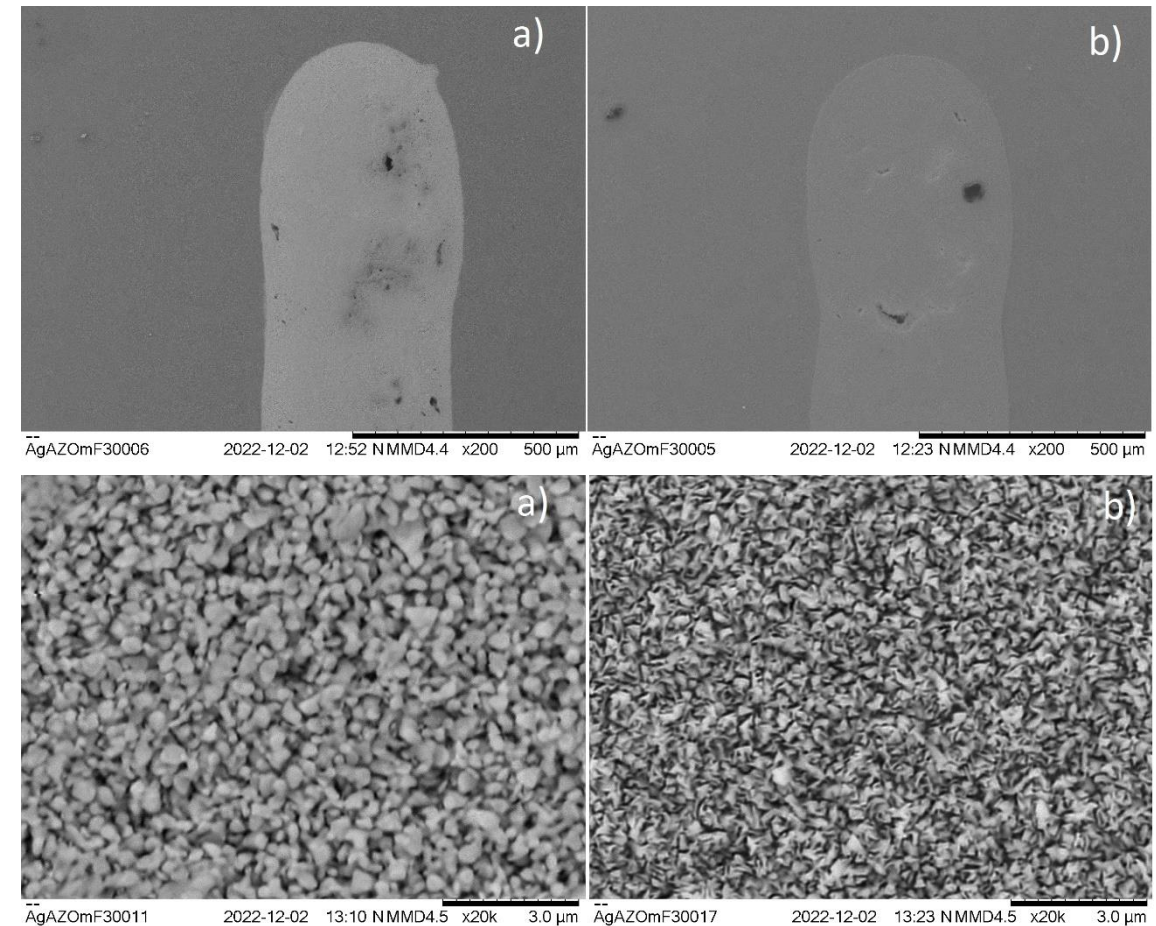
IV. Atomic oxygen robustness

Results: Silver electron collecting grid

- SEM: reveals oxidation and partial erosion of the silver
 - a) non-degraded
 - b) Completely degraded
- Darker appearance indicates **loss of conductivity**
- Less voluminous appearance indicates **erosion**
- Crystal **grains are malformed** in the degraded area

→ **loss of material constitutes a risk of contamination**
→ **effects are expected to be much stronger in LEO**

→ **Silver grid is not feasible for the use in space**



IV. Atomic oxygen robustness

Results: Overview

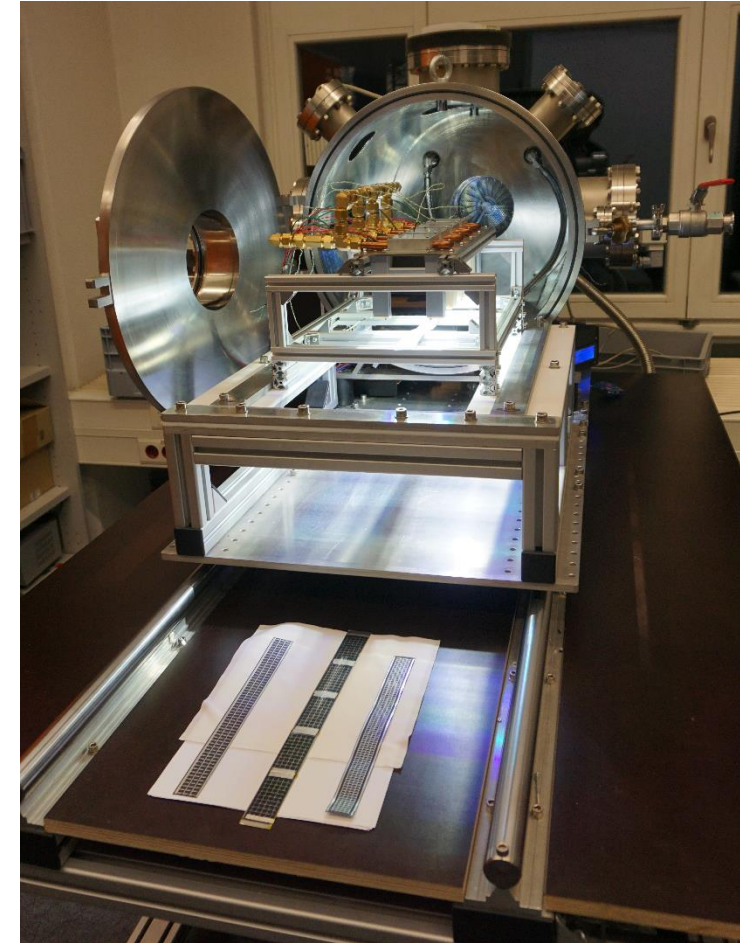
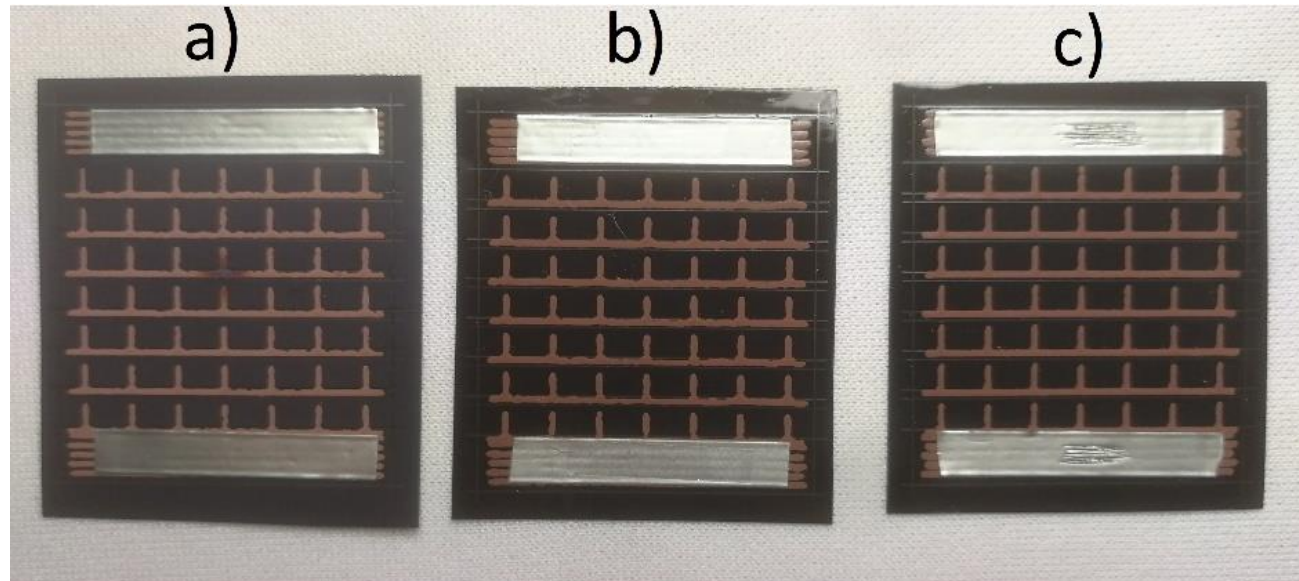
- Only Ag/AZO with no encapsulation showed a visual degradation

material comb.	robust to atomic oxygen?	tested	η_{mean} [%]
Ag/AZO no encap.	no	yes	6.05
Ag/AZO Sol encap.	yes	yes	6.62
Cu/AZO no encap.	yes	yes	7.93
Cu/AZO Sol encap.	yes	no	6.37
Cu/AZO CAG37 encap.	yes	yes	6.37
ITO no encap.	yes	yes	4.74
ITO Sol encap.	yes	no	5.28

IV. Atomic oxygen robustness

Addition: Coatings as thermal control

- Measurement of temperature curve in radiatively dominated environment
 - a. Cu/AZO without coating
 - b. Cu/AZO with Sol-coating (silicate-based)
 - c. Cu/AZO with CAG37-coating (polysilozane)



IV. Atomic oxygen robustness

Addition: Coatings as thermal control

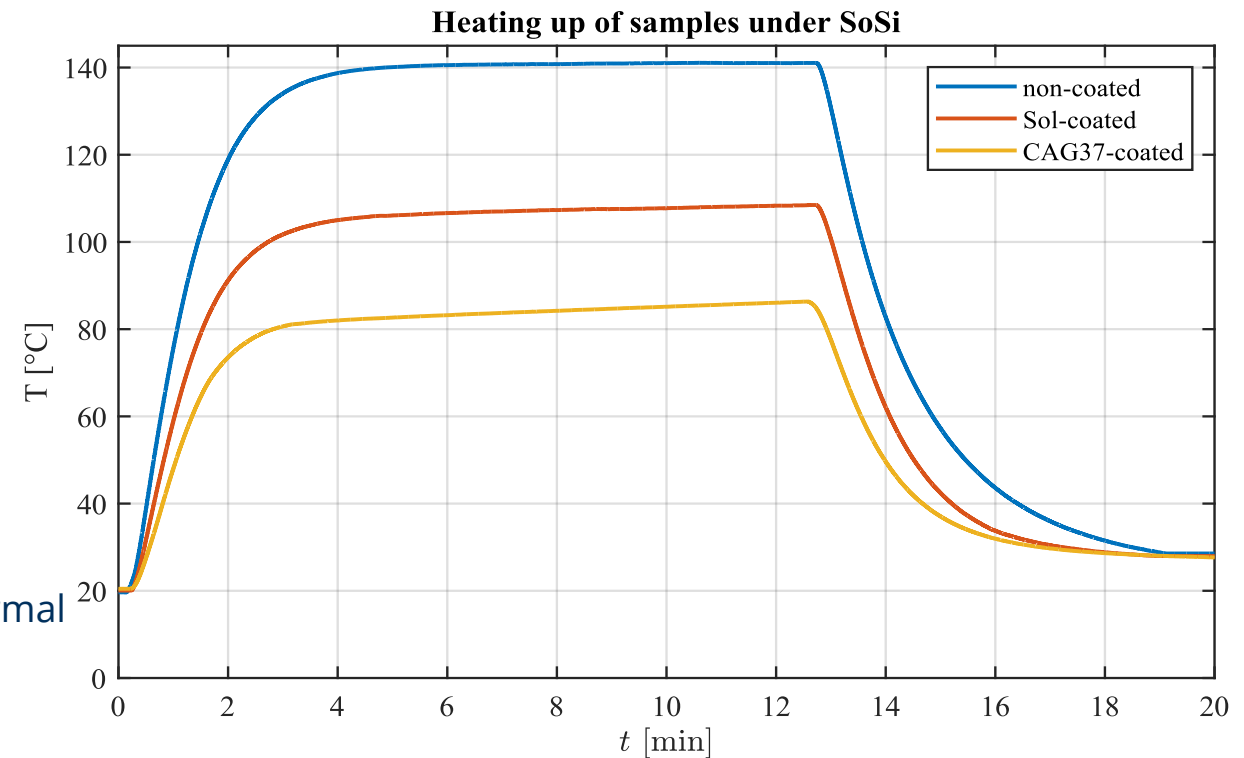
- Measurement of temperature curve in radiatively dominated environment

- Experiment was repeated three times for each sample

- Steady state temperature (4 min < t < 12 min)

- non-coated: **140 ± 5.9 °C**
- Sol-coated: **106 ± 7.2 °C**
- CAG37-coated: **85 ± 5.4 °C**

→ coatings have a significant **positive influence** on the thermal budget of the PTS!



V. Conclusion

Summary and Conclusion:

- CIGS solar cells **can be manufactured** to be exploited **for a photovoltaic tether segment (PTS)**
- Different **configurations of the PTS** were manufactured **to adapt to the partial shading problem** of a non-oriented tether-shaped photovoltaic module
- The **temperature** of the tether is the **most influential parameter** on the PTS performance
- **Coatings reduced the temperature** of the tether and **increased the robustness to atomic oxygen**

Future Prospects:

- The efficiency of the CIGS on aluminum will increase, once the manufacturing process gets optimized
- A fully assembled PTS will need optimization regarding its manufacturing and verification
- GaAs thin film solar cells and perovskite are future-candidates, once scaling and degradation effects are overcome

→ **The manufacturing of a photovoltaic tether segment based on thin film solar cells is feasible!**

19 January 2023



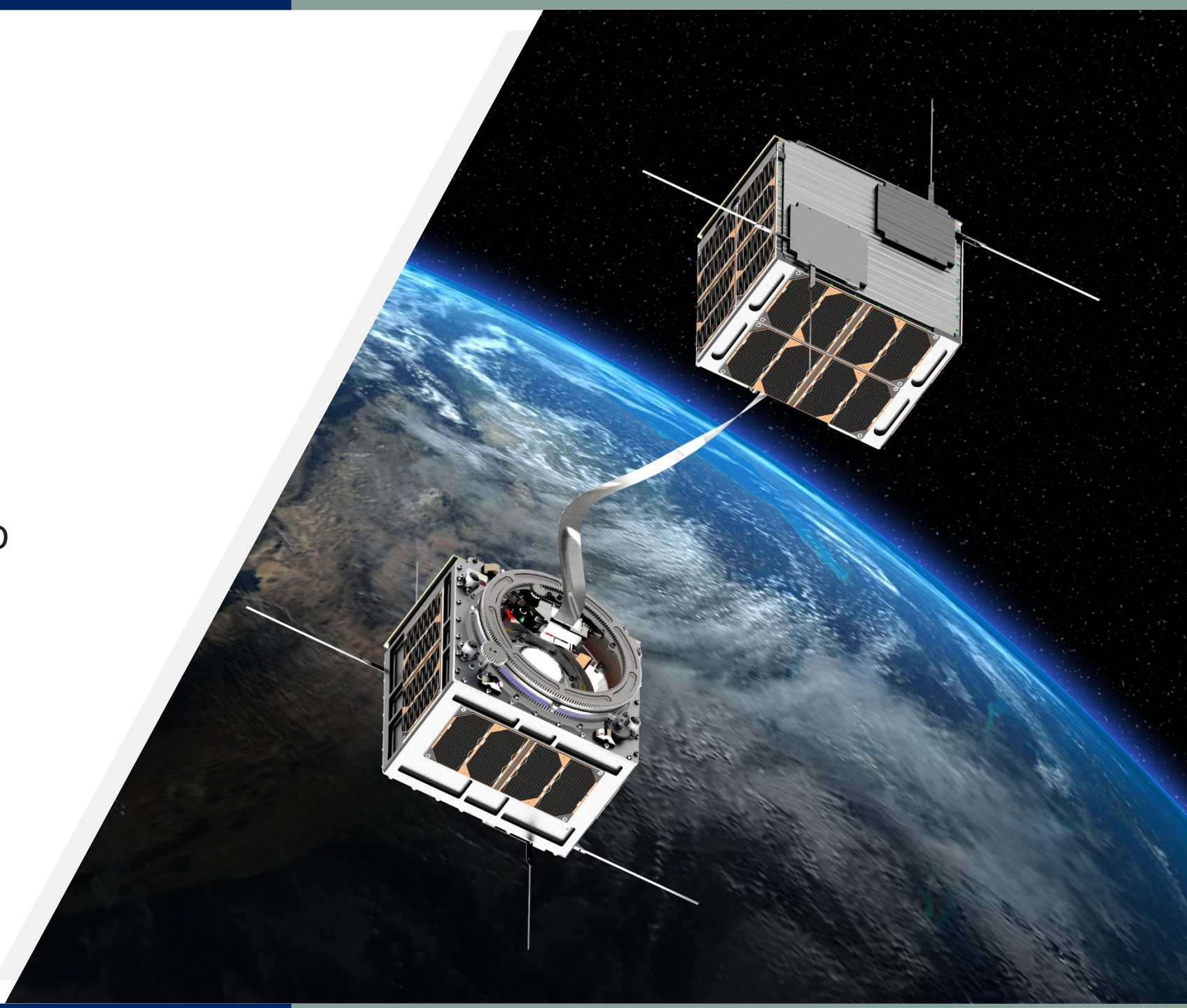
BPT
Final Presentation

Lorenzo Tarabini Castellani
Asier Ortega

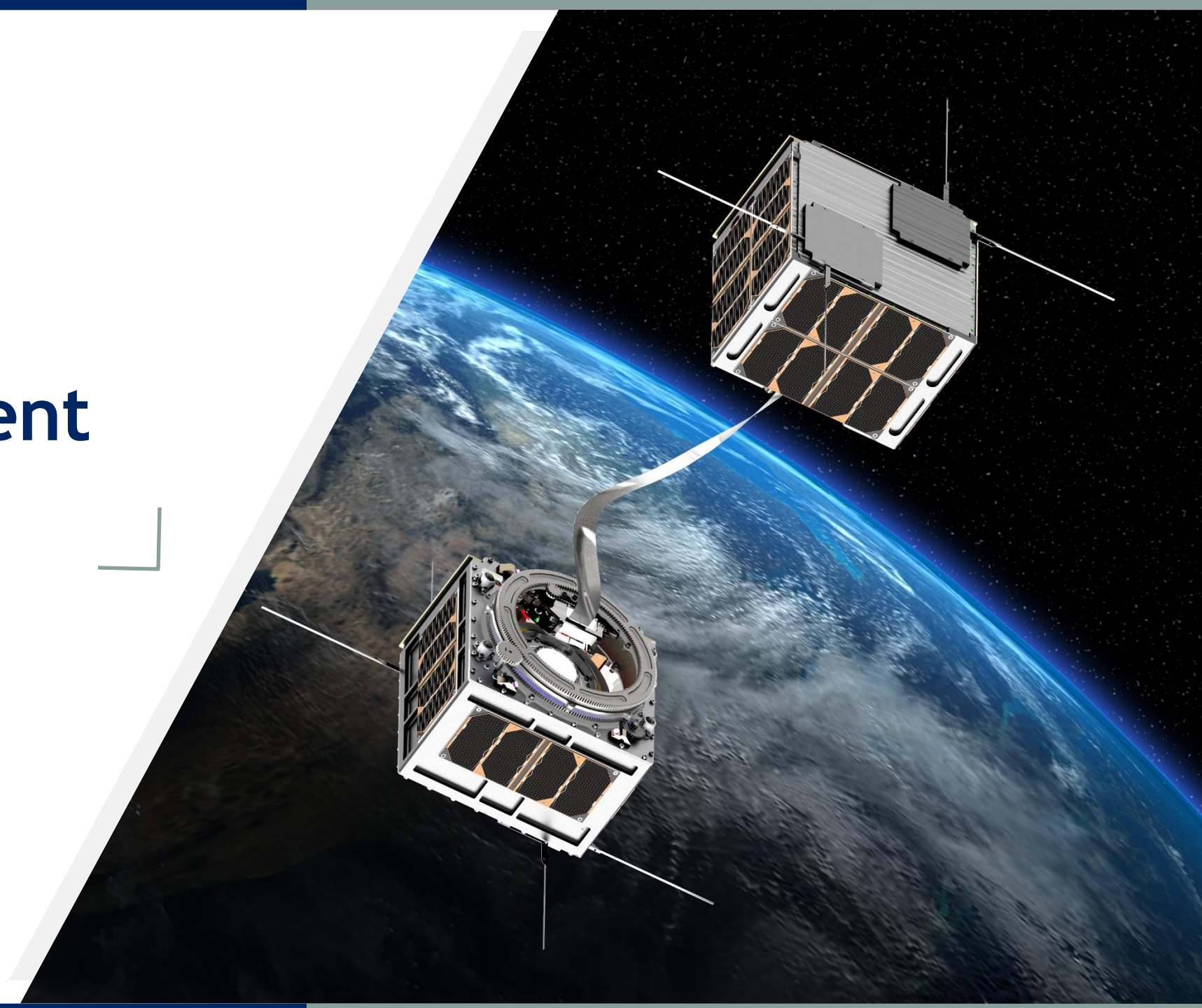
BPT DEVELOPMENT ROADMAP (for the integration in E.T.PACK)

INDEX

1. Requirement updates
2. Preliminary Design for IOD
3. BPT Planning
4. Integration Testing
5. Conclusions



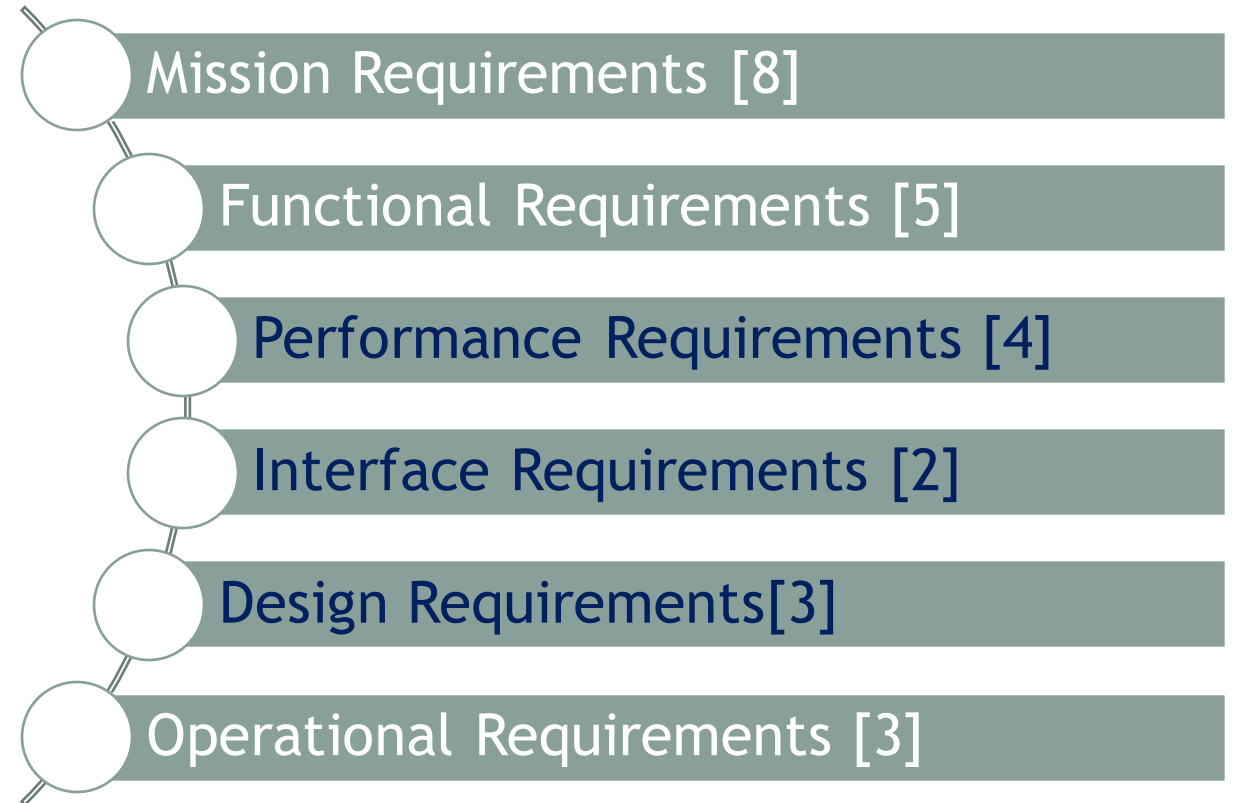
1. Requirement Updates



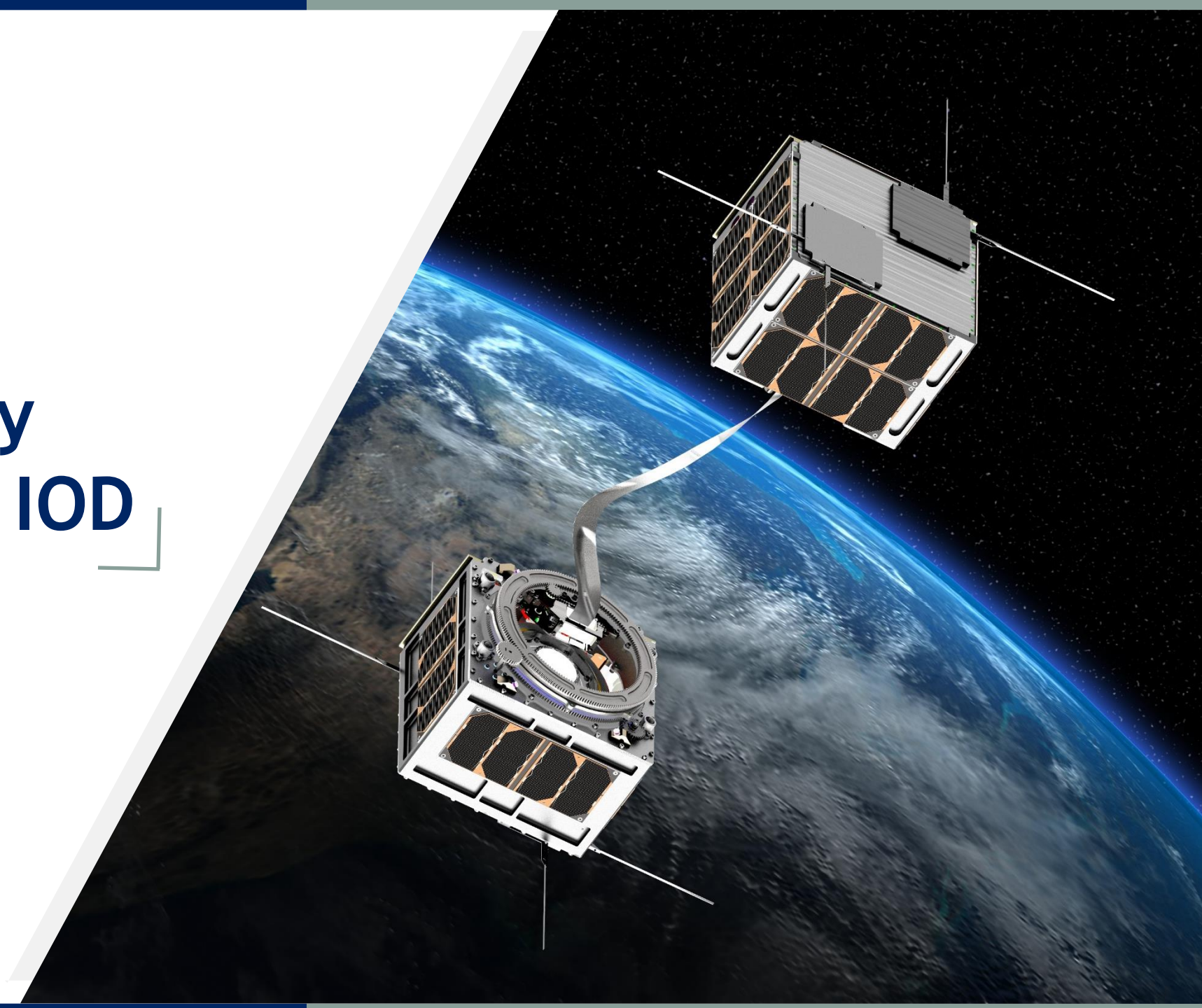
1. Requirements Updates

The 25 BPT requirements proposed at the beginning of the activity has been reviewed, completed and focused to the development of a demonstration photovoltaic segment to be flown in the ETPACK 2025 demonstration mission.

The main changes affect the performance, interface and design requirements.



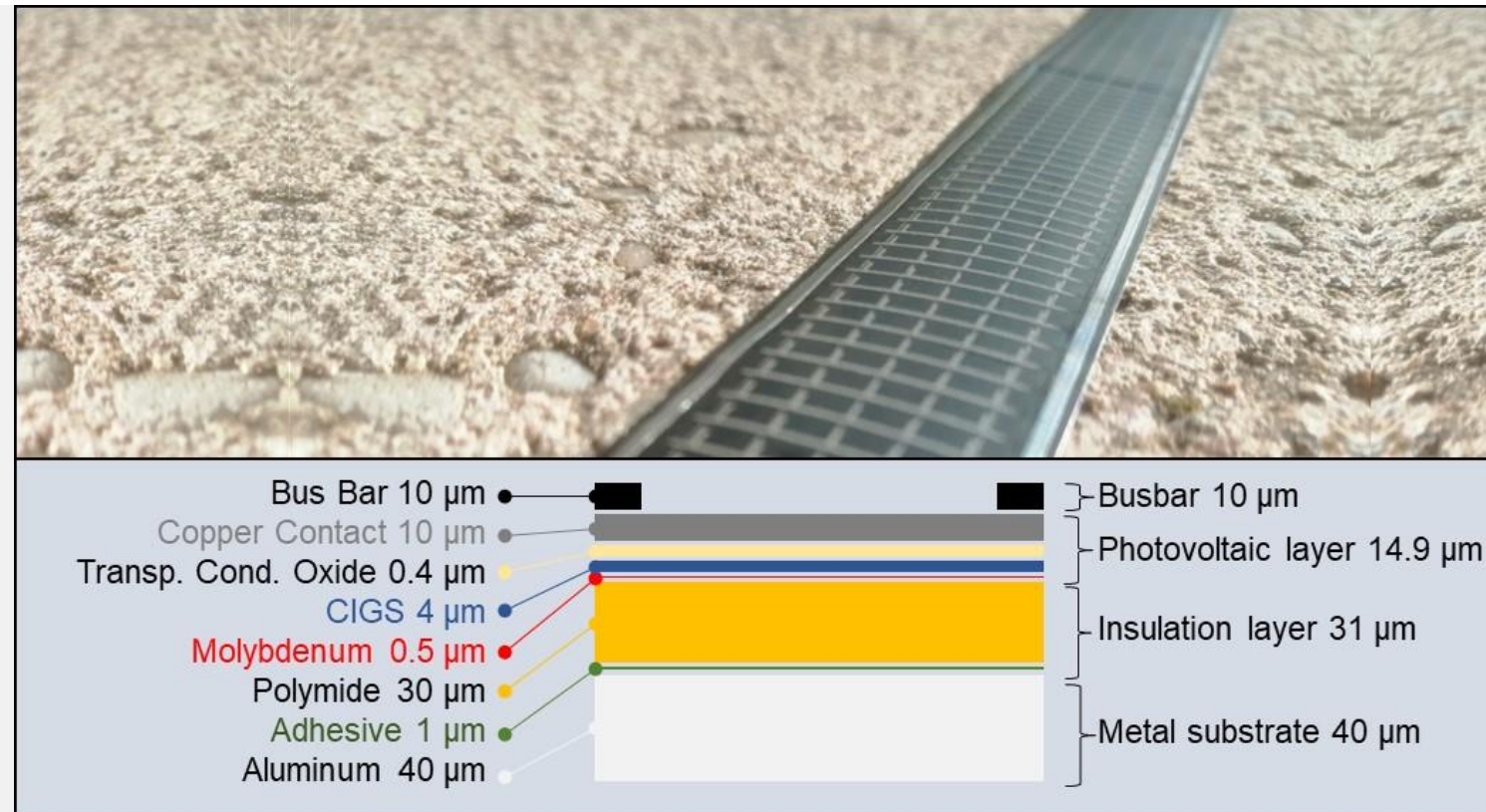
2. Preliminary Design for the IOD



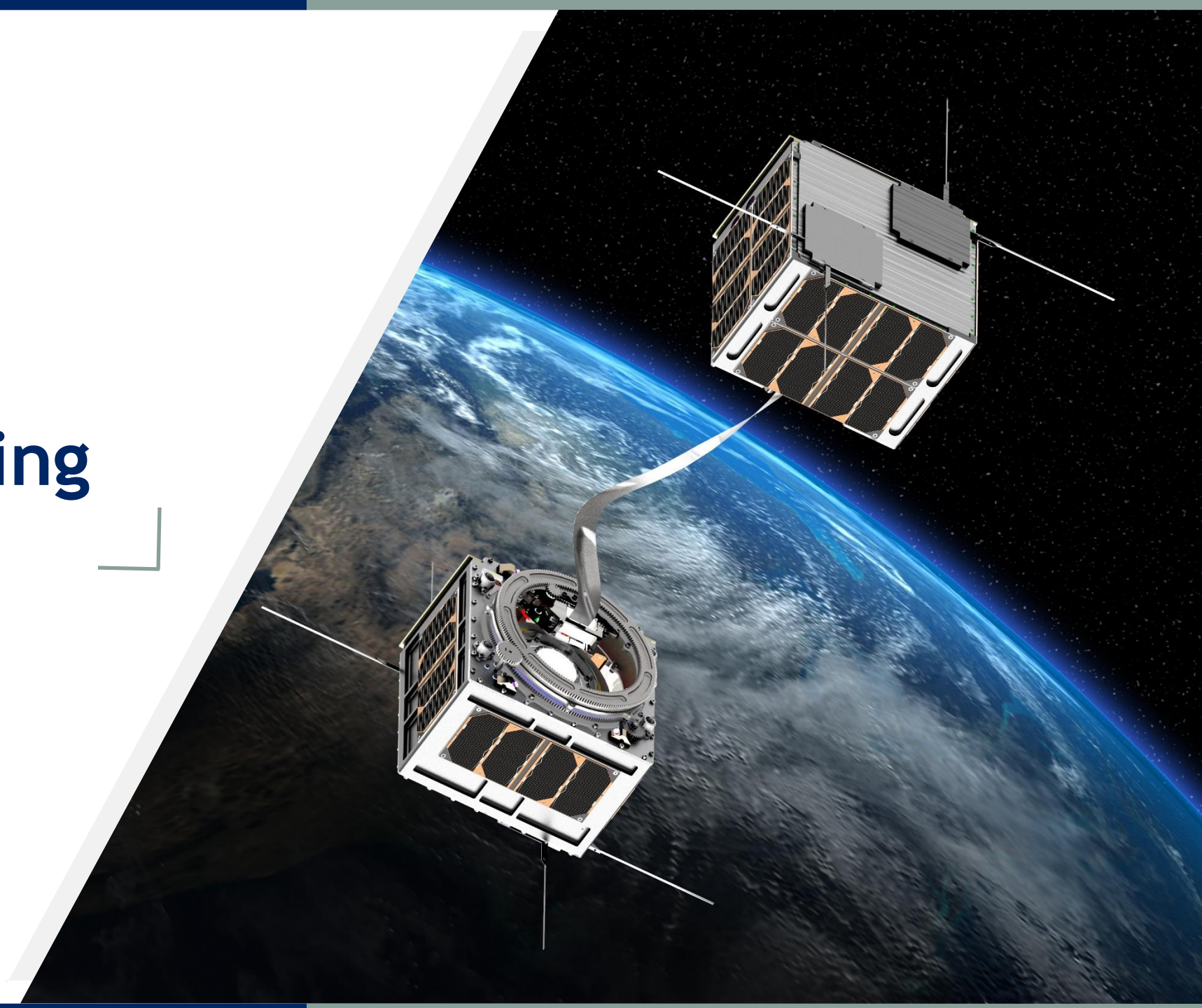
2. Preliminary Design for the IOD

For the In Orbit Demonstration, it is proposed to fly a 3m segment of BPT that could potentially provide “fully lit” about 2.4W at 100°C in vacuum. The BPT segment will have a width of 2.5 cm and an overall thickness of less than 100µm.

The BPT submodules will be designed to have an open circuit voltage of 14 V at the operation temperature of 20 °C. This will allow to directly connect the PBT to the ETPACK commercial Electric Power System (EPS) and perform testing at ambient temperature.

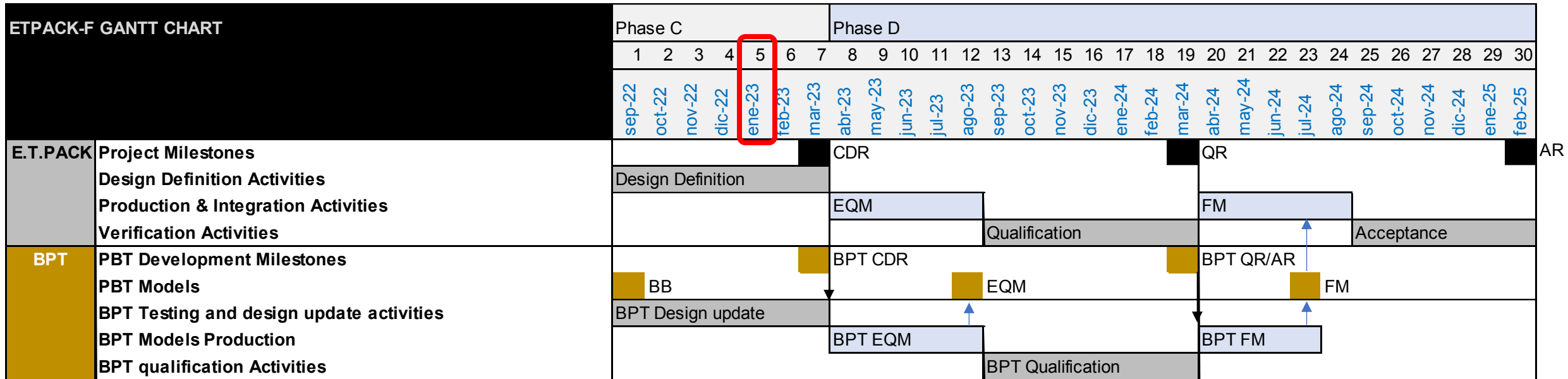


3. BPT Planning



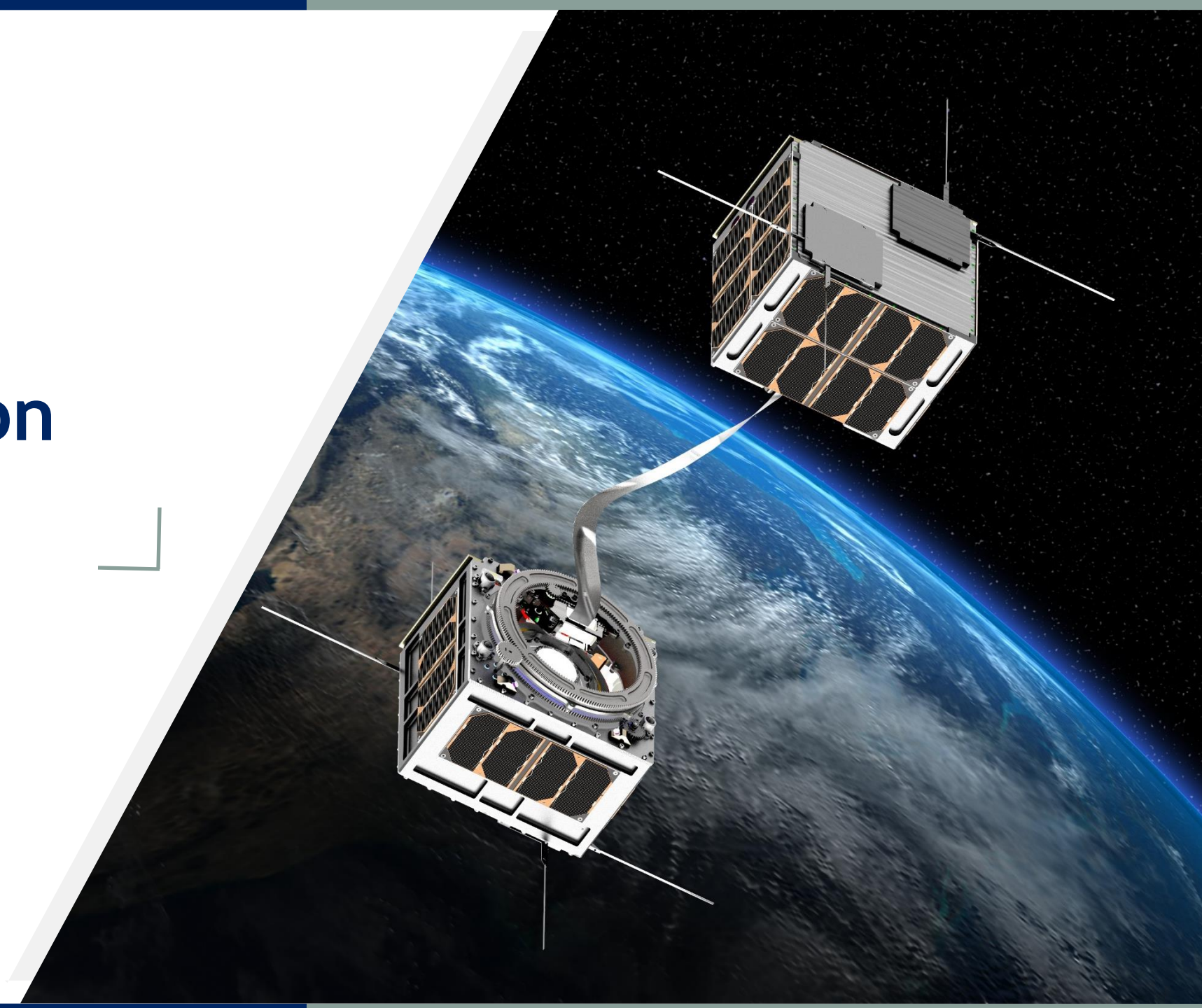
3. BPT PLanning

The BPT CDR and AR will be performed in parallel with the system CDR in order to allocate enough time to carry out the BPT development and qualification activities.



No funding for the present development is available at the time of writing this document and potential delay in getting a financial support could result in a not feasible implementation of the PBT in the E.T.PACK In Orbit Demonstration mission scheduled for 2025.

4. Integration Testing



4. Integration Testing

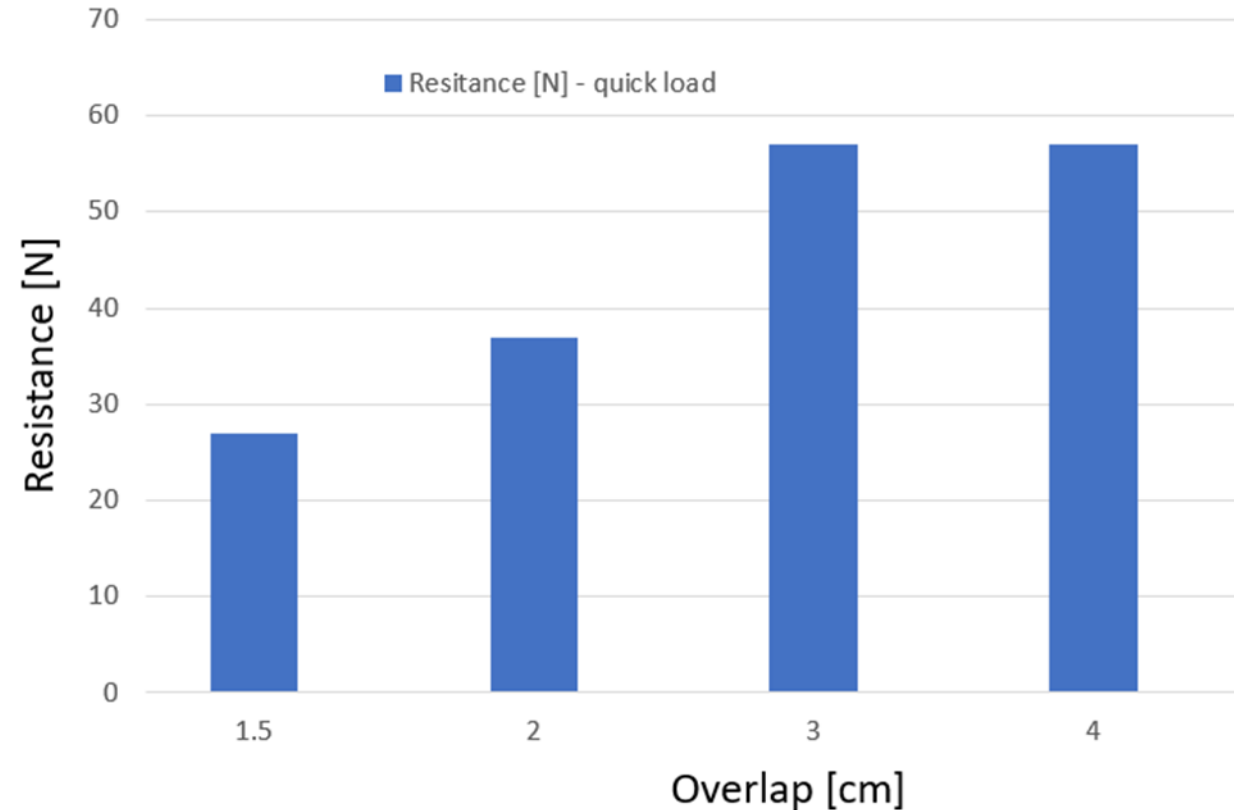
BPT mechanical connection with aluminum tape

UniPD performed the mechanical testing of the selected transfer tape* used to join together tether segments.

Overlap from 1.5 to 4 cm of tape was tested demonstrating resistance from 27N to 57N that fulfils the operational requirement maximum load of 10N.

Overlap of 3cm is selected as baseline.

Conductivity of the joint has also been successfully tested.

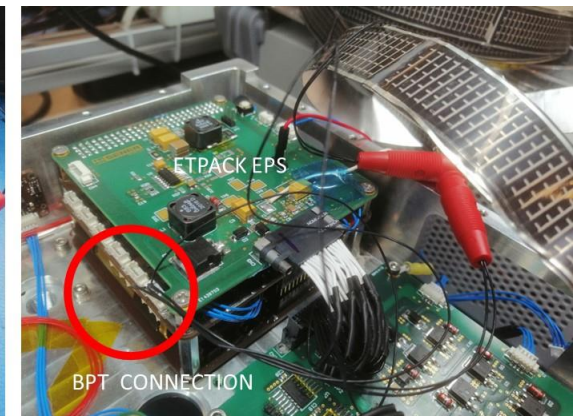
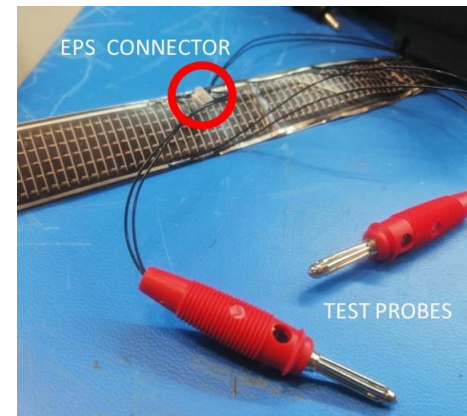


(*) 3M Conductive Adhesive Transfer Tape 9703

4. Integration Testing

BPT electrical connection with ETPACK EPS

The test was conducted on the 5th of January 2023 at 13.00. The sun inclination was 36° and the sky clear. The estimated solar irradiance was about 500 W/m^2 . The EPS was correctly sensing the voltage but was not able to charge the batteries due to the low current. In particular, the voltage of 11.5V was measured but only 3 mA of currents, while current of about 80mA was expected.



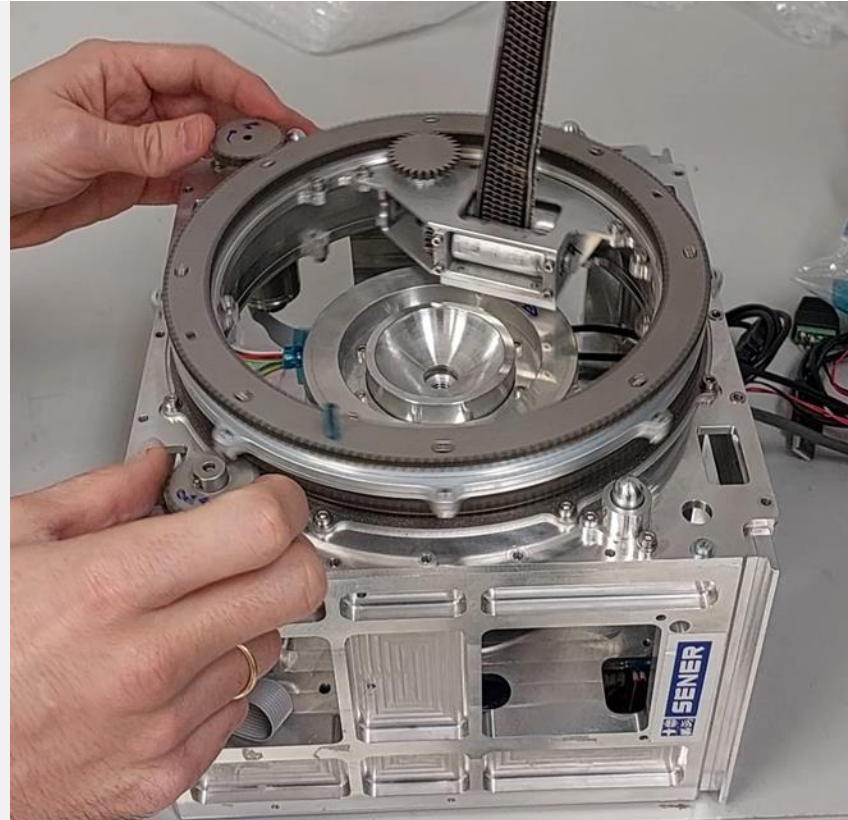
4. Integration Testing

BPT deployment

The test was conducted on the 13th of January 2023.

The BPT was coiled in the DMM and manually deployed activating the gears.

The deployment produced few scratches on the sample, but the extraction was smooth and no cracking on the BPT photovoltaic layer was observed after the test.



5. Conclusions

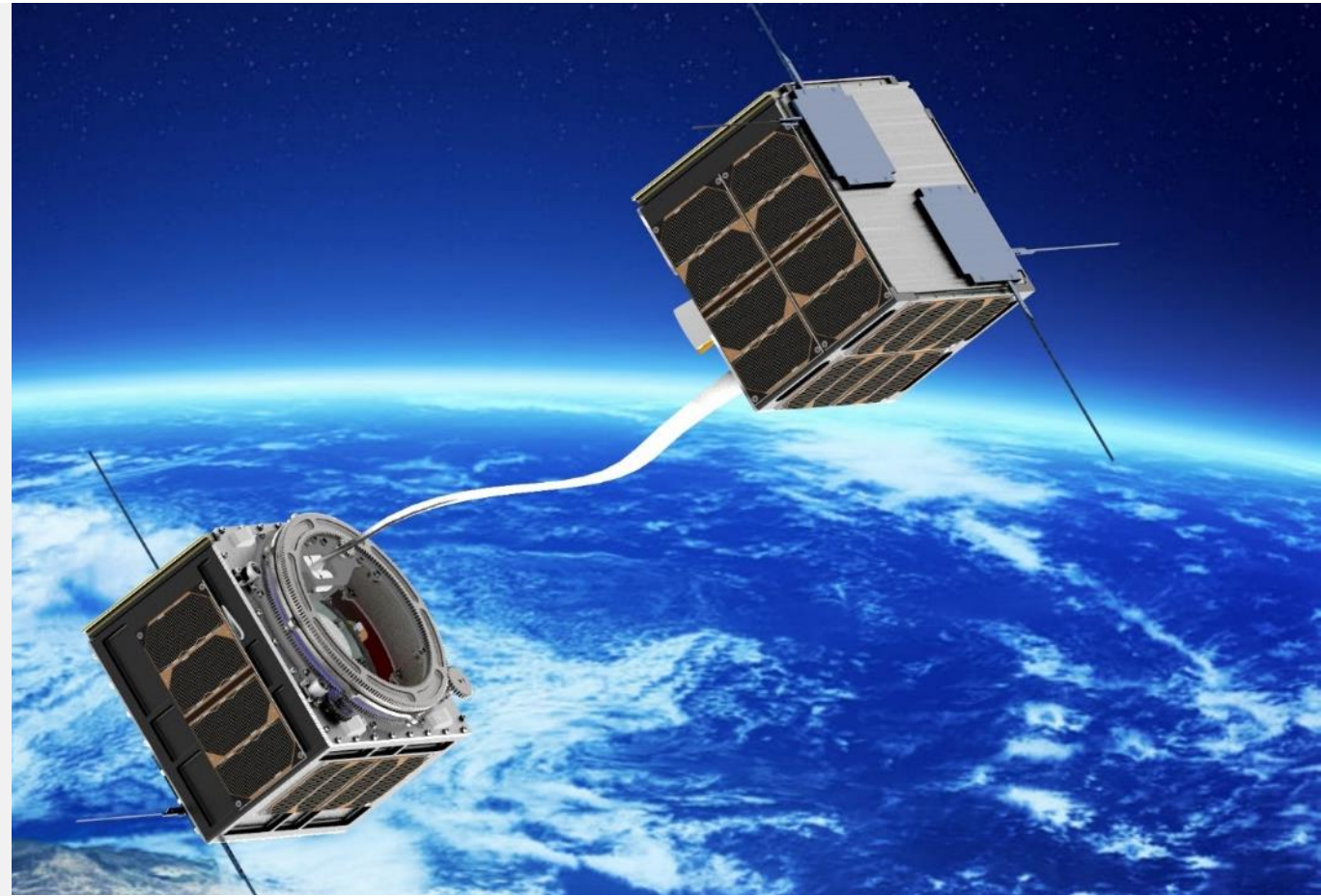


5. Conclusions

The BPT is a very promising solution for generating the required power for tether systems. Power is needed to feed the cathode and can boost the electrodynamic tether performances.

BPT is a very interesting solution to provide power for the deorbiting of launcher upper stages. Most upper stages use batteries and cannot power subsystems for extended time.

In conclusion, the results of the current study shows very good expectation for the BPT technology for the SENER's application.





SENER

Aeroespacial



THANK YOU

 www.aeroespacial.sener

 www.linkedin.com/company/sener

 www.youtube.com/user/senerengineering